MAMDANI FUZZY I-PD CONTROLLER FOR ANGULAR POSITION CONTROL OF TWO-LINK ROBOT MANIPULATOR

WICHARN CHATRATTANAWUTH

A THESIS SUBMITTED IN PARTIAL FULFILLMENT

OF THE REQUIREMENTS FOR THE DEGREE OF

MASTER OF ENGINEERING IN CONTROL ENGINEERING

SCHOOL OF GRADUATE STUDIES

KING MONGKUT'S INSTITUTE OF TECHNOLOGY LADKRABANG

2007

KMITL-EN-M-080-006

หัวข้อวิทยานิพนธ์	ตัวควบคุมแมมดานิฟัซซีไอ-พีดีสำหรับควบคุมตำแหน่งเชิงมุมของแขนกลสองข้อต่อ
นักศึกษา	นายวิชาญ ฉัตรรัตนวุฒิ
รหัสนักศึกษา	48060501
ปริญญา	วิศวกรรมศาสตรมหาบัณฑิต
สาขาวิชา	วิศวกรรมระบบควบคุม
พ.ศ.	2550
อาจารย์ที่ปรึกษาวิทยานิพนธ์	รศ.ดร.จงกล งามวิวิทย์

บทคัดย่อ

วิทยานิพนธ์นี้ นำเสนอการออกแบบตัวควบคุมแมมดานิฟัซซีไอ-พีดี เพื่อควบคุมตำแหน่งเชิงมุมของแขนกลสองข้อต่อให้มีผลตอบสนองที่รวดเร็วและไม่มีค่าผิดพลาดที่สภาวะคงตัว ซึ่งตัวควบคุมนี้ได้มาจากการนำหลักการของฟัซซีมาปรับปรุงตัวควบคุมไอ-พีดีแบบดั้งเดิมซึ่งมีพารามิเตอร์ที่ถูกออกแบบด้วยวิธีแผนผังค่าสัมประสิทธิ์ และใช้ทฤษฎีบทเกนน้อยวิเคราะห์หาเสถียรภาพที่พอเพียงของการออกแบบระบบควบคุมแมมดานิฟัซซีไอ-พีดี จากผลการจำลองและการทดลองเมื่อใช้ตัวควบคุมแมมดานิฟัซซีไอ-พีดีควบคุมตำแหน่งเชิงมุมของข้อต่อที่ 1 และข้อต่อที่ 2 ของแขนกลพบว่า ตัวควบคุมที่นำเสนอนี้ สามารถควบคุมตำแหน่งเชิงมุมของทั้งสองข้อต่อของแขนกลให้เคลื่อนที่ไปตามเส้นทางการเคลื่อนที่ที่ต้องการได้เร็วตามที่ได้ออกแบบไว้โดยมีค่าพุ่งเกินน้อย และไม่มีค่าผิดพลาดที่สภาวะคงตัว

Thesis Title	Mamdani Fuzzy I-PD Controller for Angular Position Control of Two-Link Robot Manipulator
Student	Mr. Wicharn Chatrattanawuth
Student ID.	48060501
Degree	Master of Engineering
Program	Control Engineering
Year	2007
Thesis Advisor	Assoc.Prof. Dr. Jongkol Ngamwiwit

ABSTRACT

This thesis proposes a Mamdani fuzzy I-PD controller for angular position control of two-link robot manipulator system. In order to obtain the fast response without steady-state error, the fuzzy principle is used to design the proposed controller which is the modification of the conventional I-PD controller designed by coefficient diagram method. The sufficient condition for stability of the Mamdani fuzzy I-PD control system is derived based on small gain theorem. The simulation and the experimental results of the angular position control of the 1st link and the 2nd link of the robot manipulator using the proposed Mamdani fuzzy I-PD controller are shown that the proposed controller can control both links of the robot manipulator to follow the desired trajectory rapidly without steady-state error.

Acknowledgments

First of all, as an advisee, I would like to thank my advisor, Dr. Jongkol Ngamwiwit, for her support during the course of this research work, without her suggestions, I would have never accomplish this work. As a student, I would like to thank for her guidance and her dedication for the works that also became my prototype of working and living.

Thanks to Ajarn Taworn Benjanarasuth, Ajarn Don Isarakorn, Ajarn Songmuang Nundrakwang and all the members of the Control and Mechatronics Lab for the excellent support and advice throughout the year.

Finally, I would like to express my boundless gratitude to my beloved parents, brother and sister, and for their loves and taking care of me.

CONTENTS

CONTENTS (Cont.)

CONTENTS (Cont.)

LIST OF TABLES

LIST OF FIGURES

LIST OF FIGURES (Cont.)

NOMENCLATURE

a_1	Length between gravity center position and rotational position of the 1st link
a_2	Length between gravity center position and rotational position of the 2nd link
A	Fuzzy set A
$\mathbf{A}$	State variable matrix
$B_a(s)$	Pre-filter
$B_c(s)$	Numerator polynomial of controller
$B_{fb}(s)$	Polynomial of feedback controller
$B_{ff}(s)$	Polynomial of feedforward controller
B_{M1}	Rotor damping constant of motor of the 1st link
B_{M2}	Rotor damping constant of motor of the 2nd link
$B_p(s)$	Numerator polynomial of plant
$B_p^*(s)$	Numerator polynomial of plant included the feedback controller
$\mathbf{B}$	Input variable matrix
$\mathbf{B}_M$	Rotor damping constant matrix
$\mathbf{C}$	Output variable matrix
$e(nT)$	Error
$e(nT-T)$	Error delayed by one sample
$E(s)$	Error
$\Delta e(nT)$	Change of Error
$\mathbf{f(x,u)}$	Nonlinear state variable vector
G	Syntactic rule for generating the name of the values of x
$G_p(s)$	Plant
$G_p^*(s)$	Modified plant
H_I	Adjustable constants of fuzzy I controller
H_{PD}	Adjustable constants of fuzzy PD controller
$\mathbf{h(x)}$	Nonlinear output variable matrix
J_{M1}	Moment of inertia of motor of the 1st link
J_{M2}	Moment of inertia of motor of the 2nd link
$\mathbf{J}_M$	Moment of inertia matrix of motors

NOMENCLATURE (Cont.)

k_1	Kinetic energy due to motion of the 1st link
k_2	Kinetic energy due to motion of the 2nd link
K	Kinetic energy
K_1, K_2	Fuzzy I control gain
K_3, K_4	Fuzzy PD control gain
K_I	Integral gain
K_p	Proportional gain of feedback PD controller
K_d	Derivative gain of feedback PD controller
K_{M1}	Motor torque constant of the 1st link
K_{M2}	Motor torque constant of the 2nd link
$\mathbf{K}_M$	Motor torque constant vector
ℓ_1	Length of the 1st link
ℓ_2	Length of the 2nd link
L	Lagrangian
L_e, $L_{\Delta e}$	Adjustable constants of fuzzy I controller
L_y, $L_{\Delta y}$	Adjustable constants of fuzzy PD controller
m_1	Mass of the 1st link
m_2	Mass of the 2nd link
M	Semantic rules for associating each value with its meaning.
M_{PD}	Finite constant of Mamdani fuzzy PD controller
M_I	Finite constants of Mamdani fuzzy I controller
$\mathbf{M(q)}$	Inertia matrix
$\tilde{\mathbf{M}}\mathbf{(q)}$	Inertia matrix of complete dynamics
P	Potential energy
$P(s)$	Characteristic polynomial
$\mathbf{P}(s)$	Transfer matrix in s domain
$\mathbf{P}(z)$	Transfer matrix in z domain
q_1	Angular position of the 1st link
q_2	Angular position of the 2nd link

NOMENCLATURE (Cont.)

q_{ss}	Steady-state response
$\mathbf{q}$	Joint position vector
$\mathbf{q}_M$	Angular position vector of the rotors
$\dot{\mathbf{q}}_M$	Angular velocity vector of the rotors
$\ddot{\mathbf{q}}_M$	Angular acceleration vector of the rotors
$\mathbf{Q}(s)$	Output angular position vector
$R(s)$	Input
$\mathbf{R}$	Gear ratio vector
$sp(nT)$	Set point
T	Sampling time
τ	Equivalent time constant
$\boldsymbol{\tau}$	Generalized force vector
τ_1	Supplied torque from actuator of the 1st link
τ_2	Supplied torque from actuator of the 2nd link
$T(x)$	Term set of linguistic variable x,
$\mathbf{u}_0$	Initial value of the input variable
U	Universe of discourse
$u(nT)$, $U(s)$	Control signal
$u(nT-T)$	Control signal delayed by one sample
$\Delta u_I(nT)$	Output change of the fuzzy I controller
$\Delta u_{PD}(nT)$	Output change of the fuzzy PD controller
Δu_{I_r}	Output singleton of the fuzzy I controller for the r^{th} rule
Δu_{PD_r}	Output singleton of the fuzzy PD controller the r^{th} rule
v	Velocity
v_1	Control input voltage of the 1st link
v_2	Control input voltage of the 2nd link
V_c	Constant control input voltage
$\mathbf{v}$, $\mathbf{V}(s)$	Control input voltage vector
$\mathbf{V}(\mathbf{q},\dot{\mathbf{q}})$	Coriolis/centripetal torque vector

NOMENCLATURE (Cont.)

$\tilde{\mathbf{V}}(\mathbf{q},\dot{\mathbf{q}})$	Coriolis/centripetal torque vector of complete dynamics
x	Any member in U
$\mathbf{x}$	State variable vector
$\mathbf{x}_0$	Initial value of the state variable
$y(nT),\ Y(s)$	Output
$\Delta y(nT)$	Change of output
$\mathbf{y}$	Output variable vector
α_C	Norm of controller
α_I	Norm of Mamdani fuzzy I controller
α_P	Norm of plant
α_{PD}	Norm of Mamdani fuzzy PD controller
β_C	Finite constant of controller
β_P	Finite constant of plant
β_I	Finite constant of Mamdani fuzzy I controller
β_{PD}	Finite constant of Mamdani fuzzy PD controller
μ_A	Membership function of fuzzy set A
μ_{I_r}	Membership value of Mamdani fuzzy I controller for the r^{th} rule
μ_{PD_r}	Membership value of Mamdani fuzzy PD controller for the r^{th} rule
γ_i	Stability index
γ_i^*	Stability limit

Chapter 1

Introduction

1.1 Statement and Significance of the Problems

Robot manipulator or robotic arm, which looks and works like a human being [1], was first introduced in the mass-production assembly line at the beginning of the twenty century by Ford Motor Company [2]. Following that starting point, the robot manipulator is widely used in order to manufacture the products which satisfied to the customer's requirements and passed industrial standards. It is known that the robot manipulator can be controlled to move to desired position precisely more than a human can do and the robotic arm can do the routine task without boredom and tiredness. When the robotic arm is used in assembly line, it is easy to produce the products as required and cause fewer defects. Furthermore, there are many industrial processes that can not allow the worker to deal with such as carrying weighty or high-temperature objects, coating materials by poisonous substance and so on while the robotic arm can do them as well without any damage. Hence, the robot manipulator seems like most suitable instrument for these dangerous jobs. There is no doubt that the cost can be reduced and the more profits can be obtained easy by the replacement of human with robotic arm. As a result, the study about control technique for controlling the robotic arm to move to the desired position is the most interested thing.

In recent years, many control schemes have been proposed to control the robot manipulator, such as adaptive linear compensator PD controller [3], adaptive controller [4], PID computed-torque controller [5] and implementation of observers for computed-torque control [6]. Adaptive control algorithm has been used to maintain good performance when the actual mathematical model of the controlled system is used in designing. However, it is not easy to achieve the real values of some system model components. For nonlinear control called computed-torque control, it is the same as the adaptive control. The actual mathematical model of the system is also required because the good result in control will not be performed. When the mathematical model of the interested system is vague or exhibits uncertainties, fuzzy reasoning control is seem to be the most hopeful to be used. The fuzzy control is most desirable if (1) the mathematical model of the interested system to be controlled is unfavorable but the system is known to be significantly

nonlinear, time-varying, or have time delay and/or (2) when PID control can not generate satisfactory system performance [7].

Hence, this thesis proposes a Mamdani fuzzy I-PD controller for angular position control of two-link robot manipulator system by utilizing the concepts of fuzzy principle control and I-PD control. The fuzzy principle is used to design the proposed controller which is the modification of the conventional I-PD controller designed by coefficient diagram method (CDM) [8], whose structure has a property to avoid large changes in control signal due to the proportional and derivative actions when there is a sudden change in the reference input. The simulation and the experimental results of the angular position control of the 1st link and the 2nd link of the robot manipulator using the proposed Mamdani fuzzy I-PD controller are shown that the proposed controller can control both links of the robot manipulator to follow the desired trajectory without steady-state error.

1.2 Research Objective and Approach Methodology

The need to control the angular position of two-link robot manipulator with high performance has motivated the following research objectives:

1) Studying a design method of Mamdani fuzzy I-PD controller for controlling the 1st and 2nd links of robot manipulator to follow the desired trajectory without steady-state error.

2) Derivation of two-link robot manipulator models. In this work, the two-link robot manipulator is modeled to be a linear system in order that CDM can be applied. The model parameters are determined from experimental data.

3) Analysis of the sufficient condition of bounded-input bounded-output (BIBO) stable for the Mamdani fuzzy I-PD control system based on small gain theorem.

4) Studying Mamdani fuzzy I-PD control system performances. The effectiveness of Mamdani fuzzy I-PD controller in controlling the angular positions of two-link robot manipulator will be shown by the simulation and the experimental results.

1.3 Summary of Thesis Contents

This thesis is organized in 6 chapters including references and appendices.

Chapter 2 describes the basic concepts of fuzzy set, fuzzy logic theory, fuzzy operations and linguist variable which will be useful in explaining fuzzy logic systems. Basic configuration of fuzzy logic controller which consists of fuzzification, fuzzy rules, fuzzy inference and defuzzifier will also be described, briefly.

Chapter 3 explains structure and mathematical models of two-link robot manipulator. It begins with deriving kinetic energies. Then the robot manipulator dynamics will be formulated by using Lagrange's equation. However, the robot manipulator needs the actuators to drive it. The actuator dynamics will be added to the robot manipulator dynamics to obtain the complete dynamics of the robot manipulator. From here, the linearization will be used to obtain the linear model in the initial state. Finally the identification of unmeasured parameters of the actuators will be present at the end of this chapter.

Chapter 4 introduces the structure of Mamdani fuzzy I-PD controller, fuzzy controller design and analyzing the relation between the change input and the output-change, and examining the sufficient condition of BIBO stable of the Mamdani fuzzy I-PD control system based on small gain theorem.

Chapter 5 presents the application of Mamdani fuzzy I-PD controller in controlling the angular position of two-link robot manipulator. The effectiveness of the Mamdani fuzzy I-PD controller will be evaluated by the simulation and the experimental results.

Chapter 6 will conclude the results of this research and future works.

Chapter 2

Fuzzy Set and Fuzzy Logic Theory

In order to design fuzzy logic controller for controlling the desired processes, fuzzy set and fuzzy logic theory must be known first. The basic concepts of fuzzy set and fuzzy logic which will be useful in explaining fuzzy logic system will be reviewed in this chapter.

2.1 Fuzzy Set Theory

In traditional set or crisp set theory, membership value of an object can be defined exactly with two values: 0 or 1 when the object belongs to set completely or it does not belong at all. However, in general, there are countless vague objects that can not be described easily and certainly by crisp set theory. Though the membership values of interested objects are found, it is not fairly. Fuzzy set theory is a tool which is used to remedy this dilemma.

Fuzzy set was first proposed by Professor L. A. Zadeh in 1965. The theory has laid the foundation for computing with words by generalizing 0 and 1 membership values of a crisp set to a membership function of a fuzzy set. The explanation of fuzzy set is as follows:

Definition 1 Fuzzy Set

Let U be a collection of objects and be called the universe of discourse. x is any member in U and is defined by $x \in U$. A fuzzy set A in U is characterized by membership function $\mu_A(x)$ which associates with each objects in U a real number in the interval [0,1] with the value of $\mu_A(x)$ at x representing the "grade of membership" of x in A. Thus the near the value of $\mu_A(x)$ to unity, the higher the grade of membership of x in A. When A is a set in the ordinary sense of the term, its membership function can take on only two values 0 and 1, with $\mu_A(x)$ reduces to the familiar characteristic function of a set A [9]. Fuzzy set A can be written by

$$A = \{(x, \mu_A(x)) | x \in U\}. \tag{2.3}$$

When the membership function of fuzzy set is continuous, the fuzzy set A is defined as

$$A = \int_U \mu_A(x)/x \tag{2.4}$$

and when the membership function of fuzzy set is discrete, the fuzzy set A is as

$$A = \{(x_1, \mu_A(x_1)), (x_2, \mu_A(x_2)), ..., (x_n, \mu_A(x_n))\} \tag{2.5}$$

or

$$A = \mu_A(x_1)/x_1 + \mu_A(x_2)/x_2 + ... + \mu_A(x_n)/x_n = \sum_{i=1}^{n} \mu_A(x_i)/x_i, \tag{2.6}$$

here, $\int$ and + mean unionizing the member x and the member $\mu_A(x)$ to be a set. They have no meaning of general mathematical operations as integration and summation. And / means the relation between the member x and the member $\mu_A(x)$. It is not related to the division of the members.

For explaining the concepts of the crisp set and the fuzzy set clearly, the membership function of crisp set and fuzzy set can be illustrated in figure 2.1.

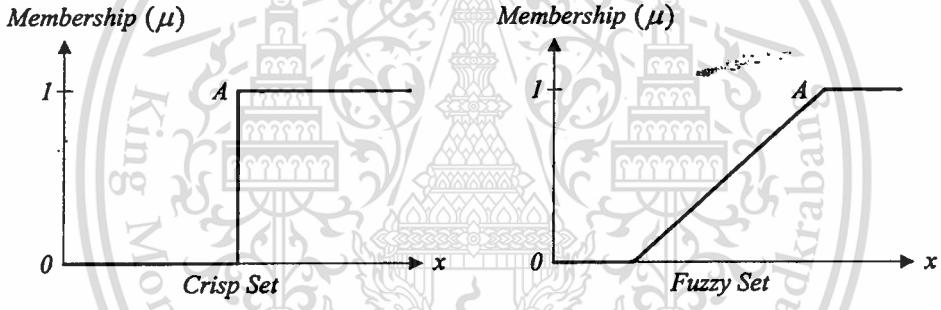

Figure 2.1 The membership function of crisp set and fuzzy set.

Definition 3 Singleton

Singleton is a fuzzy set which has nonzero membership values for one only element of the universe of discourse. Figure 2.2 shows a singleton fuzzy set whose membership values is 0 everywhere except at $x = 30$. Singleton fuzzy set is employed in consequent of fuzzy rules by the majority of typical fuzzy controllers and models.

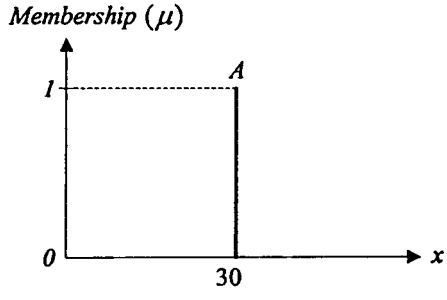

Figure 2.2 Fuzzy singleton.

Definition 4 Support

The support of a fuzzy set A is set of all elements x in the universe of discourse U such that $\mu_A(x) > 0$. It is defined by

$$supp(A) = \{x \in U | \mu_A(x) > 0\}. \tag{2.7}$$

2.2 Fuzzy Logic Operations

Let A and B are fuzzy sets in the universe of discourse U whose membership functions are μ_A and μ_B respectively. The basic operations are defined in this subsection.

Definition 7 Complement

The complement of a fuzzy set A whose $\mu_A(x) \in [0,1]$ in the universe of discourse U is represented by $\overline{A}$. Its membership function for all elements $x \in U$ are defined as

$$\mu_{\overline{A}}(x) = 1 - \mu_A(x) \qquad ;\forall x \in U. \tag{2.8}$$

Definition 8 Intersection

The intersection of a fuzzy set A and B in the universe of discourse U is represented by $A \cap B$. Its membership function for all elements $x \in U$ are defined as

$$\mu_{A \cap B}(x) = \min\{\mu_A(x), \mu_B(x)\} \qquad ;\forall x \in U. \tag{2.9}$$

Definition 9 Union

The union of fuzzy set A and B in the universe of discourse U is represent by $A \cup B$. Its membership function for all elements $x \in U$ are defined as

$$\mu_{A \cup B}(x) = \max\{\mu_A(x), \mu_B(x)\} \qquad ;\forall x \in U. \tag{2.10}$$

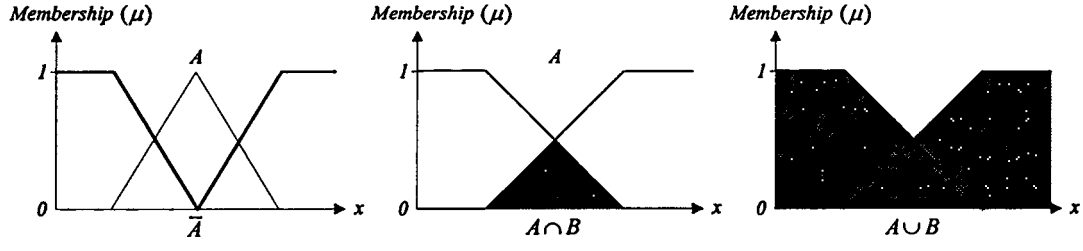

Figure 2.3 Operations: complement, intersection and union.

Definition 10 Equality

The fuzzy set A equals to the fuzzy set B when their grades of membership are equivalent.

$$A = B \leftrightarrow \mu_A(x) = \mu_B(x) \qquad ;\forall x \in U. \tag{2.11}$$

And fuzzy set A not equals to the fuzzy set B when their grades of membership are not equivalent.

$$A \neq B \leftrightarrow \mu_A(x) \neq \mu_B(x) \qquad ;\forall x \in U. \tag{2.12}$$

Definition 11 Fuzzy Subset

If every member of fuzzy set A is also a member of fuzzy set B, fuzzy set A is a subset of fuzzy set B. It is represented by

$$A \subseteq B \leftrightarrow \mu_A(x) \leq \mu_B(x) \qquad ;\forall x \in U, \tag{2.13}$$

when the grade of membership A and B are equal. If the grade of membership A and B are unequal, it can be symbolized by $A \subset B$.

Definition 12 Double-negation Law

Double-negation law is defined to be

$$\overline{\overline{A}} = A. \tag{2.14}$$

Definition 13 DeMorgan's Law

DeMorgan's law is rule for inference. It was defined as follows:

$$\overline{A \cup B} = \overline{A} \cup \overline{B}, \tag{2.15}$$

$$\overline{A \cap B} = \overline{A} \cap \overline{B}, \tag{2.16}$$

$$A \cup \overline{A} \neq U, \tag{2.17}$$

$$A \cup \overline{A} \neq \varnothing. \tag{2.18}$$

Definition 14 Cartesian Product

Let $A_1, A_2, ..., A_n$ are fuzzy sets in universes of discourse $U_1, U_2, ..., U_n$ respectively. Cartesian products of $A_1, A_2, ..., A_n$ are fuzzy sets in product space $U_1 \times U_2 \times ... \times U_n$ whose membership function is expressed by

$$\mu_{A_1 \times A_2 \times ... \times A_n}(x_1, x_2, ..., x_n) = \min\left[\mu_{A_1}(x_1), \mu_{A_2}(x_2), ..., \mu_{A_n}(x_n)\right], \quad (2.19)$$
$$x_1 \in U_1, x_2 \in U_2, ..., x_n \in U_n.$$

Definition 15 Algebraic Product

Algebraic product of fuzzy set A and fuzzy set B expressed by $A \cdot B$ whose membership function is defined as follow:

$$\mu_{A \cdot B}(x) = \mu_A(x) \cdot \mu_B(x). \quad (2.20)$$

Definition 16 Algebraic Summation

Algebraic summation of fuzzy set A and fuzzy set B is expressed by $A + B$. Its membership function is defined as follow:

$$\mu_{A+B}(x) = \mu_A(x) + \mu_B(x) - \mu_A(x) \cdot \mu_B(x). \quad (2.21)$$

Definition 17 Bounded Summation

Bounded summation of fuzzy set A and fuzzy set B is expressed by $A \oplus B$ and its membership function is defined as follow:

$$\mu_{A \oplus B}(x) = \min\{1, \mu_A(x) + \mu_B(x)\}. \quad (2.22)$$

Definition 19 Bounded Difference

Bounded difference of fuzzy set A and fuzzy set B expressed by $A \ominus B$ whose membership function is defined as follow:

$$\mu_{A \ominus B}(x) = \max\{0, \mu_A(x) - \mu_B(x)\}. \quad (2.23)$$

2.3 Linguistic Variables

A linguistic variable is characterized by a quintuple $(x, T(x), U, G, \mathrm{M})$.

Here, x is the name of variable,

$T(x)$ is the term set of linguistic variable x,

U is universes of discourse,

G is the syntactic rule for generating the name of the values of x and

M is the semantic rules for associating each value with its meaning.

The term of linguistic variable can be presented as shown in figure 2.4.

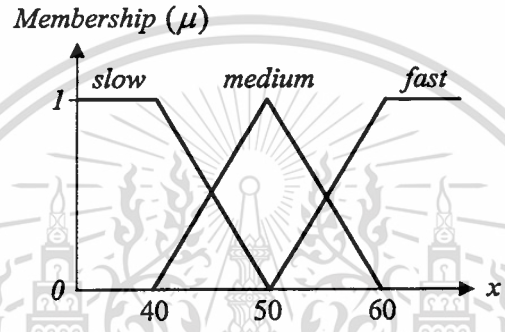

Figure 2.4 Linguistic variable called "*speed*".

2.4 Fuzzy Logic Controller

Basic configuration of fuzzy logic controller (FLC) shown in figure 2.5 consists of fuzzification, fuzzy rules, fuzzy inference and defuzzifier [10], where $x_1, x_2, ..., x_n$ are inputs of fuzzy logic controller and z is output of fuzzy logic controller.

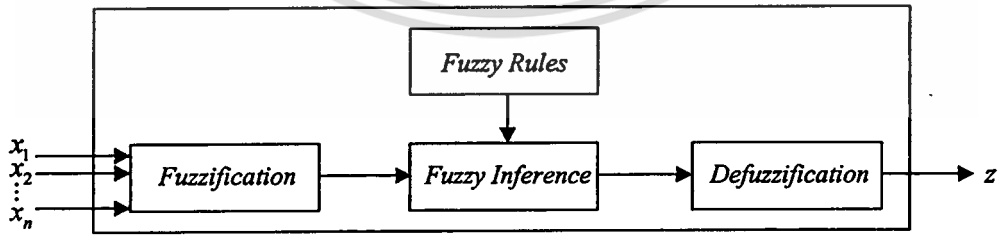

Figure 2.5 Basic configuration of fuzzy logic controller.

2.4.1 Fuzzification

Fuzzification is mathematical procedure which is used to convert the input of the fuzzy controller to be the membership value of the fuzzy set. It can be defined as

$$\mu_A(x) = fuzzification(x_0). \tag{2.23}$$

The number of fuzzy sets, their linguistic names and design parameters are determined by the fuzzy controller developer's decision included the control operator's knowledge and experience about characteristic of the system.

2.4.2 Fuzzy Rule

A fuzzy controller uses fuzzy rules which are linguistic IF-THEN statement. Fuzzy rule acts like a key in liking the input variables of fuzzy controller to the output variable. There are 2 major types of fuzzy rules. They are namely Mamdani fuzzy rule and Takagi-Sugeno (TS) fuzzy rule.

2.4.2.1 Mamdani Fuzzy Rule

Mamdani fuzzy rule is fuzzy control rule whose the rule outcome is linguistic variable. The expression of a general Mamdani fuzzy rule for a fuzzy controller involving n inputs and m outputs can be described as follows:

$$\begin{aligned} &IF\ x_1\ is\ A_1\ AND\ x_2\ is\ A_2\ AND\ ...\ AND\ x_n\ is\ A_n \\ &THEN\ y_1\ is\ B_1,\ y_2\ is\ B_2,...,\ y_n\ is\ B_n, \end{aligned} \tag{2.24}$$

where $x_1, x_2, ..., x_n$ are input variables, $y_1, y_2, ..., y_n$ are output variables, AND are fuzzy logic AND operators, $A_1, A_2, ..., A_n$ are fuzzy sets of inputs and $B_1, B_2, ..., B_n$ are fuzzy sets of outputs.

2.4.2.2 TS Fuzzy Rule

TS fuzzy rule is fuzzy control rule whose the rule outcome is functions of input variables. TS fuzzy rule for a fuzzy controller involving n inputs and m outputs can be expressed by

$$\begin{aligned} &IF\ x_1\ is\ A_1\ AND\ x_2\ is\ A_2\ AND\ ...\ AND\ x_n\ is\ A_n \\ &THEN\ y_1 = f_1(x_1,x_2,...,x_n),\ y_2 = f_2(x_1,x_2,...,x_n),...,\ y_n = f_n(x_1,x_2,...,x_n), \end{aligned} \tag{2.25}$$

where $f_1(x_1,x_2,...,x_n)$, $f_2(x_1,x_2,...,x_n)$,..., $f_n(x_1,x_2,...,x_n)$ are functions of input variables. In theory $f_n(x_1,x_2,...,x_n)$ can be chosen as any real function, linear or nonlinear function. However in practical, proper choosing or determining the mathematical formalism of nonlinear functions

for every fuzzy rule is extremely difficult. Consequently, linear function seems to be the easy option.

Fuzzy controller can be divided into two types by using fuzzy rule. They are Mamadani fuzzy controller and TS fuzzy controller.

2.4.3 Fuzzy Inference

Fuzzy inference or fuzzy reasoning is used in a fuzzy rule to determine the rule outcome from the information of rule input. Mammdani fuzzy rule and TS fuzzy rule use the different inference methods.

For Mammdani fuzzy rule, the most popular inference methods are Mamdani minimum inference, Larsen product inference, Drastic product inference and Bounded product inference. Let $\mu_{B_i}(y_i)$ be the membership function of the fuzzy set B_i, the four popular inference methods are defined by the following table:

Table 2.1 Definitions of Four Popular Inference Methods for Mamdani Fuzzy Rule.

Fuzzy Inference Method	Definition
Mamdani minimum inference, R_M	$\min\left(\mu_i, \mu_{B_i}(y_i)\right)$
Larsen product inference, R_L	$\mu_i \times \mu_{B_i}(y_i)$
Drastic product inference, R_{DP}	$\begin{cases} \mu_i & for \quad \mu_{B_i}(y_i) = 1 \\ \mu_{B_i} & for \quad \mu_i = 1 \\ 0 & for \quad \mu_i < 1 \quad and \quad \mu_{B_i}(y_i) < 1 \end{cases}$
Bounded product inference, R_{BP}	$\max\left(0, \mu_i + \mu_{B_i}(y_i) - 1\right)$

For making the meaning of the definitions of the popular fuzzy inference methods whose mathematical definitions given in table 2.1 easy to understand, graphical illustration are used and are shown in figure 2.6 and figure 2.7.

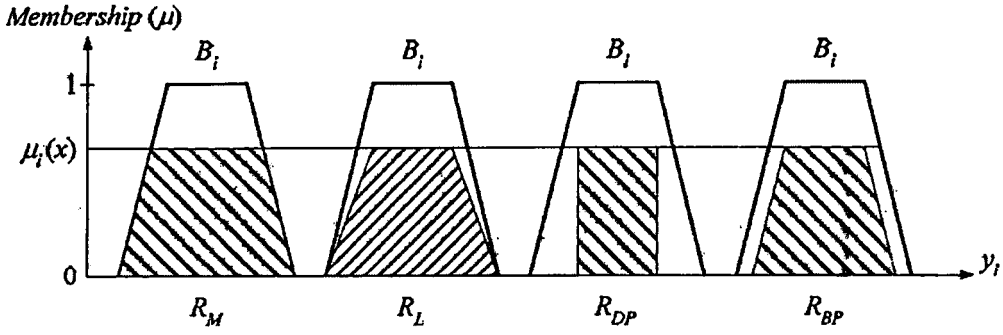

Figure 2.6 Graphical illustrations of the definitions of the four popular fuzzy inference methods.

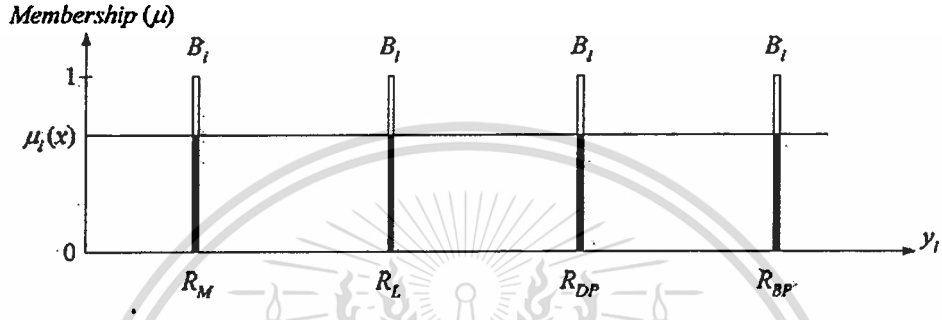

Figure 2.7 Outcome of using the four popular fuzzy inference methods.

It can be seen from figure 2.6 that when the different inference method is used for fuzzy rule consequent which is fuzzy set, the rule outcome formed in the shaded areas are not similar. However, when the different inference method is used for fuzzy rule consequent which is fuzzy singleton, the rule outcome is identical as shown in figure 2.7.

For TS fuzzy rule, the result of the fuzzy inference is $\mu_i \times f_i(x_1, x_2, ..., x_n)$. Every rule outcome is weighted by membership values of the inputs. So, the result of the fuzzy inference for TS fuzzy rule can be represented by mathematical equations easier than Mamdani fuzzy rule.

2.4.4 Defuzzification

Defuzzification is a mathematical procedure used for converting rule outcome to a real number. Every fuzzy controller uses a defuzzifier which is basically mathematical formula. The result of defuzzification will be used for controlling the process. The type of defuzzifier should be used appropriately to the output variables. In this subsection, some of popular ones will be presented.

2.4.4.1 Generalized Defuzzifier

Different type of defuzzifiers can be represented by one simple mathematic formula called generalized defuzzifier. Let Z be the output variable of fuzzy controller, N be the number

of fuzzy rules, μ_i be membership value of i^{th} rule and α be design parameter. The result of defuzzification in term of generalized defuzzifier is produced by

$$z = \frac{\sum_{i=1}^{N} \mu_i^{\alpha} \cdot y_i}{\sum_{i=1}^{N} \mu_i^{\alpha}}, \tag{2.24}$$

where y_i is the output of the fuzzy set for i^{th} rule. For the Mamdani fuzzy controller, y_i means fuzzy singleton B_i and for TS fuzzy controller, y_i means fuzzy function $f_i(x_1, x_2, ..., x_n)$.

2.4.4.2 Centriod Defuzzifier

In generalized defuzzifier, the value of the design parameter α is limited by the condition $0 \leq \alpha < \infty$. Different types of defuzzifier not use the same α values. When $\alpha = 1$, the most widely used defuzzifier called "centroid defuzzifier" is attained. The centroid type is popular because it computes the centriod of the fuzzy singleton from different rules.

Mean of maximum defuzzifier is obtained when $\alpha = \infty$. It calculates the average of maximum value of membership value. It is used for the process which needs the least computed time and a small amount of error is acceptable.

Chapter 3

Two-link Robot Manipulator

Fuzzy set and fuzzy logic theory described in chapter 2 gives important information in designing a fuzzy controller to be described in chapter 4. As the objective of the controller is to control angular positions of a two-link robot manipulator, the structure and the model of the manipulator will be described in this chapter.

3.1 Two-link Robot Manipulator Structure

The popular SCARA (Selective Compliance Assembly Robot Arm) type robot manipulator in assembly task [11] shown in figure 3.1 is used in the experiments. It consists of two links made from rigid material. They are driven by AC servos (see in the appendix A) with no gear, so that this robot can be called "direct drive robot (DDR)". The end of the 2nd link is called "end-effector" which is position for setting up tools. The end of the 1st link is attached to a metallic plate which is the base of the robot manipulator. The control signal transmission line and the feedback signal line are also connected via the base.

Figure 3.1 SCARA type robot manipulator (top view).

3.2 Mathematical Model of Two-link Robot Manipulator

In this section, mathematical models of two-link robot manipulator shown in figure 3.1 are derived. The mathematical models are the relation between the input current command voltage $\mathbf{V}(s)$ and the output angular position $\mathbf{Q}(s)$ for the 1st link and the 2nd link. The models can be

obtained from the dynamic equations of motion and the dynamics of the actuators. The dynamic equations of motion are given by deriving the kinetic energy of the manipulator by using Lagrange's equations of motion. The dynamic equations of actuators are obtained by the AC servos that drive the robot arm.

3.2.1 Kinetic Energy

The structure of the manipulator can be schematically shown in figure 3.2. q_1 and q_2 are the angular positions, m_1 and m_2 are the masses, ℓ_1 and ℓ_2 are the lengths, a_1 and a_2 are the lengths between the gravity center positions and rotational positions of the 1st and the 2nd links, respectively.

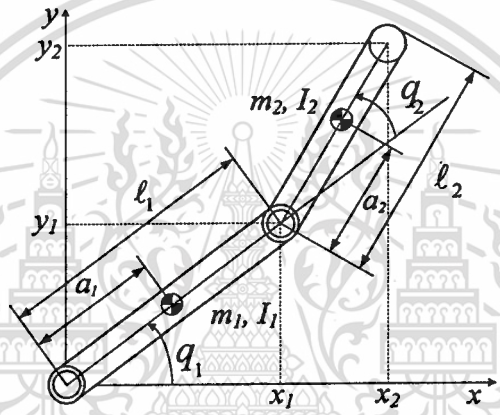

Figure 3.2 Schematic structure of the two-link robot manipulator (top view).

The gravity center positions of the 1st and the 2nd links of the robot shown in figure 3.2 are given by coordinates of x_1, x_2, y_1 and y_2 respectively,

$$x_1 = a_1 c_1 \quad y_1 = a_1 s_1 \tag{3.1}$$

$$x_2 = \ell_1 c_1 + a_2 c_{12} \quad y_2 = \ell_1 s_1 + a_2 s_{12}, \tag{3.2}$$

where $c_1 = \cos q_1$, $s_1 = \sin q_1$, $c_{12} = \cos(q_1 + q_2)$ and $s_{12} = \sin(q_1 + q_2)$. The velocities squares of the 1st and the 2nd link are

$$v_1^2 = \dot{x}_1^2 + \dot{y}_1^2 = a_1^2 \dot{q}_1^2 \tag{3.3}$$

$$v_2^2 = \dot{x}_2^2 + \dot{y}_2^2 = \ell_1^2 \dot{q}_1^2 + a_2^2 (\dot{q}_1^2 + 2\dot{q}_1 \dot{q}_2 + \dot{q}_2^2) + 2\ell_1 a_2 c_1 \dot{q}_1 (\dot{q}_1 + \dot{q}_2), \tag{3.4}$$

and the kinetic energies due to motions of the 1st and the 2nd links

$$k_1 = \frac{1}{2} m_1 v_1^2 = \frac{1}{2} m_1 a_1^2 \dot{q}_1^2 \tag{3.5}$$

$$k_2 = \frac{1}{2} m_2 v_2^2 = \frac{1}{2} m_2 (\ell_1^2 \dot{q}_1^2 + a_2^2 (\dot{q}_1^2 + 2\dot{q}_1 \dot{q}_2 + \dot{q}_2^2) + 2\ell_1 a_2 c_1 \dot{q}_1 (\dot{q}_1 + \dot{q}_2)) \tag{3.6}$$

are also given respectively. Since SCARA type robot is designed to move only in horizontal plane, the changes in height of the manipulator for the both links are considered to be zeros. The potential energies are also considered to zero.

3.2.2 Lagrange's Equation

In order to obtain the dynamic models of the manipulator, Lagrange's equation will be used. Lagrange's equations for a conservative system are given by [12]

$$\frac{d}{dt}\frac{\partial L}{\partial \dot{q}} - \frac{\partial L}{\partial q} = \tau \tag{3.7}$$

where q is the n-vector of generalized coordinates, τ is the n-vector of generalized forces and the Lagrangian is the difference between the kinetic and potential energies

$$L = K - P \tag{3.8}$$

where K is the kinetic energy and P is potential energy. By substituting the kinetic energies shown in equations (3.5) and (36.) to equation (3.8), the Lagrangian for the two-link robot manipulator is obtain as

$$L = k_1 + k_2. \tag{3.9}$$

From equation (3.9), when the joint variables is

$$\mathbf{q} = \begin{bmatrix} q_1 & q_2 \end{bmatrix}^T \tag{3.10}$$

and the generalized force is

$$\boldsymbol{\tau} = \begin{bmatrix} \tau_1 & \tau_2 \end{bmatrix}^T \tag{3.11}$$

where τ_1 and τ_2 are supplied torques from actuators, the Lagrange's equation of both links are

$$\frac{d}{dt}\frac{\partial L}{\partial \dot{q}_1} - \frac{\partial L}{\partial q_1} = \tau_1 \tag{3.12}$$

$$\frac{d}{dt}\frac{\partial L}{\partial \dot{q}_2} - \frac{\partial L}{\partial q_2} = \tau_2. \tag{3.13}$$

According to Lagrange's equation, the dynamic models of the manipulator are given by the two coupled nonlinear differential equations as

$$\begin{aligned}\tau_1 = {} & (m_1 a_1^2 + m_2 \ell_1^2 + m_2 a_2^2 + 2m_2 \ell_1 a_2 c_2)\ddot{q}_1 + (m_2 a_2^2 + m_2 \ell_1 a_2 c_2)\ddot{q}_2 \\ & - m_2 \ell_1 a_2 s_2 (2\dot{q}_1 \dot{q}_2 + \dot{q}_2^2)\end{aligned} \tag{3.14}$$

$$\tau_2 = (m_2 a_2^2 + m_2 \ell_1 a_2 c_2)\ddot{q}_1 + m_2 a_2^2 \ddot{q}_2 + m_2 \ell_1 a_2 s_2 \dot{q}_1^2 \tag{3.15}$$

where $\dot{q}_1$ and $\dot{q}_2$ are joint velocities of the 1st and the 2nd link, and $\ddot{q}_1$ and $\ddot{q}_2$ are joint accelerations of the 1st and the 2nd link. The simple form of τ_1 and τ_2 in equations (3.14) and (3.15) can be written as

$$\tau_1 = (J_1 + J_2 + 2rc_2)\ddot{q}_1 + (J_2 + 2rc_2)\ddot{q}_2 - rs_2(2\dot{q}_1\dot{q}_2 + \dot{q}_2^2) \tag{3.16}$$

$$\tau_2 = (J_2 + 2rc_2)\ddot{q}_1 + J_2\ddot{q}_2 + rs_2\dot{q}_1^2 \tag{3.17}$$

where $J_1 = m_1 a_1^2 + m_2 \ell_1^2$, $J_2 = m_2 a_2^2$ and $r = m_2 \ell_1 a_2$. The manipulator dynamic equations may be written in standard form as

$$\mathbf{M}(\mathbf{q})\ddot{\mathbf{q}} + \mathbf{V}(\mathbf{q}, \dot{\mathbf{q}}) = \boldsymbol{\tau} \tag{3.18}$$

where $\mathbf{q} \in R^2$ is joint variable vector, $\mathbf{M}(\mathbf{q})$ is the inertia matrix and $\mathbf{V}(\mathbf{q}, \dot{\mathbf{q}})$ is the Coriolis/centripetal torque vector. The parameters in $\mathbf{M}(\mathbf{q})$ and $\mathbf{V}(\mathbf{q}, \dot{\mathbf{q}})$ are

$$\mathbf{M}(\mathbf{q}) = \begin{bmatrix} J_1 + J_2 + 2rc_2 & J_2 + rc_2 \\ J_2 + rc_2 & J_2 \end{bmatrix} \tag{3.19}$$

and

$$\mathbf{V}(\mathbf{q}, \dot{\mathbf{q}}) = \begin{bmatrix} -2rs_2\dot{q}_1\dot{q}_2 - rs_2\dot{q}_2^2 \\ rs_2\dot{q}_1^2 \end{bmatrix}. \tag{3.20}$$

3.2.3 Actuator Dynamics

The dynamics of the robot manipulator in joint space and Cartesian coordinates are described in section 3.2.2. However, the robot manipulator needs actuators to move it. The actuator dynamics will be added to the robot manipulator dynamics to obtain the complete dynamic description of the robot manipulator.

By assuming that the actuators are ideal servos, there is no loss in the power transmutation circuit, and the frictions of the rotors are neglected. Then the dynamics of the actuators is given by [13]

$$\mathbf{J}_M \ddot{\mathbf{q}}_M + \mathbf{B}_M \dot{\mathbf{q}}_M + \boldsymbol{\tau} = \mathbf{K}_M \mathbf{v} \tag{3.21}$$

where $\mathbf{q}_M = vec\{q_{Mi}\}$, with q_{Mi} the angular position of the i^{th} rotor, $\dot{\mathbf{q}}_M = vec\{\dot{q}_{Mi}\}$, with $\dot{q}_{Mi}$ the angular velocity of the i^{th} rotor and $\ddot{\mathbf{q}}_M = vec\{\ddot{q}_{Mi}\}$, with $\ddot{q}_{Mi}$ the angular acceleration of the i^{th} rotor. $\mathbf{v} \in R^2$ is the current command voltage vector. The actuator coefficient matrices are all constants and are given by

$$\mathbf{J}_M = diag\{J_{Mi}\} \tag{3.22}$$

$$\mathbf{B}_M = diag\{B_{Mi}\} \tag{3.23}$$

$$\mathbf{R} = diag\{r_i\} \tag{3.24}$$

$$\mathbf{K}_M = diag\{K_{Mi}\} \tag{3.25}$$

where J_{Mi} is moment of inertia of the i^{th} motor, B_{Mi} is the rotor damping constant of the i^{th} motor and K_{Mi} is torque constant of the i^{th} motor.

The gear ratio of the coupling from the i^{th} motor to the i^{th} link is r_i. Here, the relation between q and q_M can be express as

$$q_i = r_i q_{Mi} \quad \text{or} \quad \mathbf{q} = \mathbf{R}\mathbf{q}_M . \tag{3.26}$$

3.2.4 Complete Dynamics

Since the robot used in the experiment is direct drive robot that has no gear, therefore the gear ratios are equal to one. By substituting τ from the equation (3.18) to actuator dynamics in

equation (3.21), the complete dynamics of the two-link robot manipulator plus actuators can be found by

$$(\mathbf{J}_M + \mathbf{M}(\mathbf{q}))\ddot{\mathbf{q}} + (\mathbf{B}_M\dot{\mathbf{q}} + \mathbf{V}(\mathbf{q},\dot{\mathbf{q}})) = \mathbf{K}_M\mathbf{v} \tag{3.27}$$

or

$$\tilde{\mathbf{M}}(\mathbf{q})\ddot{\mathbf{q}} + \tilde{\mathbf{V}}(\mathbf{q},\dot{\mathbf{q}}) = \mathbf{K}_M\mathbf{v} \tag{3.28}$$

where

$$\tilde{\mathbf{M}}(\mathbf{q}) = \begin{bmatrix} J_1 + J_2 + J_{M1} + 2rc_2 & J_2 + rc_2 \\ J_2 + rc_2 & J_2 + J_{M2} \end{bmatrix}$$

$$\tilde{\mathbf{V}}(\mathbf{q},\dot{\mathbf{q}}) = \begin{bmatrix} -r(2\dot{q}_1\dot{q}_2 + \dot{q}_2^2)s_2 + B_{M1}\dot{q}_1 \\ rs_2\dot{q}_1^2 + B_{M2}\dot{q}_2 \end{bmatrix}.$$

Solving for $\ddot{\mathbf{q}}$, yields

$$\ddot{\mathbf{q}} = -\tilde{\mathbf{M}}^{-1}(\mathbf{q})\tilde{\mathbf{V}}(\mathbf{q},\dot{\mathbf{q}}) + \tilde{\mathbf{M}}^{-1}\mathbf{K}_M\mathbf{v}, \tag{3.29}$$

or

$$\ddot{q}_1 = \frac{-(J_2 + rc_2)\left(-rs_2\dot{q}_1^2 - B_{M2}\dot{q}_2 + K_{M2}v_2\right)}{J_1J_2 + J_{M1}J_2 + J_1J_{M2} + J_2J_{M2} + J_{M1}J_{M2} + 2J_{M2}rc_2 - r^2c_2^2} + \frac{(J_2 + J_{M2})\left(r(2\dot{q}_1\dot{q}_2 + \dot{q}_2^2)s_2 - B_{M1}\dot{q}_1 - K_{M1}v_1\right)}{J_1J_2 + J_{M1}J_2 + J_1J_{M2} + J_2J_{M2} + J_{M1}J_{M2} + 2J_{M2}rc_2 - r^2c_2^2}$$

$$\ddot{q}_2 = \frac{-(J_2 + rc_2)\left(r(2\dot{q}_1\dot{q}_2 + \dot{q}_2^2)s_2 - B_{M1}\dot{q}_1 + K_{M1}v_1\right)}{J_1J_2 + J_{M1}J_2 + J_1J_{M2} + J_2J_{M2} + J_{M1}J_{M2} + 2J_{M2}rc_2 - r^2c_2^2} - \frac{(J_1 + J_2 + J_{M1} + 2rc_2)\left(rs_2\dot{q}_1^2 - B_{M2}\dot{q}_2 + K_{M2}v_2\right)}{J_1J_2 + J_{M1}J_2 + J_1J_{M2} + J_2J_{M2} + J_{M1}J_{M2} + 2J_{M2}rc_2 - r^2c_2^2}.$$

The state-space formulations of the robot manipulator dynamics can be obtained by defining the angular position/velocity state as

$$\mathbf{x} = \begin{bmatrix} q_1 & q_2 & \dot{q}_1 & \dot{q}_2 \end{bmatrix}. \tag{3.30}$$

Then the nonlinear angular position/velocity state-space can be obtained as

$$\dot{\mathbf{x}} = \mathbf{f}(\mathbf{x},\mathbf{u})$$
$$\mathbf{y} = \mathbf{h}(\mathbf{x})$$

where

$$\mathbf{f}(\mathbf{x},\mathbf{u}) = \begin{bmatrix} \dot{\mathbf{q}} \\ -\tilde{\mathbf{M}}^{-1}(\mathbf{q})\tilde{\mathbf{V}}(\mathbf{q},\dot{\mathbf{q}}) \end{bmatrix} + \begin{bmatrix} \mathbf{0} \\ \tilde{\mathbf{M}}^{-1}(\mathbf{q}) \end{bmatrix} \mathbf{K}_m \mathbf{v}$$
$$\mathbf{h}(\mathbf{x}) = \begin{bmatrix} \mathbf{I} & \mathbf{0} \end{bmatrix} \mathbf{x}.$$

3.2.5 Linearization

Since the manipulator system is nonlinear system, it must be linearized in order to design the controller easily.. The linear equation of motion at the initial state $\mathbf{u}_0 = \mathbf{0}$ and $\mathbf{x}_0 = \begin{bmatrix} 0 & 0 & 0 & 0 \end{bmatrix}^T$ is given by

$$\begin{aligned} \dot{\mathbf{x}} &= \mathbf{A}\mathbf{x} + \mathbf{B}\mathbf{u} \\ \mathbf{y} &= \mathbf{C}\mathbf{x} \end{aligned} \tag{3.31}$$

where

$$\mathbf{A} = \left. \frac{\partial \mathbf{f}(\mathbf{x},\mathbf{u})}{\partial x} \right|_{\mathbf{x}=\mathbf{x}_0, \mathbf{u}=\mathbf{u}_0}$$

$$\mathbf{B} = \left. \frac{\partial \mathbf{f}(\mathbf{x},\mathbf{u})}{\partial u} \right|_{\mathbf{x}=\mathbf{x}_0, \mathbf{u}=\mathbf{u}_0} \tag{3.32}$$

$$\mathbf{C} = \mathbf{h}(\mathbf{x}).$$

From equations (3.31),

$$\mathbf{A} = \begin{bmatrix} 0 & 0 & 1 & 0 \\ 0 & 0 & 0 & 1 \\ 0 & 0 & a_{33} & a_{34} \\ 0 & 0 & a_{43} & a_{44} \end{bmatrix}, \quad \mathbf{B} = \begin{bmatrix} 0 & 0 \\ 0 & 0 \\ b_{31} & b_{32} \\ b_{41} & b_{42} \end{bmatrix} \text{ and } \mathbf{C} = \begin{bmatrix} 1 & 0 & 0 & 0 \\ 0 & 1 & 0 & 0 \end{bmatrix}$$

are obtained where

$$a_{33} = \frac{(J_{m2} + J_2)B_{m1}}{-J_{m1}J_{m2} - J_{m1}J_2 - J_1J_{m2} - J_1J_2 - J_2J_{m2} - 2rJ_{m2} + r^2}$$

$$a_{34} = \frac{-(J_2 + r)B_{m2}}{-J_{m1}J_{m2} - J_{m1}J_2 - J_1J_{m2} - J_1J_2 - J_2J_{m2} - 2rJ_{m2} + r^2}$$

$$a_{43} = \frac{(-J_2 - r)B_{m1}}{-J_{m1}J_{m2} - J_{m1}J_2 - J_1J_{m2} - J_1J_2 - J_2J_{m2} - 2rJ_{m2} + r^2}$$

$$a_{44} = \frac{J_{m1} + J_1 + J_2 + 2r}{-J_{m1}J_{m2} - J_{m1}J_2 - J_1J_{m2} - J_1J_2 - J_2J_{m2} - 2rJ_{m2} + r^2}$$

$$b_{31} = \frac{(J_{m2} + j_2)K_{m1}}{-J_{m1}J_{m2} - J_{m1}J_2 - J_1J_{m2} - J_1J_2 - J_2J_{m2} - 2rJ_{m2} + r^2}$$

$$b_{32} = \frac{(-j_2 - r)K_{m2}}{-J_{m1}J_{m2} - J_{m1}J_2 - J_1J_{m2} - J_1J_2 - J_2J_{m2} - 2rJ_{m2} + r^2}$$

$$b_{41} = \frac{(-j_2 - r)K_{m1}}{-J_{m1}J_{m2} - J_{m1}J_2 - J_1J_{m2} - J_1J_2 - J_2J_{m2} - 2rJ_{m2} + r^2}$$

$$b_{42} = \frac{(J_{m1} + j_1 + j_2 + 2r)K_{m2}}{-J_{m1}J_{m2} - J_{m1}J_2 - J_1J_{m2} - J_1J_2 - J_2J_{m2} - 2rJ_{m2} + r^2}.$$

The transfer matrix in s domain of the equation (3.31) is given by

$$\mathbf{P}(s) = \frac{\mathbf{Y}(s)}{\mathbf{U}(s)} = \mathbf{C}(s\mathbf{I} - \mathbf{A})^{-1}\mathbf{B} = \begin{bmatrix} P_{11}(s) & P_{12}(s) \\ P_{21}(s) & P_{22}(s) \end{bmatrix} \tag{3.33}$$

where $P_{11}(s) = \dfrac{(s - a_{44})b_{31} + a_{34}b_{41}}{s(s^2 - sa_{44} - a_{33}s + a_{33}a_{44} - a_{34}a_{43})}$

$$P_{12}(s) = \frac{(s - a_{44})b_{32} + a_{34}b_{42}}{s(s^2 - sa_{44} - a_{33}s + a_{33}a_{44} - a_{34}a_{43})}$$

$$P_{21}(s) = \frac{(s - a_{33})b_{41} + a_{43}b_{31}}{s(s^2 - sa_{44} - a_{33}s + a_{33}a_{44} - a_{34}a_{43})}$$

$$P_{22}(s) = \frac{(s - a_{33})b_{42} + a_{43}b_{32}}{s(s^2 - sa_{44} - a_{33}s + a_{33}a_{44} - a_{34}a_{43})}.$$

3.2.6 Parameter Identification

When the effects of the coupling of the 1st link and 2nd link are neglected, the linear models or independent joint dynamics can be obtained by rewriting the complete dynamics with two components as

$$(J_{M1} + J_1 + J_2 + 2rc_2)\ddot{q}_1 + B_{M1}\dot{q}_1 = K_{M1}v_1 \tag{3.34}$$

$$(J_{M2} + J_2)\ddot{q}_1 + B_{M2}\dot{q}_2 = K_{M2}v_2, \tag{3.35}$$

where v_1 and v_2 are the current command voltages. Taking the Laplace transform of equations (3.34) and (3.35), respectively, with zero initial conditions, then

$$(J_{M1} + J_1 + J_2 + 2r)s^2Q_1(s) + B_{M1}sQ_1(s) = K_{M1}V_1(s) \tag{3.36}$$

$$(J_{M2} + J_2)s^2Q_2(s) + B_{M2}sQ_1(s) = K_{M2}V_2(s) \tag{3.37}$$

are obtained. Finally, the linear transfer functions between the current command voltages and output angular positions for the 1st and the 2nd link are respectively obtained as follows:

$$\frac{Q_1(s)}{V_1(s)} = \frac{K_{M1}/B_{M1}}{s\left((T_1s+1)\right)} \tag{3.38}$$

$$\frac{Q_2(s)}{V_2(s)} = \frac{K_{M2}/B_{M2}}{s\left((T_2s+1)\right)} \tag{3.39}$$

where $T_1 = (J_{M1} + J_1 + J_2 + 2r)/B_{M1}$ and $T_2 = (J_{M2} + J_2)/B_{M2}$.

For the 1st link, applying the step input of the current command voltage $V_1(s) = \frac{V_C}{s}$ to the 1st joint, its output can be obtained as

$$Q_1(s) = \frac{K_{M1}}{s\left(M_1s + B_{M1}\right)}\frac{V_c}{s}, \tag{3.40}$$

where V_c is the magnitude of the step input of the current command voltage and $M_1 = T_{M1} \cdot B_{M1}$. Expanding $Q_1(s)$ into partial fractions gives

$$Q_1(s) = \frac{K_{M1}V_c}{B_{M1}}\left[\frac{1}{s^2} - T\frac{1}{s} + \frac{T^2}{Ts+1}\right], \tag{3.41}$$

and taking the inverse Laplace transform of equation (3.41), yields

$$q_1(t) = \frac{K_{M1}V_c}{B_{M1}}\left[t - T + Te^{-t/T}\right], \text{ for } t \geq 0. \tag{3.42}$$

The response curve of equation (3.42) to the step input is shown in figure 3.3. As t approaches infinity, the equation for the steady-state response q_{ss} can be written by

$$q_{ss} = \frac{K_{M1}V_c}{B_{M1}}(t - T). \tag{3.43}$$

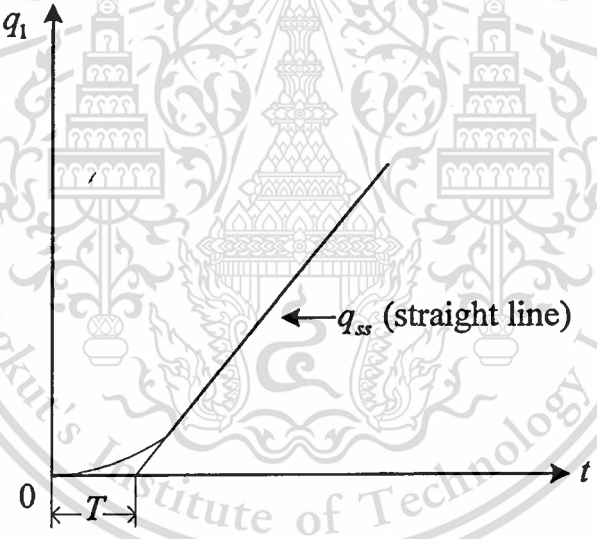

Figure 3.3 Response to step input of the current command voltage.

From equation (3.43),

(1) The straight line q_{ss} extrapolated back to $q_1 = 0$ and intersects the time axis at $t = T$. Thus, T can be found first.

(2) The slider mass M_1 is generally defined by a designer since motor mounting procedure. From equation (3.43), B_{M1} can be found.

(3) From the slope of the steady-state response, q_{ss}, $\left(\frac{K_{M1}V_{c1}}{B_{M1}}\right)$ and K_{M1} can be found.

For the 2nd link, K_{M2} can also be found by using the same manner state above.

The torque constants K_{M1} and K_{M2} can be found from the experiments and are used for obtaining the linear models of the two-link robot manipulator. The linear models will give the relation between the input voltages and the output angular positions which are necessary for assigning the controller gains in chapter 5.

Chapter 4

Mamdani Fuzzy I-PD Controller Design

In this chapter, the Mamdani fuzzy I-PD controller structure which is the modification of the conventional I-PD controller, fuzzy controller design, the output change analysis and stability analysis will be described respectively. Since the structure of the fuzzy controller for each link of the manipulator is same structure, the following details for designing the fuzzy controller will be shown for controlling either the 1st link or the 2nd link of the robot manipulator to follow the desired trajectory without steady-state error.

4.1 Conventional I-PD Controller Structure

The conventional I-PD control system which consists of a plant, an integral controller and a PD feedback controller is shown in figure 4.1. Here, K_i is the integral gain of the integral controller, and K_p and K_d are the proportional gain and derivative gain of the PD feedback controller, respectively.

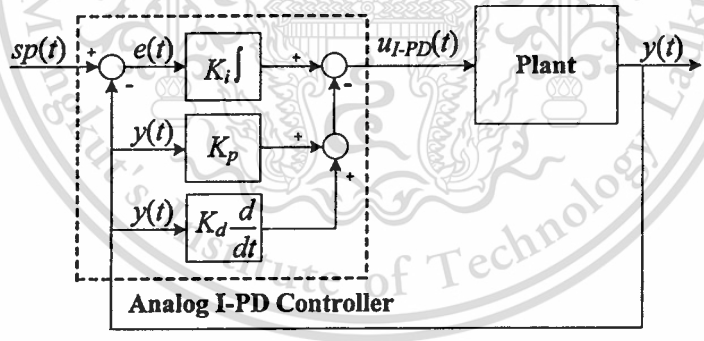

Figure 4.1 Conventional I-PD control system structure.

The control signal of the conventional I-PD controller of the control system shown in figure 4.1 can be expressed as

$$u_{I-PD}(t) = K_i \int_0^t e(t)dt - K_p y(t) - K_d \frac{dy(t)}{dt}. \tag{4.1}$$

After taking Lapalce transform of equation (4.1), it becomes

$$U_{I-PD}(s) = \frac{K_I}{s}E(s) - K_p Y(s) - K_d sY(s) \tag{4.2}$$

where

$$U_I(s) = \frac{K_I}{s}E(s) \tag{4.3}$$

and

$$U_{PD}(s) = K_p Y(s) + K_d sY(s). \tag{4.4}$$

4.2 Mamdani Fuzzy I-PD Controller Structure

The structure of the fuzzy I-PD controller, which is the modification of the conventional I-PD controller structure, will be described in this section.

By approximating the equation (4.3) with the trapezoidal formula, the output of Mamdani fuzzy I controller $u_I(nT)$ can be computed as

$$u_I(nT) = K_1 e(nT) - K_2 \Delta e(nT) + u_I(nT - T), \tag{4.5}$$

where the error $e(nT) = sp(nT) - y(nT)$, the change of error $\Delta e(nT) = e(nT) - e(nT - T)$, $K_1 = K_i T$, $K_2 = K_i T/2$ and T denotes to the sampling time.

In the same manner, the output of Mamdani fuzzy PD controller $u_{PD}(nT)$ can be directly computed from equation (4.4) by approximating the derivative term with two-point difference form. Then

$$u_{PD}(nT) = K_3 y(nT) + K_4 \Delta y(nT) \tag{4.6}$$

can be obtained, where $y(nT)$ is the output, $\Delta y(nT)$ is the change of output, $K_3 = K_p$ and $K_4 = K_d/T$. As the result of equations (4.5) and (4.6), the output of digital I-PD controller $u_{I-PD}(nT)$ can be obtained by

$$u_{I-PD}(nT) = K_1 e(nT) - K_2 \Delta e(nT) + u_I(nT - T) - K_3 y(nT) - K_4 \Delta y(nT) \tag{4.7}$$

or

$$u_{I-PD}(nT) = u_I(nT) - u_{PD}(nT), \tag{4.8}$$

and the structure of digital I-PD control system can be illustrated as shown in figure 4.2.

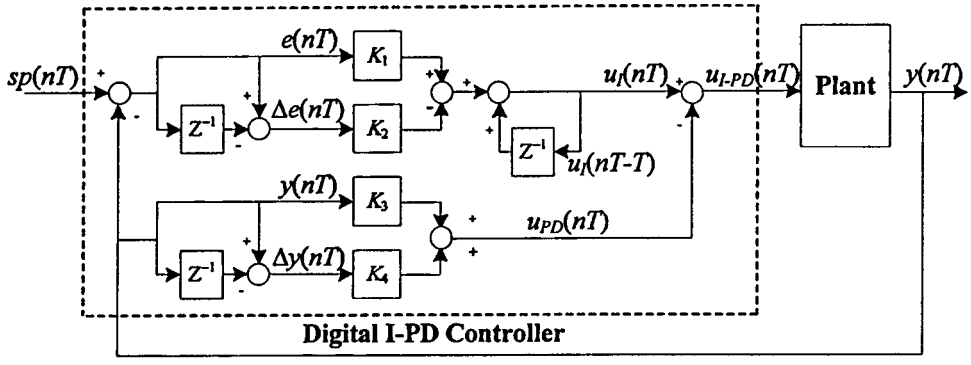

Figure 4.2 Digital I-PD control system structure.

When the term $K_1e(nT)-K_2\Delta e(nT)$ is replaced by the output change $\Delta u_I(nT)$ of the fuzzy I controller, the control signal of fuzzy I controller is given by

$$u_I(nT)=\Delta u_I(nT)+u_I(nT-T), \tag{4.9}$$

and when the term $K_3y(nT)+K_4\Delta y(nT)$ is replaced by the output change $\Delta u_{PD}(nT)$ of the fuzzy PD controller, the control signal of fuzzy PD controller is obtained as

$$u_{I-PD}(nT)=\Delta u_{PD}(nT). \tag{4.10}$$

Consequently, the control signal of the fuzzy I-PD controller shown in figure 4.3 can be expressed as follows:

$$u_{I-PD}(nT)=\Delta u_I(nT)+u_I(nT-T)-\Delta u_{PD}(nT). \tag{4.11}$$

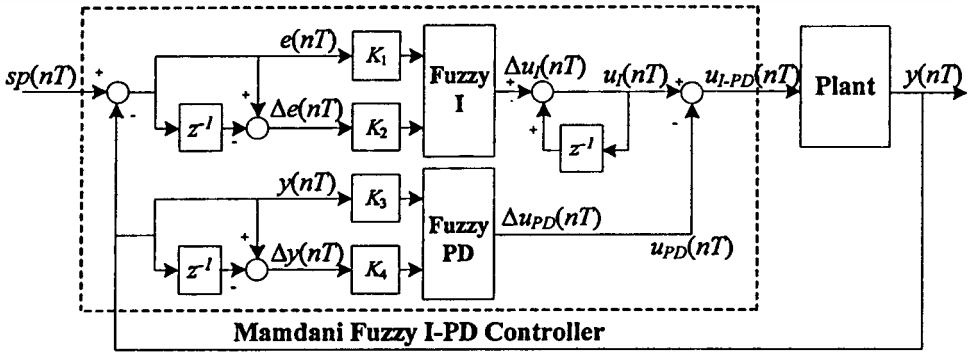

Figure 4.3 Mamdani Fuzzy I-PD control system structure.

4.3 Fuzzy Controller Design

Fuzzy logic controller described in chapter 2 consists of fuzzification, fuzzy rules, fuzzy inference and defuzzifier. In the fuzzification stage, the membership functions used for calculating the membership values for the inputs of fuzzy I controller $\left(K_1 e(nT)\right.$ and $\left.K_2 \Delta e(nT)\right)$ and fuzzy PD controller $\left(K_3 y(nT)\right.$ and $\left.K_4 \Delta y(nT)\right)$ are similarly defined as shown in figure 4.4 and 4.5. For the controller outputs $\Delta u_I(nT)$ and $\Delta u_{PD}(nT)$, the output membership functions are defined by using fuzzy singletons as shown in figure 4.5 and figure 4.6, respectively.

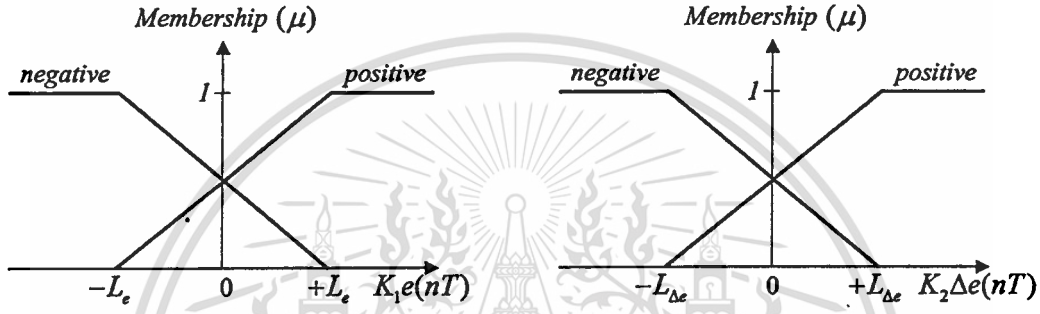

(a) Membership functions of $K_1 e(nT)$. (b) Membership functions of $K_2 \Delta e(nT)$.

Figure 4.4 Input membership functions for fuzzy I controller.

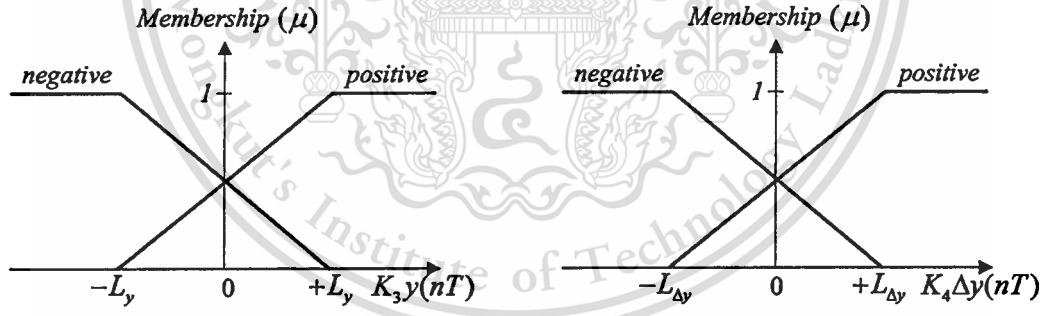

(a) Membership functions of $K_3 y(nT)$. (b) Membership functions of $K_4 \Delta y(nT)$.

Figure 4.5 Input membership functions for fuzzy PD controller.

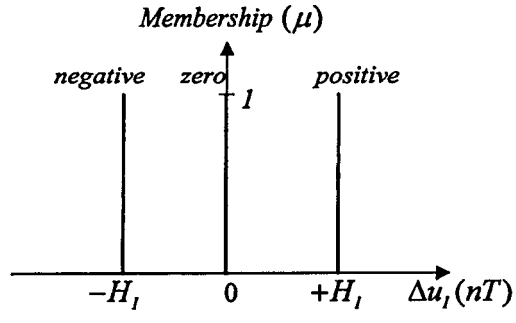

Figure 4.6 Output membership functions for fuzzy I controller.

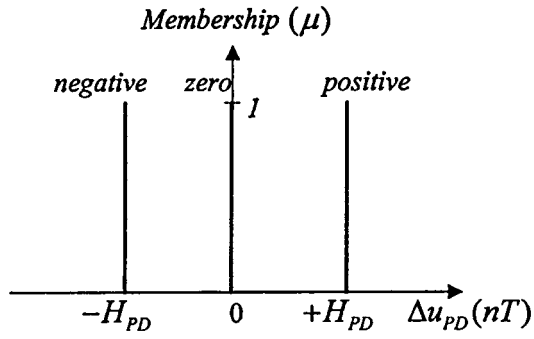

Figure 4.7 Output membership functions for fuzzy PD controller.

Referring to figures 4.4 and 4.5, the input membership functions for the 1st link and the 2nd link of the robot manipulator can be written as

$$\mu_{en} = \begin{cases} 1 & ;(-\infty, -L_e] \\ \dfrac{L_e - K_1 e(nT)}{2L_e} & ;[-L_e, L_e] \\ 0 & ;[+L_e, +\infty) \end{cases} ; \mu_{ep} = \begin{cases} 0 & ;(-\infty, -L_e] \\ \dfrac{L_e + K_1 e(nT)}{2L_e} & ;[-L_e, L_e] \\ 1 & ;[+L_e, +\infty) \end{cases}$$

$$\mu_{\Delta en} = \begin{cases} 1 & ;(-\infty, -L_{\Delta e}] \\ \dfrac{L_{\Delta e} - K_2 \Delta e(nT)}{2L_{\Delta e}} & ;[-L_{\Delta e}, L_{\Delta e}] \\ 0 & ;[+L_{\Delta e}, +\infty) \end{cases} ; \mu_{\Delta ep} = \begin{cases} 0 & ;(-\infty, -L_{\Delta e}] \\ \dfrac{L_{\Delta e} + K_2 \Delta e(nT)}{2L_{\Delta e}} & ;[-L_{\Delta e}, L_{\Delta e}] \\ 1 & ;[+L_{\Delta e}, +\infty) \end{cases}$$

$$\mu_{yn} = \begin{cases} 1 & ;(-\infty, -L_y] \\ \dfrac{L_y - K_3 y(nT)}{2L_y} & ;[-L_y, L_y] \\ 0 & ;[+L_y, +\infty) \end{cases} ; \mu_{yp} = \begin{cases} 0 & ;(-\infty, -L_y] \\ \dfrac{L_y + K_3 y(nT)}{2L_y} & ;[-L_y, L_y] \\ 1 & ;[+L_y, +\infty) \end{cases}$$

$$\mu_{\Delta yn} = \begin{cases} 1 & ;(-\infty, -L_{\Delta y}] \\ \dfrac{L_{\Delta y} - K_4 \Delta y(nT)}{2L_y} & ;[-L_{\Delta y}, L_{\Delta y}] \\ 0 & ;[+L_{\Delta y}, +\infty) \end{cases} ; \mu_{\Delta yp} = \begin{cases} 0 & ;(-\infty, -L_{\Delta y}] \\ \dfrac{L_{\Delta y} + K_4 \Delta y(nT)}{2L_{\Delta y}} & ;[-L_{\Delta y}, L_{\Delta y}] \\ 1 & ;[+L_{\Delta y}, +\infty) \end{cases}$$

where $\mu_{en}(nT)$ is a fuzzy set called "error negative",

$\mu_{ep}(nT)$ is a fuzzy set called "error positive",

$\mu_{\Delta en}(nT)$ is a fuzzy set called "change of error negative",

$\mu_{\Delta ep}(nT)$ is a fuzzy set called "change of error positive",

$\mu_{yn}(nT)$ is a fuzzy set called "output negative",

$\mu_{yp}(nT)$ is a fuzzy set called "output positive",

$\mu_{\Delta yn}(nT)$ is a fuzzy set called "change of output negative",

$\mu_{\Delta yp}(nT)$ is a fuzzy set called "change of output positive",

L_e, $L_{\Delta e}$, L_y, $L_{\Delta y}$, H_I and H_{PD} are adjustable constants of fuzzy I-PD controller.

Based on the input membership functions in fuzzification stage and the output membership functions shown in figures 4.6 and 4.7, the Mamdani fuzzy rules for the fuzzy I controller are

(R1): IF $K_1 e(nT)$ is *negative* AND $K_2 \Delta e(nT)$ is *negative* THEN $\Delta u_{I_1}(nT)$ is *negative*
(R2): IF $K_1 e(nT)$ is *negative* AND $K_2 \Delta e(nT)$ is *positive* THEN $\Delta u_{I_2}(nT)$ is *zero*
(R3): IF $K_1 e(nT)$ is *positive* AND $K_2 \Delta e(nT)$ is *negative* THEN $\Delta u_{I_3}(nT)$ is *zero* (4.12)
(R4): IF $K_1 e(nT)$ is *positive* AND $K_2 \Delta e(nT)$ is *positive* THEN $\Delta u_{I_4}(nT)$ is *positive*.

Similar rules are also applied for assigning the fuzzy PD controller. Hence,

(R1): IF $K_3 y(nT)$ is *negative* AND $K_4 \Delta y(nT)$ is *negative* THEN $\Delta u_{PD_1}(nT)$ is *negative*
(R2): IF $K_3 y(nT)$ is *negative* AND $K_4 \Delta y(nT)$ is *positive* THEN $\Delta u_{PD_2}(nT)$ is *zero*
(R3): IF $K_3 y(nT)$ is *positive* AND $K_4 \Delta y(nT)$ is *negative* THEN $\Delta u_{PD_3}(nT)$ is *zero* (4.13)
(R4): IF $K_3 y(nT)$ is *positive* AND $K_4 \Delta y(nT)$ is *positive* THEN $\Delta u_{PD_4}(nT)$ is *positive*.

Since Mamdani fuzzy rules are used for designing the fuzzy I-PD controller, the proposed controller will be called as "Mamdani fuzzy I-PD controller" in this thesis.

The centroid defuzzifier is used to calculate the output change $\Delta u_I(nT)$ of the Mamdani fuzzy I controller and $\Delta u_{PD}(nT)$ of the Mamdani fuzzy PD controller. The defuzzification results are respectively obtained from

$$\Delta u_I(nT) = \frac{\sum_{r=1}^{4} \Delta u_{I_r} \cdot \mu_{I_r}}{\sum_{r=1}^{4} \mu_{I_r}} \tag{4.14}$$

and

$$\Delta u_{PD}(nT) = \frac{\sum_{r=1}^{4} \Delta u_{PD_r} \cdot \mu_{PD_r}}{\sum_{r=1}^{4} \mu_{PD_r}}, \tag{4.15}$$

where Δu_{I_r} and Δu_{PD_r} are the output singletons, and μ_{I_r} and μ_{PD_r} are the membership values for the r^{th} rule.

4.4 Analysis of the Changes of Fuzzy Controller Output

Figure 4.8 and figure 4.9 show the input spaces of Mamdani fuzzy I and Mamdani fuzzy PD controller that each controller can be decomposed into 12 different input spaces (ICs).

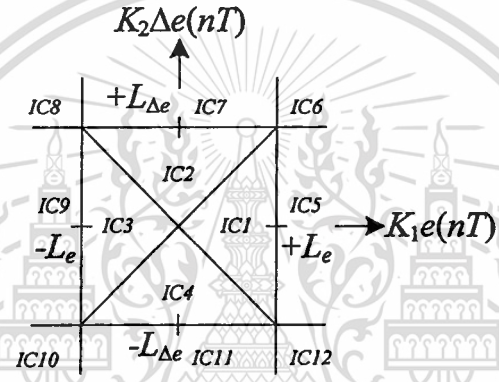

Figure 4.8 Input spaces of Mamdani fuzzy I controller.

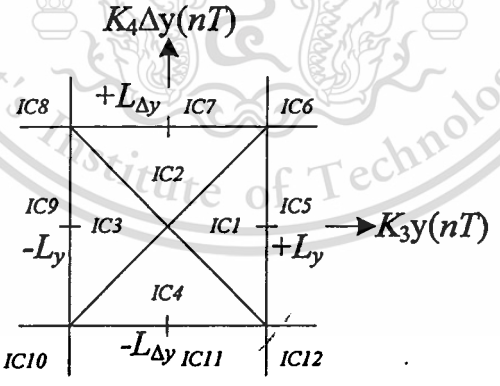

Figure 4.9 Input spaces of Mamdani fuzzy PD controller.

In order to calculate the output change, the input membership value in each IC must be found. For the input space IC1 in figure 4.8, the membership value μ_{I_1} for the rule (R1) shown in equation (4.12) can be found by interfering the input linguistic variables with Mamdani minimum inference method. The remaining of the membership values of μ_{I_2}, μ_{I_3} and μ_{I_4} can be obtained

in the same manner of μ_{I_1}. Consequently, the following membership values are obtained and can be expressed as follows:

$$(R1)\ \mu_{I_1} = \min\{\mu_{en}, \mu_{\Delta en}\} = \min\left\{\frac{L_e - K_1 e(nT)}{2L_e}, \frac{L_{\Delta e} - K_2 \Delta e(nT)}{2L_{\Delta e}}\right\} = \frac{L_e - K_1 e(nT)}{2L_e}$$

$$(R2)\ \mu_{I_2} = \min\{\mu_{en}, \mu_{\Delta ep}\} = \min\left\{\frac{L_e - K_1 e(nT)}{2L_e}, \frac{L_{\Delta e} + K_2 \Delta e(nT)}{2L_{\Delta e}}\right\} = \frac{L_e - K_1 e(nT)}{2L_e}$$

$$(R3)\ \mu_{I_3} = \min\{\mu_{ep}, \mu_{\Delta en}\} = \min\left\{\frac{L_e + K_1 e(nT)}{2L_e}, \frac{L_{\Delta e} - K_2 \Delta e(nT)}{2L_{\Delta e}}\right\} = \frac{L_{\Delta e} - K_2 \Delta e(nT)}{2L_{\Delta e}}$$

$$(R4)\ \mu_{I_4} = \min\{\mu_{ep}, \mu_{\Delta ep}\} = \min\left\{\frac{L_e + K_1 e(nT)}{2L_e}, \frac{L_{\Delta e} + K_2 \Delta e(nT)}{2L_{\Delta e}}\right\} = \frac{L_{\Delta e} + K_2 \Delta e(nT)}{2L_{\Delta e}}.$$

For the remaining input space ICs, the corresponding input membership values for each rule can be obtained in the same manner as input space IC1. Hence, the expression of input membership values for the Mamdani fuzzy I and PD controllers are summarized in the Table 4.1 and 4.2, respectively.

Table 4.1 Input Membership Values of Mamdani Fuzzy I Controller in IC1 to IC12.

#IC	μ_{I_1}	μ_{I_2}	μ_{I_3}	μ_{I_4}
IC1	$\frac{L_e - K_1 e(nT)}{2L_e}$	$\frac{L_e - K_1 e(nT)}{2L_e}$	$\frac{L_{\Delta e} - K_2 e(nT)}{2L_{\Delta e}}$	$\frac{L_{\Delta e} + K_2 e(nT)}{2L_{\Delta e}}$
IC2	$\frac{L_{\Delta e} - K_2 e(nT)}{2L_{\Delta e}}$	$\frac{L_e - K_1 e(nT)}{2L_e}$	$\frac{L_{\Delta e} - K_2 e(nT)}{2L_{\Delta e}}$	$\frac{L_e + K_1 e(nT)}{2L_e}$
IC3	$\frac{L_{\Delta e} - K_2 e(nT)}{2L_{\Delta e}}$	$\frac{L_{\Delta e} + K_2 e(nT)}{2L_{\Delta e}}$	$\frac{L_e + K_1 e(nT)}{2L_e}$	$\frac{L_e + K_1 e(nT)}{2L_e}$
IC4	$\frac{L_e - K_1 e(nT)}{2L_e}$	$\frac{L_{\Delta e} + K_2 e(nT)}{2L_{\Delta e}}$	$\frac{L_e + K_1 e(nT)}{2L_e}$	$\frac{L_{\Delta e} + K_2 e(nT)}{2L_{\Delta e}}$
IC5	0	0	$\frac{L_{\Delta e} - K_2 e(nT)}{2L_{\Delta e}}$	$\frac{L_{\Delta e} + K_2 e(nT)}{2L_{\Delta e}}$
IC6	0	0	0	1
IC7	0	$\frac{L_e - K_1 e(nT)}{2L_e}$	0	$\frac{L_e + K_1 e(nT)}{2L_e}$
IC8	0	1	0	0
IC9	$\frac{L_{\Delta e} - K_2 e(nT)}{2L_{\Delta e}}$	$\frac{L_{\Delta e} + K_2 e(nT)}{2L_{\Delta e}}$	0	0
IC10	1	0	0	0
IC11	$\frac{L_e - K_1 e(nT)}{2L_e}$	0	$\frac{L_e + K_1 e(nT)}{2L_e}$	0
IC12	0	0	1	0

Table 4.2 Input Membership Values of Mamdani Fuzzy PD Controller in IC1 to IC12.

#IC	μ_{PD_1}	μ_{PD_2}	μ_{PD_3}	μ_{PD_4}
IC1	$\frac{L_y - K_3 y(nT)}{2L_y}$	$\frac{L_y - K_3 y(nT)}{2L_y}$	$\frac{L_{\Delta y} - K_4 \Delta y(nT)}{2L_{\Delta y}}$	$\frac{L_{\Delta y} + K_4 \Delta y(nT)}{2L_{\Delta y}}$
IC2	$\frac{L_{\Delta y} - K_4 \Delta y(nT)}{2L_{\Delta y}}$	$\frac{L_y - K_3 y(nT)}{2L_y}$	$\frac{L_{\Delta y} - K_4 \Delta y(nT)}{2L_{\Delta y}}$	$\frac{L_y + K_3 y(nT)}{2L_y}$
IC3	$\frac{L_{\Delta y} - K_4 \Delta y(nT)}{2L_{\Delta y}}$	$\frac{L_{\Delta y} + K_4 \Delta y(nT)}{2L_{\Delta y}}$	$\frac{L_y + K_3 y(nT)}{2L_y}$	$\frac{L_y + K_3 y(nT)}{2L_y}$
IC4	$\frac{L_y - K_3 y(nT)}{2L_y}$	$\frac{L_{\Delta y} + K_4 \Delta y(nT)}{2L_{\Delta y}}$	$\frac{L_y + K_3 y(nT)}{2L_y}$	$\frac{L_{\Delta y} + K_4 \Delta y(nT)}{2L_{\Delta y}}$
IC5	0	0	$\frac{L_{\Delta y} - K_4 \Delta y(nT)}{2L_{\Delta y}}$	$\frac{L_{\Delta y} + K_4 \Delta y(nT)}{2L_{\Delta y}}$
IC6	0	0	0	1
IC7	0	$\frac{L_y - K_3 y(nT)}{2L_y}$	0	$\frac{L_y + K_3 y(nT)}{2L_y}$
IC8	0	1	0	0
IC9	$\frac{L_{\Delta y} - K_4 \Delta y(nT)}{2L_{\Delta y}}$	$\frac{L_{\Delta y} + K_4 \Delta y(nT)}{2L_{\Delta y}}$	0	0
IC10	1	0	0	0
IC11	$\frac{L_y - K_3 y(nT)}{2L_y}$	0	$\frac{L_y + K_3 y(nT)}{2L_y}$	0
IC12	0	0	1	0

In order to find the output change $\Delta u_I(nT)$ which is the output changes of Madani fuzzy I controller in each input space, the output singletons of Δu_{I_1}, Δu_{I_2}, Δu_{I_3} and Δu_{I_4} must be found. For the input space IC1 in figure 4.8, when the output linguistic variables *negative*, *zero* and *positive* of the rules in equation (4.12) are interfered by the constants $-H_I$, 0 and $+H_I$ then the output singletons are $\Delta u_{I_1} = -H_I$, $\Delta u_{I_2} = 0$, $\Delta u_{I_3} = 0$ and $\Delta u_{I_4} = +H_I$. Thus, the output change $\Delta u_I(nT)$ obtained from the corresponding output singletons and input membership values can be found from

$$\Delta u_I(nT) = \frac{H_I L_{\Delta e} K_1 e(nT) - H_I L_e K_2 \Delta e(nT)}{4L_e L_{\Delta e} - 2L_{\Delta e} K_1 e(nT)}.$$

The output change $\Delta u_I(nT)$ of the remaining input spaces can be found in the same manner as space IC1. Furthermore, the output change $\Delta u_{PD}(nT)$ which is output changes of Madani fuzzy PD controller of all input spaces can also be found in the same manner as $\Delta u_I(nT)$. The output changes of Madani fuzzy I and PD controllers for all input spaces are summarized in Table 4.3.

Table 4.3 Output Changes of Mamdani Fuzzy I and PD Controllers in IC1 to IC12.

#IC	$\Delta u_I(nT)$	$\Delta u_{PD}(nT)$
IC1	$\frac{H_I L_{\Delta e} K_1 e(nT) - H_I L_e K_2 \Delta e(nT)}{4L_e L_{\Delta e} - 2L_{\Delta e} K_1 e(nT)}$	$\frac{H_{PD} L_{\Delta y} K_3 y(nT) + H_{PD} L_y K_4 \Delta y(nT)}{4L_y L_{\Delta y} - 2L_{\Delta y} K_3 y(nT)}$
IC2	$\frac{H_I L_{\Delta e} K_1 e(nT) + H_I L_e K_2 \Delta e(nT)}{4L_e L_{\Delta e} - 2L_e K_2 \Delta e(nT)}$	$\frac{H_{PD} L_{\Delta y} K_3 y(nT) + H_{PD} L_y K_4 \Delta y(nT)}{4L_y L_{\Delta y} - 2L_y K_4 \Delta y(nT)}$
IC3	$\frac{H_I L_{\Delta e} K_1 e(nT) + H_I L_e K_2 \Delta e(nT)}{4L_e L_{\Delta e} + 2L_{\Delta e} K_1 e(nT)}$	$\frac{H_{PD} L_{\Delta y} K_3 y(nT) + H_{PD} L_y K_4 \Delta y(nT)}{4L_y L_{\Delta y} + 2L_{\Delta y} K_3 y(nT)}$
IC4	$\frac{H_I L_{\Delta e} K_1 e(nT) + H_I L_e K_2 \Delta e(nT)}{4L_e L_{\Delta e} + 2L_e K_2 \Delta e(nT)}$	$\frac{H_{PD} L_{\Delta y} K_3 y(nT) + H_{PD} L_y K_4 \Delta y(nT)}{4L_y L_{\Delta y} + 2L_y K_4 \Delta y(nT)}$
IC5	$\frac{H_I K_2 \Delta e(nT) + H_I L_{\Delta e}}{2L_{\Delta e}}$	$\frac{H_{PD} K_4 \Delta y(nT) + H_{PD} L_{\Delta y}}{2L_{\Delta y}}$
IC6	0	0
IC7	$\frac{H_I K_1 e(nT) + H_I L_e}{2L_e}$	$\frac{H_{PD} K_3 y(nT) + H_{PD} L_y}{2L_y}$
IC8	$-H_I$	$-H_{PD}$
IC9	$\frac{H_I K_2 \Delta e(nT) - H_I L_{\Delta e}}{2L_{\Delta e}}$	$\frac{H_{PD} K_4 \Delta y(nT) - H_{PD} L_{\Delta y}}{2L_{\Delta y}}$
IC10	0	0
IC11	$\frac{H_I K_1 e(nT) - H_I L_e}{2L_e}$	$\frac{H_{PD} K_3 y(nT) - H_{PD} L_y}{2L_y}$
IC12	H_I	H_{PD}

4.5 Stability Analysis

The aim of analyzing the stability of the controlled system is to study the system stability when there is a disturbance or perturbation in the system.

In this thesis, BIBO (bounded-input bounded-output) stability analysis will be used for considering the stability of the control system. The control system is said to be BIBO stable if a

bounded control input to the system always produces a bounded output through the system. The sufficient conditions of BIBO stable can be found by using the small gain theorem.

4.5.1 Small Gain Theorem

The small gain theorem is used for considering the sufficient condition of the stability. It can be applied to both continuous and discrete systems and to both SISO and MIMO systems, whose block diagram is shown in figure 4.10 where C is a controller, P is a process, $sp(nT)$ is the input of the system, $u(nT) = C \cdot e(nT)$ is the output of the controller, $u(nT)$ is the input of the process and $y(nT) = P \cdot u(nT)$ is the output of the controlled system.

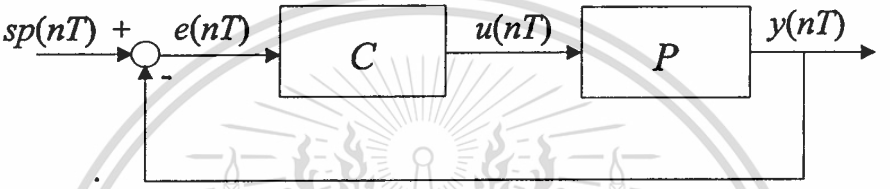

Figure 4.10 Feedback control system.

The norms of the output of the controller and the output of the system shown in figure 4.10 are given by

$$\|C \cdot e(nT)\| \le \alpha_C \|e(nT)\| + \beta_C; \quad \alpha_C, \beta_C \ge 0 \tag{4.16}$$

$$\|P \cdot u(nT)\| \le \alpha_P \|u(nT)\| + \beta_P; \quad \alpha_P, \beta_P \ge 0 \tag{4.17}$$

where α_C, α_P, β_C and β_P are constants, and the norm $\|\cdot\|$ in this thesis means the infinity norm $\|\cdot\|_\infty$. From equations (4.16) and (4.17) the norm of the error $\|e(nT)\|$ is obtained by

$$\|e(nT)\| \le \frac{\|sp(nT)\| + \alpha_P \|u_2(nT)\| + \alpha_P \beta_C + \beta_P}{1 - \alpha_C \cdot \alpha_P}. \tag{4.18}$$

When the term $\|sp(nT)\| + \alpha_P \|u_2(nT)\| + \alpha_P \beta_C + \beta_P$ is considered as a constant, and if the value of the term $\alpha_C \cdot \alpha_P$ is less than one, then the value of the error will be bound in limited range. Therefore, the sufficient condition of BIBO stable of a feedback control system is

$$\alpha_C \cdot \alpha_P < 1. \tag{4.19}$$

4.5.2 Sufficient Condition for Mamdani Fuzzy I-PD Control System Stability

The block diagram of Mamdani fuzzy I-PD control system for analyzing the stability is shown in figure 4.11 where C_I is a I controller, C_{PD} is a PD controller, P is a process to be controlled, $sp(nT)$ is the input of the system, $u(nT) = u_{I-PD}(nT)$ is the output of the controller, $u(nT)$ is the input of the process, $y(nT) = P \cdot u(nT)$ is the output of the controlled system and $u_I(nT-T)$ is the Mamdani fuzzy I controller output delayed by one sample.

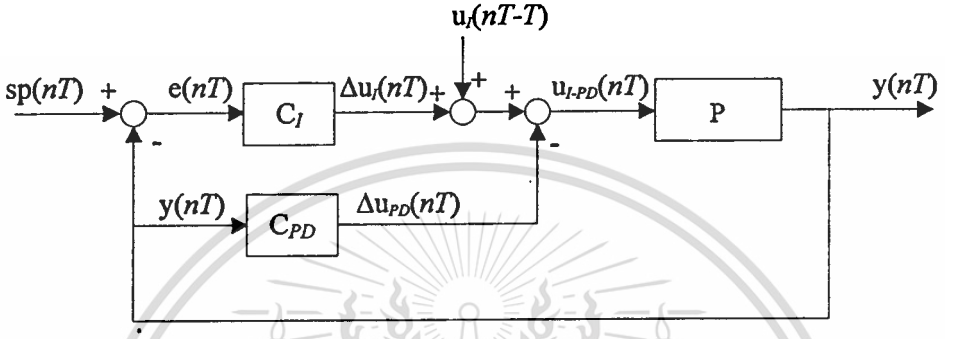

Figure 4.11 Mamdani fuzzy I-PD control system.

The norms of the output of the Mamdani fuzzy I-PD controller and the output of the system are then given by

$$\|u_I(nT)\| \le \|\Delta u_I(nT)\| + M_I \le \alpha_I \cdot \|e(nT)\| + \beta_I + M_I \tag{4.20}$$

$$\|u_{PD}(nT)\| \le \|\Delta u_{PD}(nT)\| \le \alpha_{PD} \cdot \|e(nT)\| + \beta_{PD} \tag{4.21}$$

$$\|u(nT)\| = \|\Delta u_{I-PD}(nT)\| \le (\alpha_I + \alpha_{PD}) \cdot \|e(nT)\| + \alpha_{PD} \cdot \|sp(nT)\| + \beta_I + \beta_{PD} + M_I \tag{4.22}$$

$$\|y(nT)\| = \|P \cdot u(nT)\| \le \|P\| \cdot \|u_{I-PD}(nT)\|, \tag{4.23}$$

where β_I, $\beta_{PD} \ge 0$ and $M_I = \|u(nT-T)\|$. From equations (4.20) to (4.23), the norm of the error can be obtained as

$$\|e(nT)\| \le \frac{(\alpha_{PD} \cdot \|P\| - 1)\|sp(nT)\| + \|P\| \cdot (\beta_I + \beta_{PD} + M_I)}{1 - (\alpha_I + \alpha_{PD}) \cdot \|P\|}. \tag{4.24}$$

The sufficient condition of BIBO stable for a Mamdani fuzzy I-PD control system is

$$(\alpha_I + \alpha_{PD}) \cdot \|P\| < 1, \tag{4.25}$$

where α_I and α_{PD} are found from the norms of Mamdani fuzzy I and Mamdani fuzzy PD controllers and $\|P\|$ is obtained from the norm of the manipulator.

4.5.3 Norm of a Mamdani Fuzzy I-PD Controller

The norm of the Mamdani fuzzy I-PD controller for each input space IC must be considered. For input space IC1, the norm of $\Delta u_I(nT)$ shown in Table 4.3 is given by

$$\|\Delta u_I(nT)\| = \left\| \frac{H_I L_{\Delta e} K_1 e(nT) - H_I L_e K_2 \Delta e(nT)}{4L_e L_{\Delta e} - 2L_{\Delta e} K_1 e(nT)} \right\|. \tag{4.26}$$

Since, the norm of $\Delta u_I(nT)$ in input space IC1 is maximum when $K_1 e(nT) = 0$, then

$$\|\Delta u_I(nT)\| \le \left| \frac{H_I L_{\Delta e} K_1 + H_I L_e K_2}{4L_e L_{\Delta e}} \right| \cdot \|e(nT)\| + \left| \frac{H_I L_e K_2}{4L_e L_{\Delta e}} \right| \cdot \|e(nT-T)\| \tag{4.27}$$

can be obtained. By substituting $M_I = \sup_{n\ge 1} |e(nT-T)|$ to equation (4.27), then

$$\|\Delta u_I(nT)\| \le \alpha_I \cdot \|e(nT)\| + \beta_I \tag{4.28}$$

is obtained where $\alpha_I = \left| \frac{H_I L_{\Delta e} K_1 + H_I L_e K_2}{4L_e L_{\Delta e}} \right|$ is the norm of Mamdani fuzzy I controller and $\beta_I = \left| \frac{H_I L_e K_2}{4L_e L_{\Delta e}} \right| \cdot M_I$ is a constant. Similarly the norm of $\Delta u_{PD}(nT)$ shown in Table 4.3 is given by

$$\|\Delta u_{PD}(nT)\| = \left\| \frac{H_{PD} L_{\Delta y} K_3 y(nT) - H_{PD} L_y K_4 \Delta y(nT)}{4L_y L_{\Delta y} - 2L_{\Delta y} K_3 y(nT)} \right\|. \tag{4.29}$$

Since, the norm of $\Delta u_{PD}(nT)$ in input space IC1 is maximum when $K_3 y(nT) = 0$, then

$$\|\Delta u_{PD}(nT)\| \le \left| \frac{H_{PD} L_{\Delta y} K_3 + H_{PD} L_y K_4}{4L_y L_{\Delta y}} \right| \cdot \|y(nT)\| + \left| \frac{H_{PD} L_y K_4}{4L_y L_{\Delta y}} \right| \cdot \|y(nT-T)\| \tag{4.30}$$

can be obtained. By substituting $M_{PD} = \sup_{n\ge 1} |y(nT-T)|$ in equation (4.30), then

$$\left\|\Delta u_{PD}(nT)\right\| \le \alpha_{PD} \cdot \left\|y(nT)\right\| + \beta_{PD} \tag{4.31}$$

is obtained where $\alpha_{PD} = \left|\frac{H_{PD}L_{\Delta y}K_3 + H_{PD}L_yK_4}{4L_yL_{\Delta y}}\right|$ is the norm of Mamdani fuzzy PD controller and $\beta_{PD} = \left|\frac{H_{PD}L_yK_4}{4L_yL_{\Delta y}}\right| \cdot M_{PD}$ is a constant.

For the remaining input space ICs, the the norms of the Mamdani fuzzy I and PD controller can be obtained in the same manner as the input space IC1. Then the maximum norm for every input space is summarized in Table 4.4.

Table 4.4 Norms of Mamadani fuzzy I and Mamadani fuzzy PD controller in IC1 to IC12.

#IC	α_I	α_{PD}
IC1, IC2, IC3, IC4	$\left\|\frac{H_IL_{\Delta e}K_1 + H_IL_eK_2}{4L_eL_{\Delta e}}\right\|$	$\left\|\frac{H_{PD}L_{\Delta y}K_3 + H_{PD}L_yK_4}{4L_yL_{\Delta y}}\right\|$
IC5, IC9	$\left\|\frac{H_IK_2}{2L_{\Delta e}}\right\|$	$\left\|\frac{H_{PD}K_4}{2L_{\Delta y}}\right\|$
IC7, IC11	$\left\|\frac{H_IK_2}{2L_e}\right\|$	$\left\|\frac{H_{PD}K_4}{2L_y}\right\|$
IC6, IC8, IC10, IC12	0	0

Chapter 5

Simulation and Experimental Results

In this chapter, the effectiveness of the proposed Mamdani fuzzy I-PD controller in controlling the angular positions of the 1st and the 2nd links of the robot manipulator will be evaluated by comparing to the conventional I-PD control system. The simulation and the experimental results will also be shown.

5.1 Experimental System

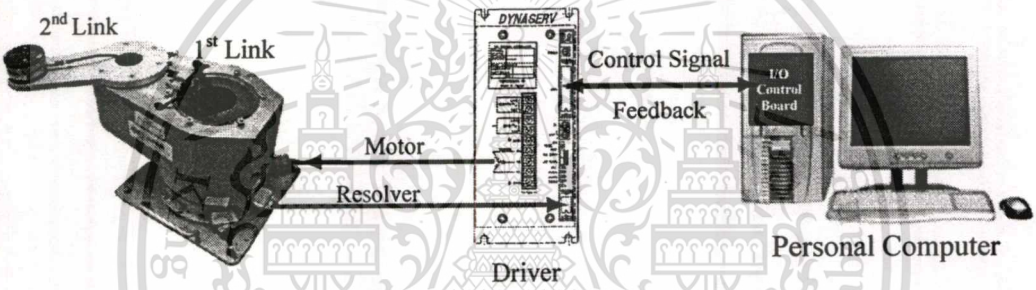

Figure 5.1 Experimental system.

The experimental system of angular position control for two-link robot manipulator is set up as shown in figure 5.1. The masses, rotor inertias and the lengths of robot arms are m_1 = 12.27 kg, m_2 = 1.24 kg, $J_{M1} = 85\text{x}10^{-3}$ kgm, $J_{M2} = 60\text{x}10^{-3}$ kgm, $\ell_1 = \ell_2 = 200$ mm, a_1 = 63 mm and a_2 = 80 mm. Maximum torque of the 1st and the 2nd joints are 70 Nm and 15 Nm when the maximum torque commands are produced at ±8 V by 2 channels 24 bits D/A PC interface card. Optical encoders of the 1st joint and the 2nd joint are 614,400 and 507,904 pulse/rev.

5.2 Mamdani Fuzzy I-PD Controller Parameters

The parameters of Mamdani fuzzy I-PD controller have to be assigned for simulations and experiments. Hence, the parameters of the 1st link and the 2nd link are first determined from experimental data based on the technique described in chapter 3. Applying the +1 V current command voltage from personal computer to both links through the servo DYNASERV

DR1070E and DR1015B, the open-loop responses of both links can be obtained as shown in figures 5.2 and 5.3.

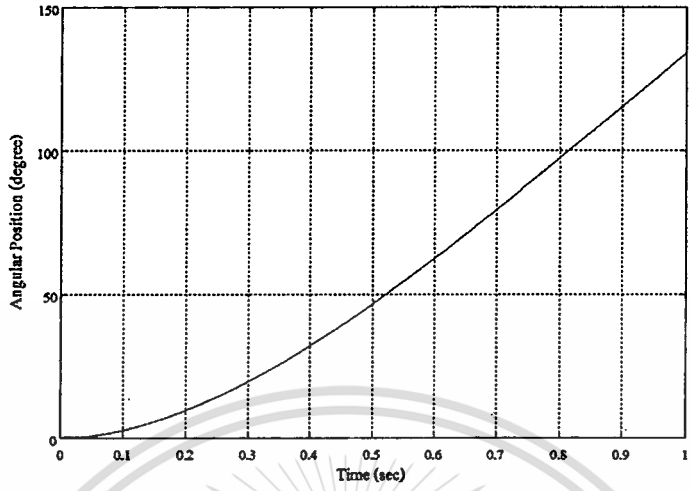

Figure 5.2 Open-loop response of the 1st link.

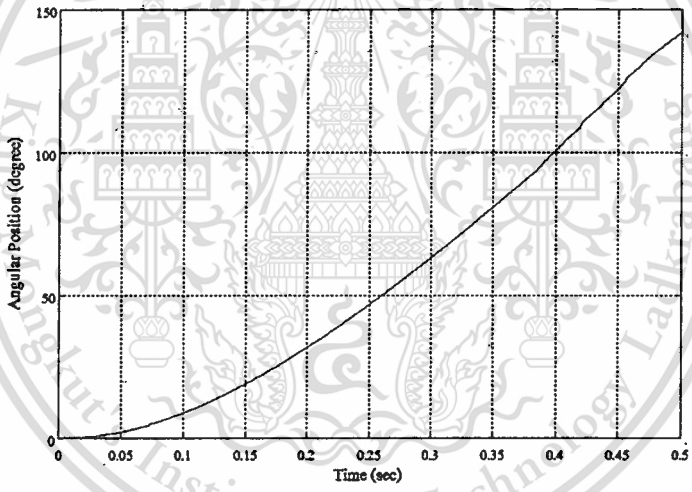

Figure 5.3 Open-loop response of the 2nd link.

From the open-loop response curves in figure 5.3 and 5.4, the slope of the steady-state responses of the 1st link and the 2nd link are 182.1213 and 412.122, the straight lines of steady-state responses extrapolated back to the time axis and intersects this axis at 0.2657 second and 0.1563 second. Thus, the torque constants K_{M1} and K_{M2} are 158.0801 Nm/V and 76.0955 Nm/V. Hence, their model can be found as

$$\frac{\mathbf{Q}(s)}{\mathbf{V}(s)} = \begin{bmatrix} \dfrac{28.4155s+181.8685}{s(0.0367s^2+0.4219s+1)} & \dfrac{-13.1301s}{s(0.0367s^2+0.4219s+1)} \\ \dfrac{-27.2763s}{s(0.0367s^2+0.4219s+1)} & \dfrac{109.1570s+410.8829}{s(0.0367s^2+0.4219s+1)} \end{bmatrix}. \tag{5.9}$$

In this work, the parameters K_I, K_p and K_d can be obtained by using CDM. This method uses polynomials for system representation. The denominator and the numerator of the transfer function are considered independently from each other. Thus, the better results can be achieved against pole-zero cancellation (see the details of CDM method in Appendix A).

The controller parameters for the 1st link are designed by setting the stability indices γ_1 = 3.5, γ_2 = 3.9809 and γ_3 = 1.7717 and the equivalent time constant τ = 0.75 second. Then K_I = 0.7678, K_p = 0.6332 and K_d = 0.0408 are obtained based on CDM. When the sampling time is T = 0.001 second, the parameters K_1, K_2, K_3 and K_4 of the Mamdani fuzzy I-PD controller can be computed as K_1 = 7.6775x10^{-4}, K_2 = 3.8388x10^{-4}, K_3 = 0.6332 and K_4 = 40.7557. The adjustable constant L_e, $L_{\Delta e}$, L_y, $L_{\Delta y}$, H_I and H_{PD} which are used for computing the membership values, are selected as L_e = 14, $L_{\Delta e}$ = 50, L_y = 75, $L_{\Delta y}$ = 95, H_I = 205 and H_{PD} = 100.

The controller parameters for the 2nd link are designed as the same manner of the 1st link by setting the stability indices γ_1 = 3.5, γ_2 = 4.6377 and γ_3 = 6.7118 and the equivalent time constant τ = 0.9 second. Then K_I = 0.8426, K_p = 0.6780 and K_d = 0.0445 are obtained. The parameters K_1 = 8.4260x10^{-4}, K_2 = 4.2130x10^{-4}, K_3 = 0.6780 and K_4 = 44.5353 can be found. The adjustable constants are selected as L_e = 16, $L_{\Delta e}$ = 50, L_y = 95, $L_{\Delta y}$ = 92.5, H_I = 205 and H_{PD} = 110.

The norm of the Mamdani fuzzy I-PD controller for the 1st link and the 2nd link can be computed and be summarized in Table 5.1.

Table 5.1 Norms of Mamadani Fuzzy I and PD Controllers in IC1-IC12.

#IC	$\alpha_I + \alpha_{PD}$ for 1st link controller	$\alpha_I + \alpha_{PD}$ for 2nd link controller
IC1, IC2, IC3, IC4	10.9395	13.4396
IC5, IC9	21.4511	26.4813
IC7, IC11	13.5880	12.8945
IC6, IC8, IC10, IC12	0	0

From the Table 5.1, the maximum value of the norm of the controller is $\alpha_I + \alpha_{PD}$ = 26.4813. The norm of the process can be found by the relation between the output $\mathbf{Q}(s)$ with the input $\mathbf{V}(s)$ shown in equation (5.9). The discrete time equivalent of this system is found by using the zero-order hold circuit with the sampling time $T = 0.001$ as

$$\mathbf{P}(z)=\frac{\mathbf{Q}(z)}{\mathbf{V}(z)}=\begin{bmatrix}P_{11}(z) & P_{12}(z)\\ P_{21}(z) & P_{22}(z)\end{bmatrix} \tag{5.10}$$

where $P_{11}(z)=\dfrac{0.0003865z^2+0.000001.81z-0.0003834}{z^3-2.989z^2+2.977z-0.9886}$

$P_{12}(z)=\dfrac{-0.0001782z-0.0001775}{z^2-1.989z+0.9886}$

$P_{21}(z)=\dfrac{-0.0003702z-0.0003688}{z^2-1.989z+0.9886}$

$P_{22}(z)=\dfrac{0.001483z^2+0.000001755z-0.001474}{z^3-2.989z^2+2.977z-0.9886}.$

Then the norm of the process can be obtained as

$$\left\|\mathbf{P}(z)\right\|=\sup_{|z|=1}\left|\frac{\mathbf{Q}(z)}{\mathbf{V}(z)}\right|=0.0179. \tag{5.11}$$

By substituting value of the norm of the process $\left\|\mathbf{P}(z)\right\|=0.0179$ and the value of the norm of the controller $\alpha_I+\alpha_{PD}=26.4813$ in the sufficient condition equation (4.25), then $0.4747<1$ is obtained. It is shown that the designed controllers can be used to control the 1st link and the 2nd link of the robot manipulator and the controlled system will be stable.

5.3 Simulation Results of Angular Position Control

The simulation result of controlling the angular positions of robot manipulator both in no-load condition and load condition will be shown is this section.

5.3.1 Angular Position Control for the 1st Link

The simulation results of controlling the 1st link (the 2nd link is not controlled) of the robot manipulator with no load mass at the end-effector are shown in figure 5.4. It is seen from figure 5.4 that the Mamdani fuzzy I-PD controller can rapidly control the 1st link to follow the desired cubic polynomial trajectory (see Appendix C) faster than the conventional I-PD controller. However both control systems can reach to the desired angular position at 90 degrees without steady-state error. It is also seen that the tracking error of the Mamdani fuzzy I-PD control system is quite smaller than the conventional I-PD control system while the control signal is slightly larger than the latter one.

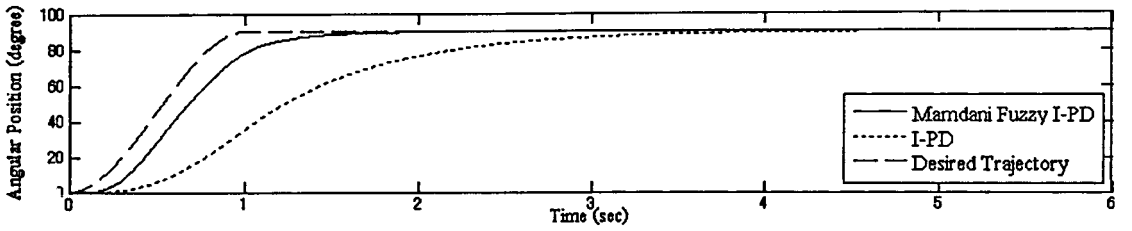

(a) Responses of the 1st link.

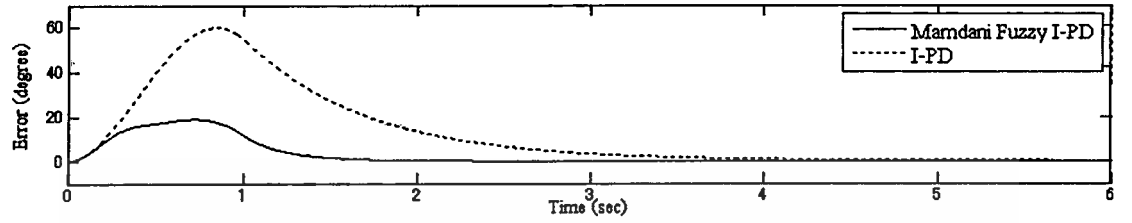

(b) Errors of the 1st link.

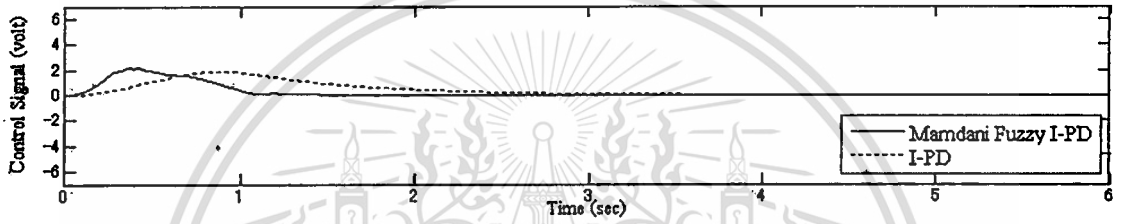

(c) Control signals of the 1st link.

Figure 5.4 Simulation results for the 1st link (no load).

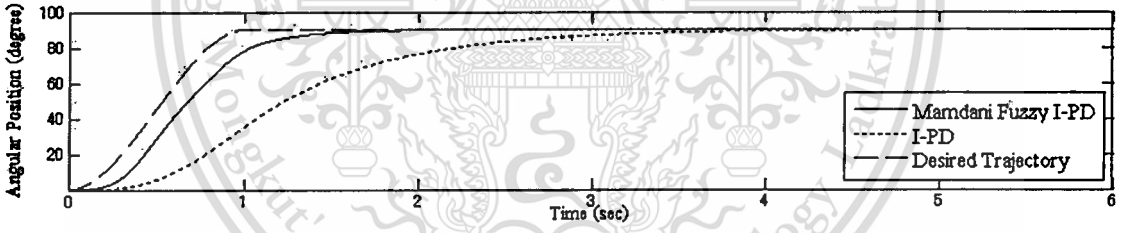

(a) Responses of the 1st link.

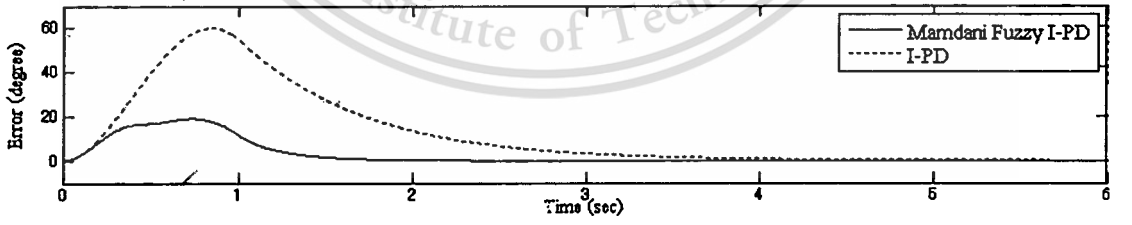

(b) Errors of the 1st link.

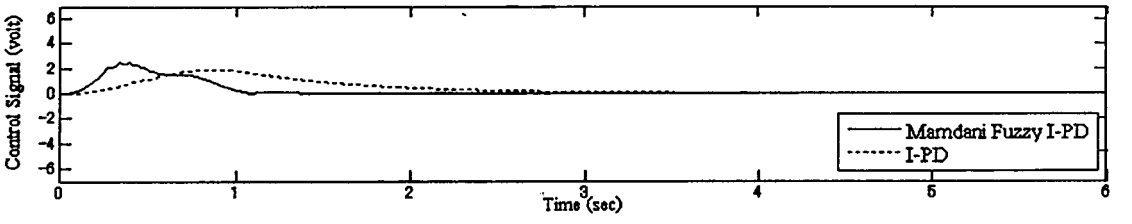

(c) Control signals of the 1st link.

Figure 5.5 Simulation results for the 1st link (0.8 kg load).

In order to demonstrate the effectiveness of the Mamdani fuzzy I-PD controller, the 0.8 kg load mass is placed on the end-effector without changing the controller parameters. The system tracking response for the same desired trajectory for the 1st link can be shown in figure 5.5. It is seen that the response of the Mamdani fuzzy I-PD system still can track the desired trajectory faster than the conventional I-PD system, even if there is 0.8 kg load mass at the end-effector, and small amount of tracking error of the Mamdani fuzzy I-PD system can be seen.

5.3.2 Angular Position Control for the 2nd Link

When applying the designed controller to control the 2nd link (the 1st link is not controlled) with no load mass, the simulation results are shown in figure 5.6. It is seen that the Mamdani fuzzy I-PD controller can also rapidly control the 2nd link to follow the desired cubic polynomial trajectory faster than the conventional I-PD controller with smaller tracking error.

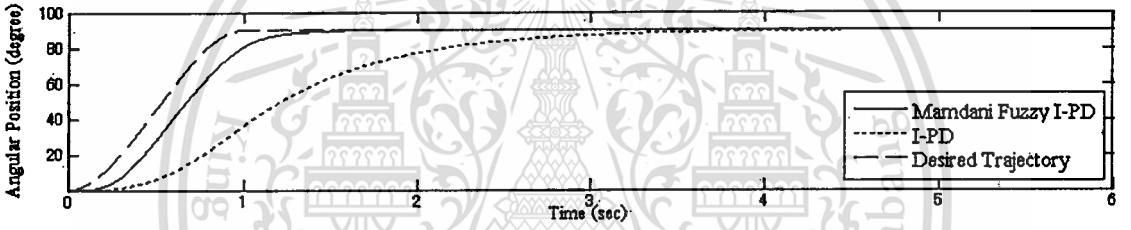

(a) Responses of the 2nd link.

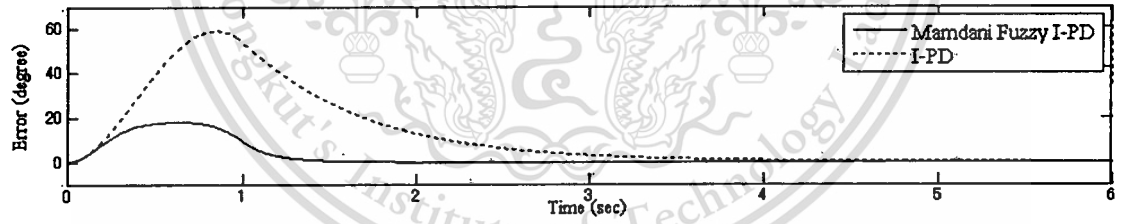

(b) Errors of the 2nd link.

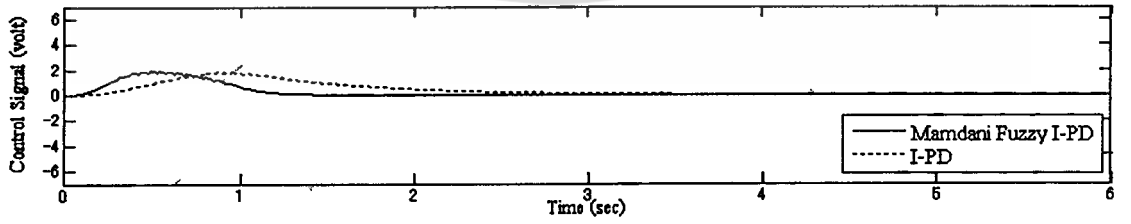

(c) Control signals of the 2nd link.

Figure 5.6 Simulation results for the 2nd link (no load).

When the 0.8 kg load mass is placed on the end-effector without changing the parameters of the controller for the 2nd link, the tracking responses for the same desired trajectory can be shown in figure 5.7. It is seen that the response of the Mamdani fuzzy I-PD system still can track the desired trajectory faster than the conventional I-PD system with small amount of tracking error. However, it is also seen that the larger control signal occurred when the controller is Mamdani fuzzy I-PD controller.

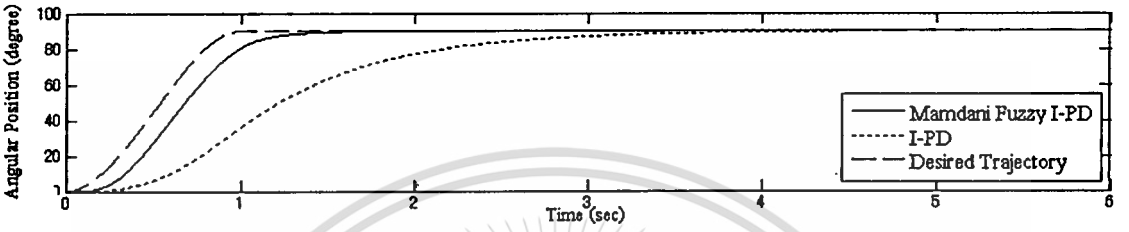

(a) Responses of the 2nd link.

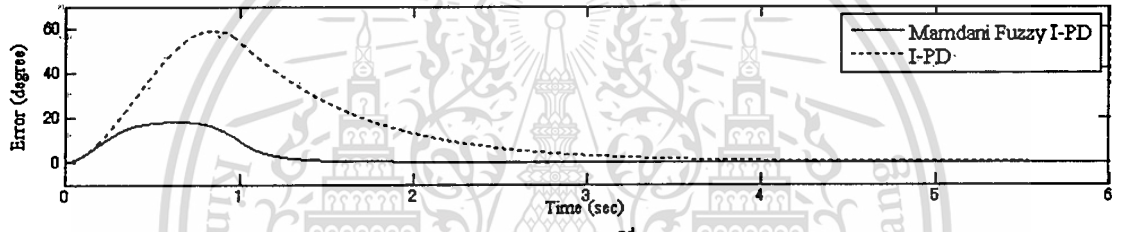

(b) Errors of the 2nd link.

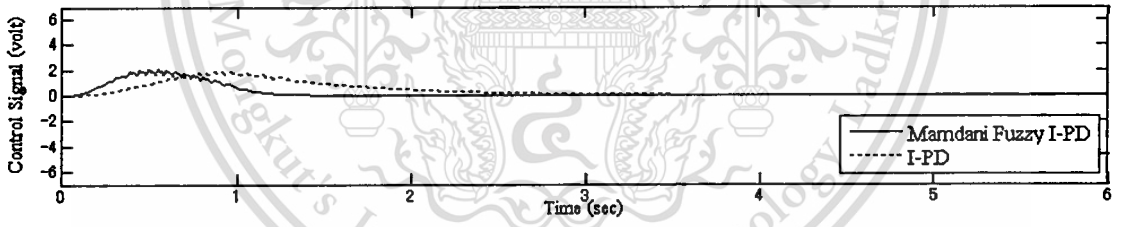

(c) Control signals of the 2nd link.

Figure 5.7 Simulation results for the 2nd link (0.8 kg load).

5.3.3 Effect of Joint Coupling

In this sub-section, the tracking responses of the angular position control when both links are being operated to the same desired trajectory at the same time. The effects of the control system with no-load and load are also considered.

The simulation results of controlling the 1st and the 2nd links with no load are shown in figure 5.8. It is seen that the responses of both links can track the desired trajectory rapidly, even if there are the coupling forces caused by the rotational movements of the both links. The tracking errors are also small. The larger oscillatory control signal is occurred when the controllers are Mamdani fuzzy I-PD controllers.

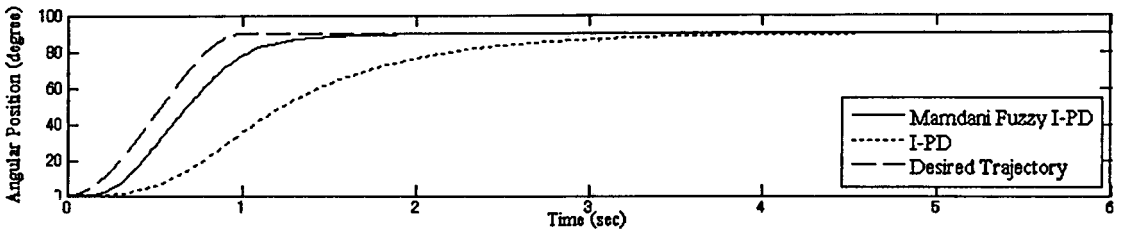

(a) Responses of the 1st link.

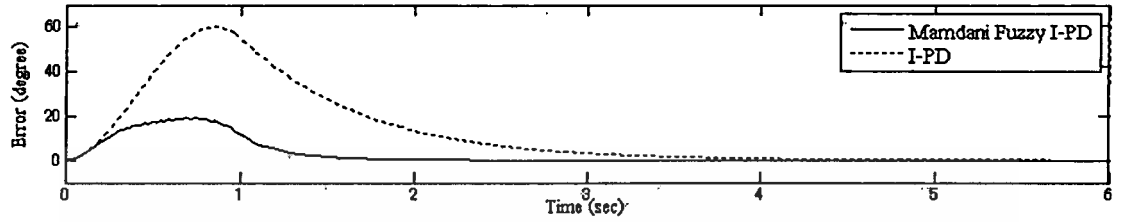

(b) Errors of the 1st link.

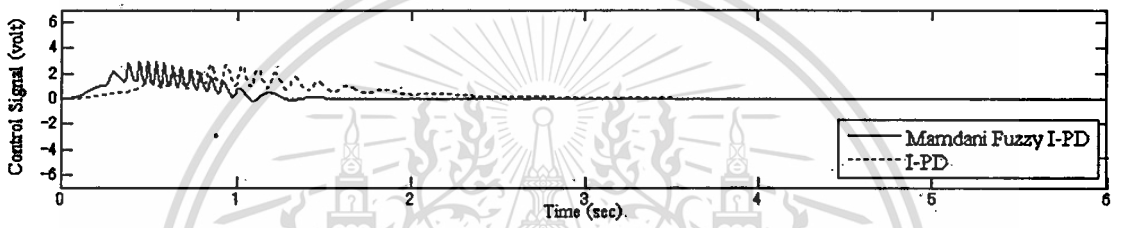

(c) Control signals of the 1st link.

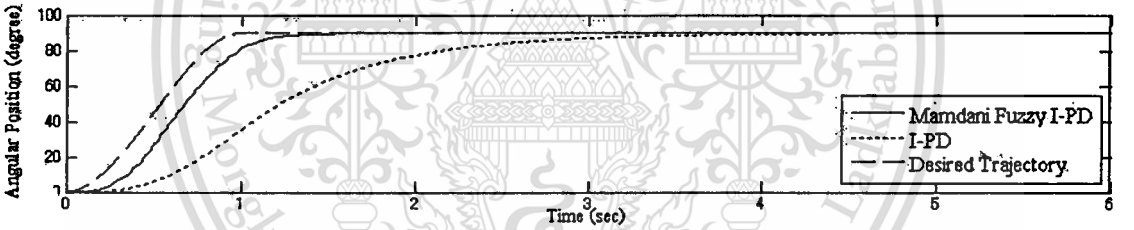

(d) Responses of the 2nd link.

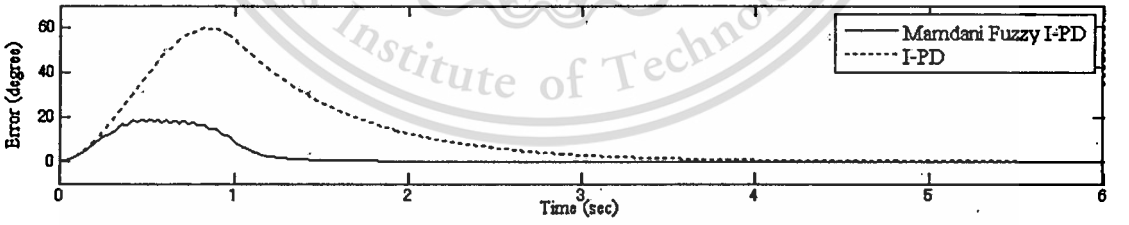

(e) Errors of the 2nd link.

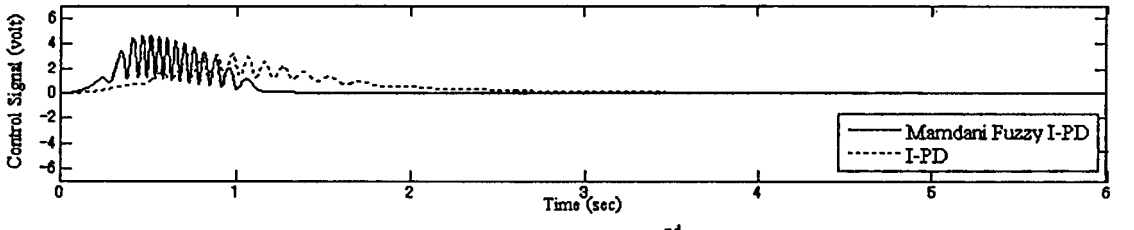

(f) Control signals of the 2nd link.

Figure 5.8 Simulation results for simultaneously control of both links (no load).

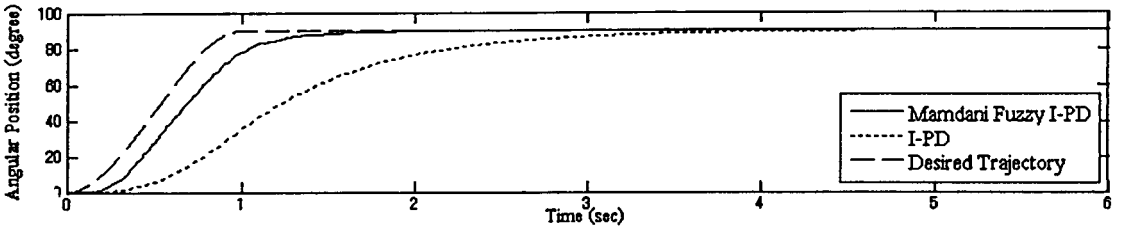

(a) Responses of the 1st link.

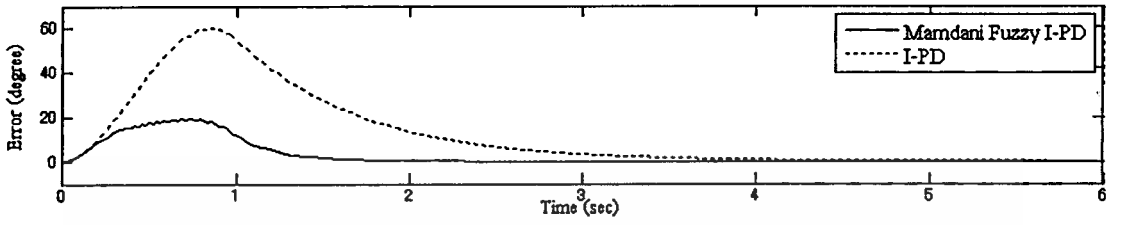

(b) Errors of the 1st link.

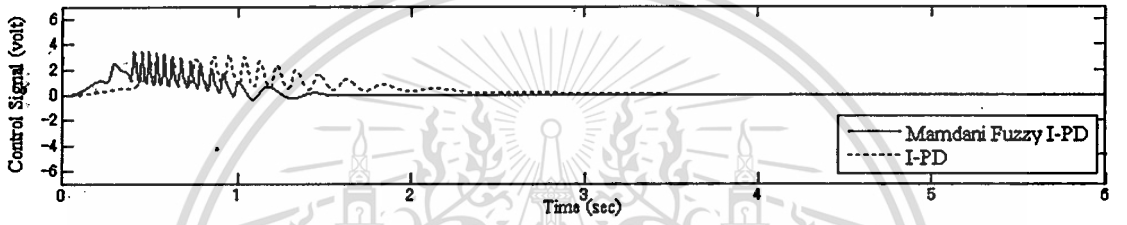

(c) Control signals of the 1st link.

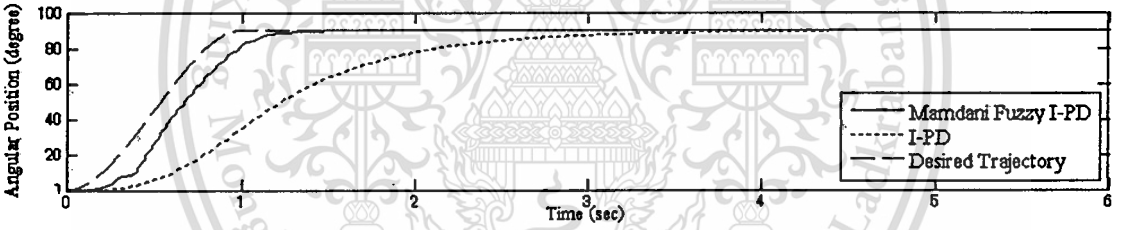

(d) Responses of the 2nd link.

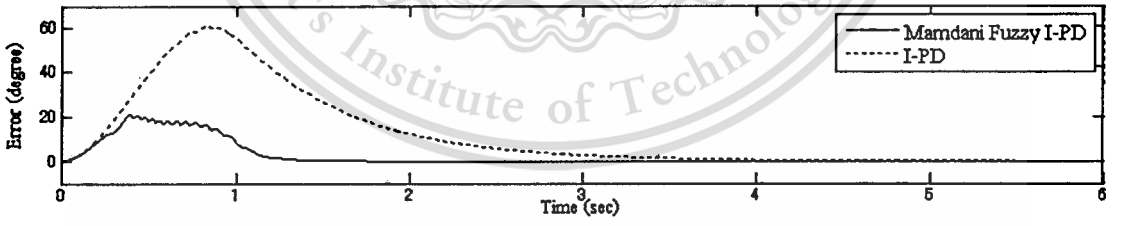

(e) Errors of the 2nd link.

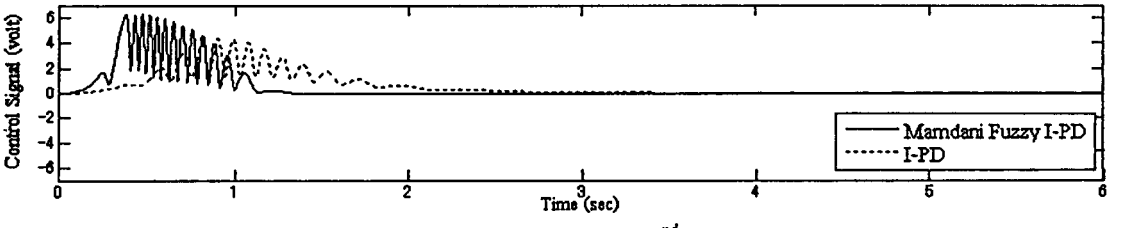

(f) Control signals of the 2nd link.

Figure 5.9 Simulation results for simultaneously control of both links (0.8 kg load).

For load condition the simulation responses for 0.8 kg load condition are shown in figure 5.9. The responses still can track the desired trajectory, even if there is the 0.8kg load mass at the end-effector and there are the coupling forces caused by the rotational movements of the both links of the robot manipulator. It can also see that the larger oscillatory control signals appeared when the controllers are Mamdani fuzzy I-PD controller.

5.4 Experimental Results of Angular Position Control

In this section, the experiments will be carried out to verify the effectiveness of the Mamdani fuzzy I-PD tracking angular position control system of the two-link robot manipulator. The experimental result will be performed both no-load and load conditions.

5.4.1 Angular Position Control for the 1st Link

Figure 5.10 shows the experimental results of controlling the 1st link (the 2nd link is not controlled) of the robot manipulator when there is no load mass at the end-effector. It is seen that the Mamdani fuzzy I-PD controller can rapidly control the 1st link to follow the desired trajectory faster than the conventional I-PD controller where the tracking error the Mamdani fuzzy I-PD control system is smaller than the conventional I-PD control system similar to the simulation. But the larger control signal of the Mamdani fuzzy I-PD control system can be seen.

The effectiveness of the Mamadani fuzzy I-PD controller can be demonstrated by placing 0.8 kg load mass at the end-effector without changing controller parameters. The experimental results of the 1st link of the robot manipulator are shown in figure 5.11. It is seen that the Mamdani fuzzy I-PD controller still can control the 1st link to follow the desired trajectory faster than the conventional I-PD controller while the tracking error of the Mamdani fuzzy I-PD control system is smaller than the conventional I-PD control system. The larger control signal of the Mamdani fuzzy I-PD control system also is seen.

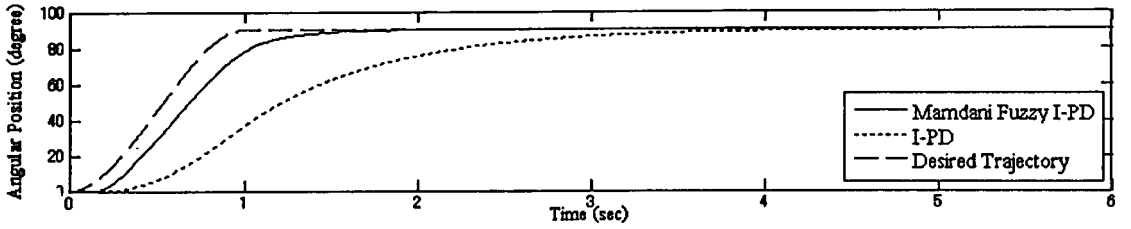

(a) Responses of the 1st link.

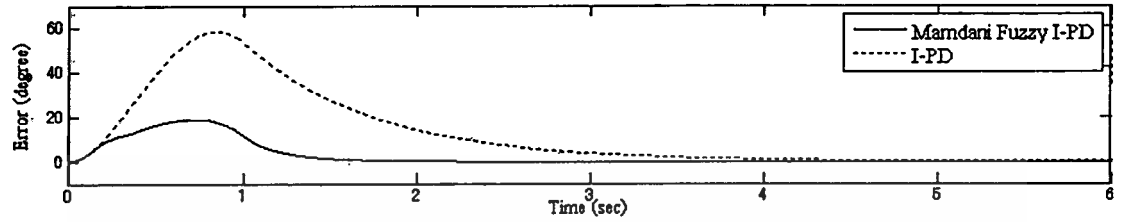

(b) Errors of the 1st link.

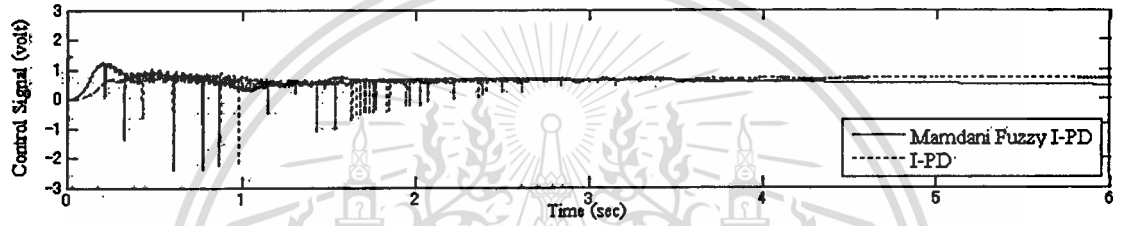

(c) Control signals of the 1st link.

Figure 5.10 Experimental results for the 1st link (no load).

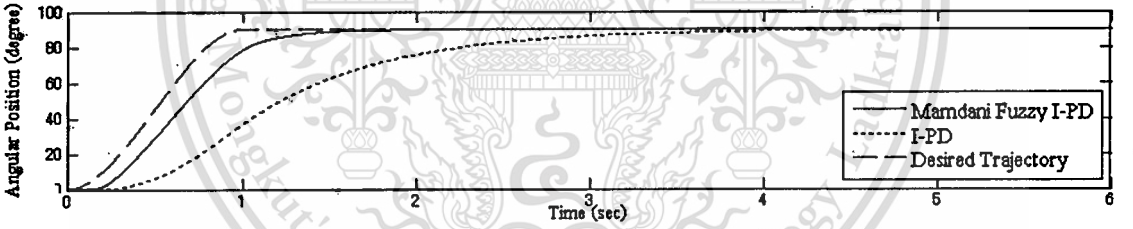

(a) Responses of the 1st link.

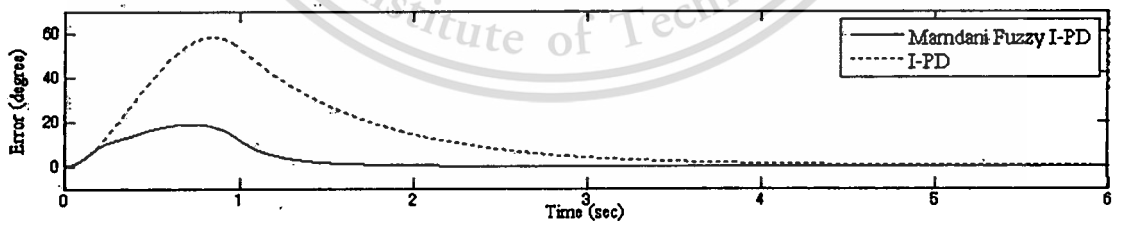

(b) Errors of the 1st link.

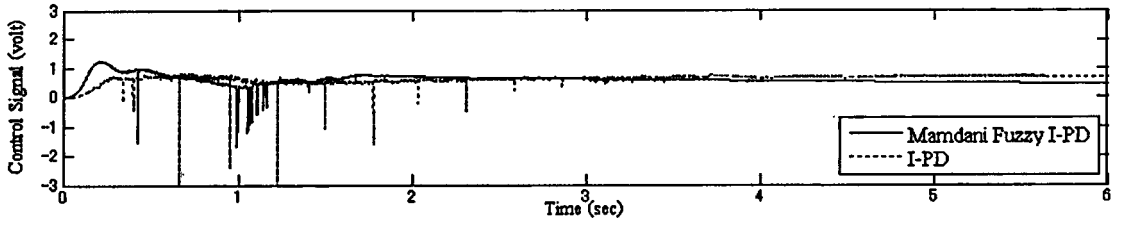

(c) Control signals of the 1st link.

Figure 5.11 Experimental results for the 1st link (0.8 kg load).

5.4.2 Angular Position Control for the 2nd Link

The experimental results of controlling the 2nd link (the 1st link is not controlled) of the robot manipulator when there is no load mass at the end-effector are shown in figure 5.12. It is seen that the responses of the 2nd link of the robot manipulator can be controlled to reach to the desired angular at 90 degrees without steady-state error. The tracking error of the Mamdani fuzzy I-PD control system is smaller than the conventional I-PD control system. However, it is seen from the figure that there is the lager control signal in the Mamdani fuzzy I-PD control system.

When placing the 0.8 kg load mass at the end-effector without changing controller parameters, the responses of the 2nd link of the robot manipulator shown in figure 5.13 still can be controlled to reach to the desired angular position without steady-state errors while the tracking error of the Mamdani fuzzy I-PD control system is smaller than the conventional I-PD control system. The lager control signal of the Mamdani fuzzy I-PD control system still occurred with larger magnitude than the case with no load mass.

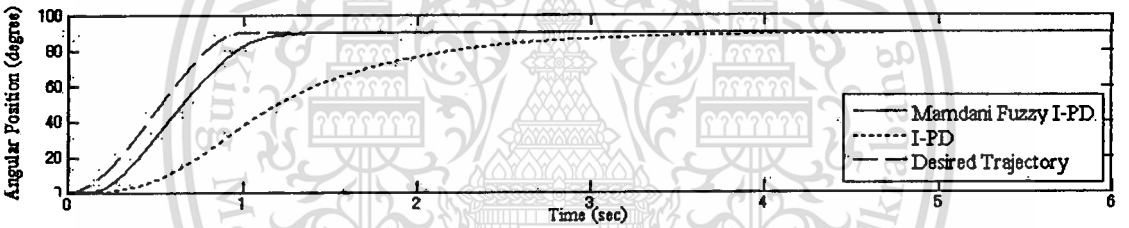

(a) Responses of the 2nd link.

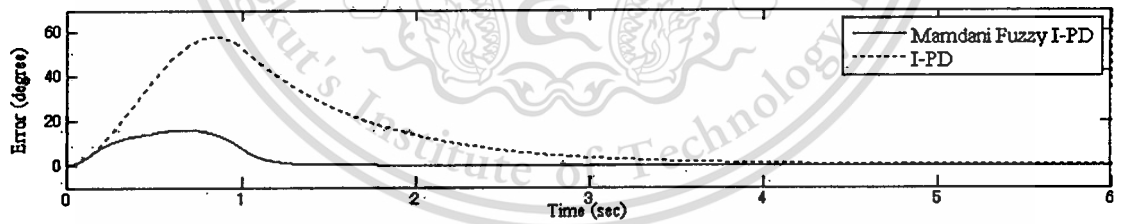

(b) Errors of the 2nd link.

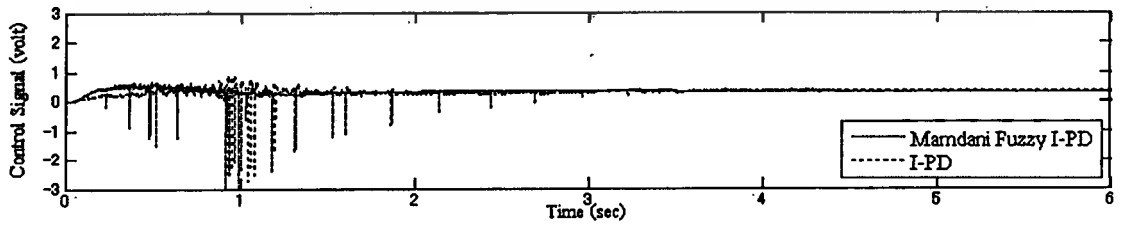

(c) Control signals of the 2nd link.

Figure 5.12 Experimental results for the 2nd link (no load).

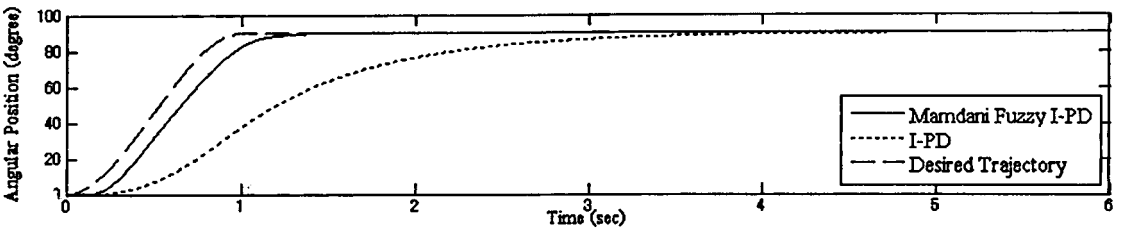

(a) Responses of the 2nd link.

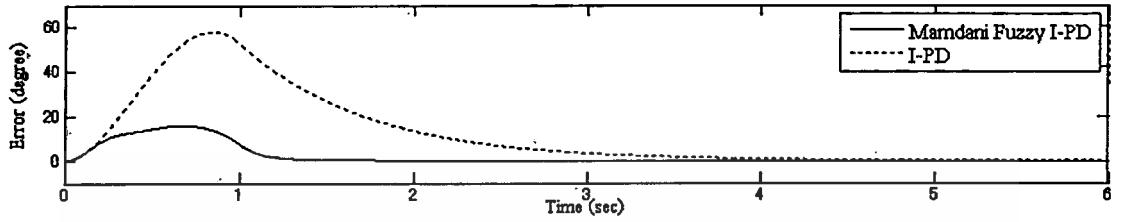

(b) Errors of the 2nd link.

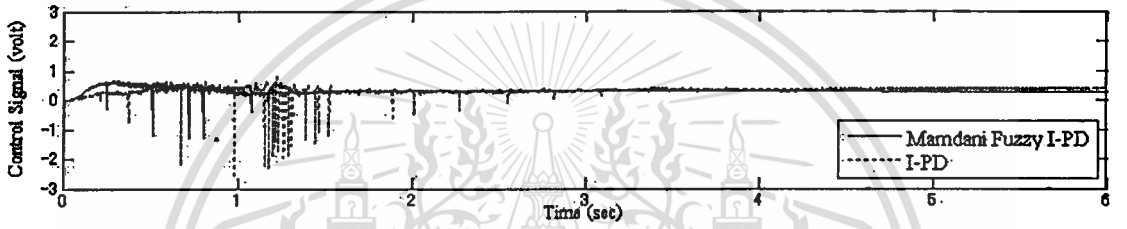

(c) Control signals of the 2nd link.

Figure 5.13 Experimental results for the 2nd link (0.8 kg load).

5.4.3 Effect of Joint Coupling

When both links of the robot manipulator are being operated simultaneously, the coupling effects between links will be caused. The tracking responses of the angular position control for the 1st and the 2nd link of the robot manipulator in this situation will be considered for both with no-load and load conditions. The experimental results for no-load condition are shown in figure 5.14, and the experimental results for 0.8 kg load condition are shown in figure 5.15.

Form figure (5.14), it is seen that the responses of the both system can track the desired trajectory, however it is noticed that the tracking errors of Mamdani fuzzy I-PD control system is smaller, and the Mamdani fuzzy I-PD control system can track the desired trajectory faster than the conventional I-PD system. It also be seen that the larger oscillatory control signals occurred when the controllers are Mamdani fuzzy I-PD controllers.

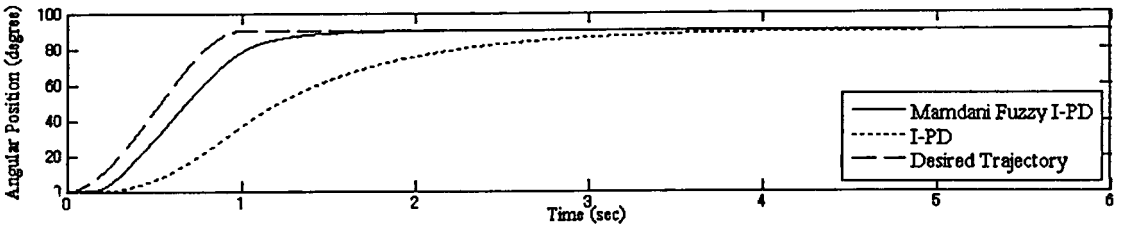

(a) Responses of the 1st link.

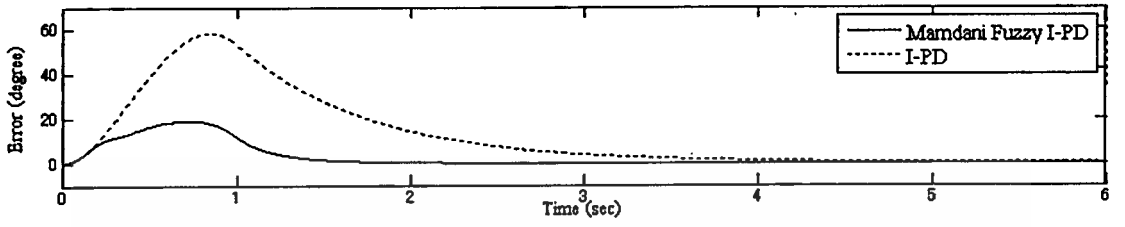

(b) Errors of the 1st link.

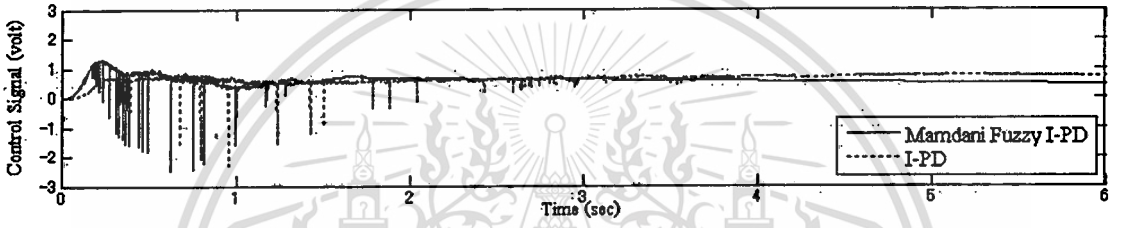

(c) Control signals of the 1st link.

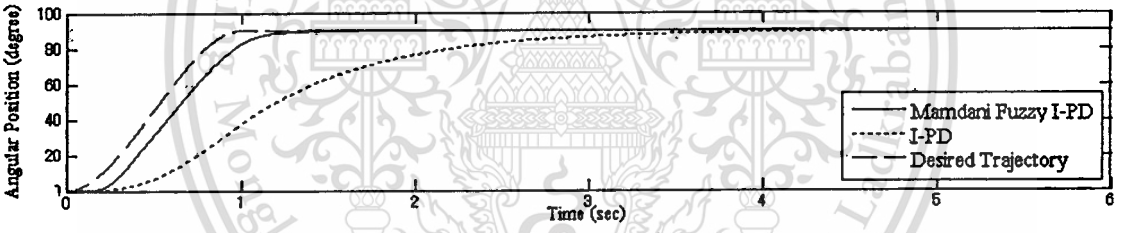

(d) Responses of the 2nd link.

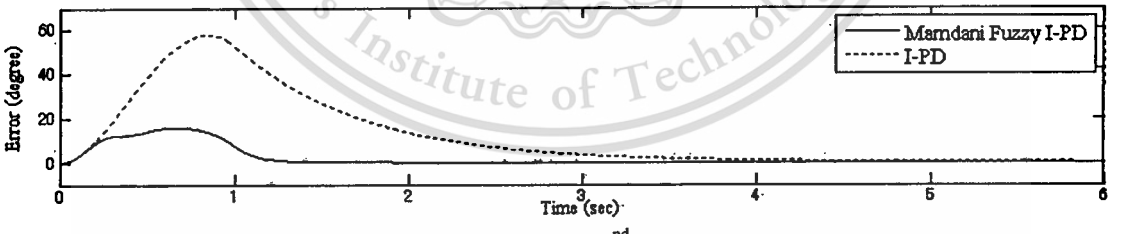

(e) Errors of the 2nd link.

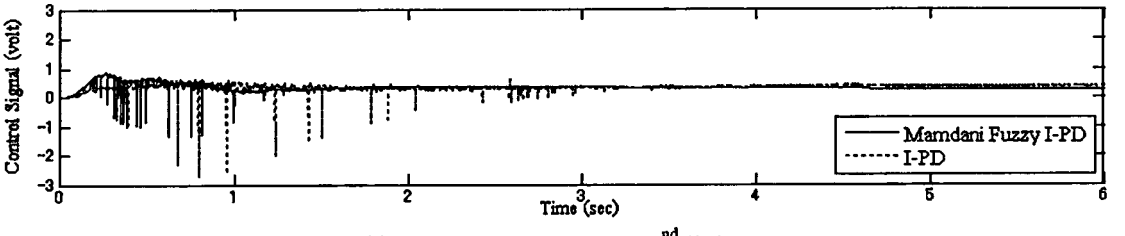

(f) Control signals of the 2nd link.

Figure 5.14 Experimental results for simultaneously control of both links (no load).

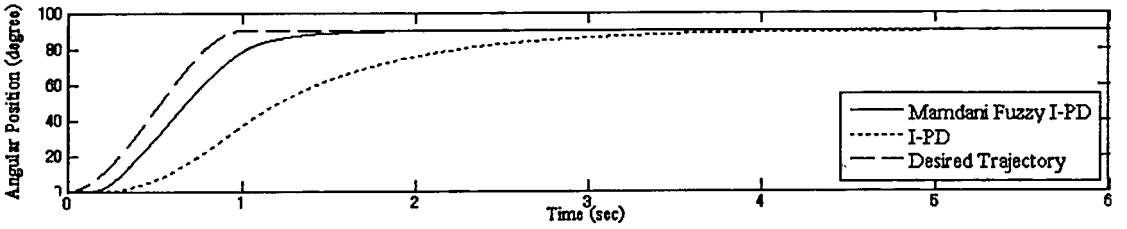

(a) Responses of the 1st link.

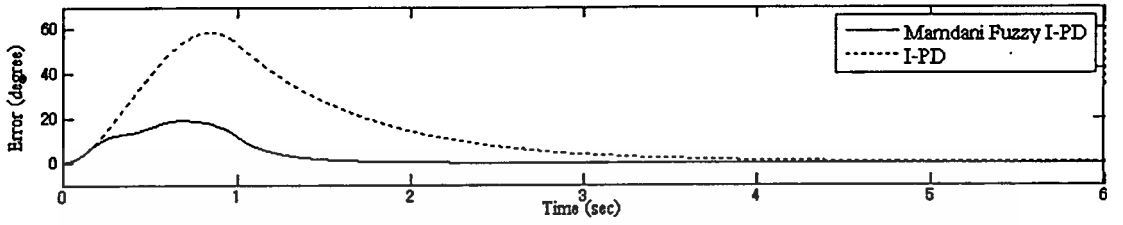

(b) Errors of the 1st link.

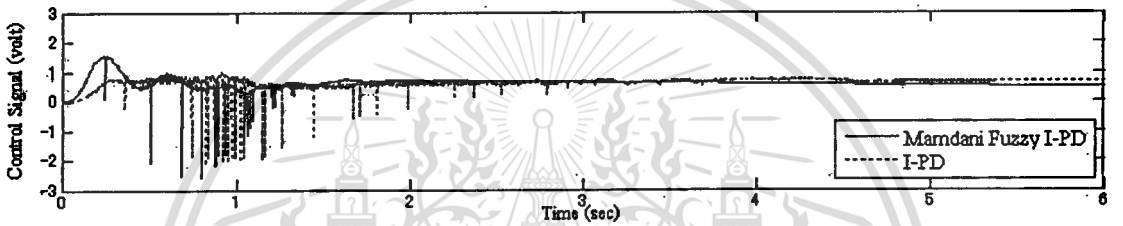

(c) Control signals of the 1st link.

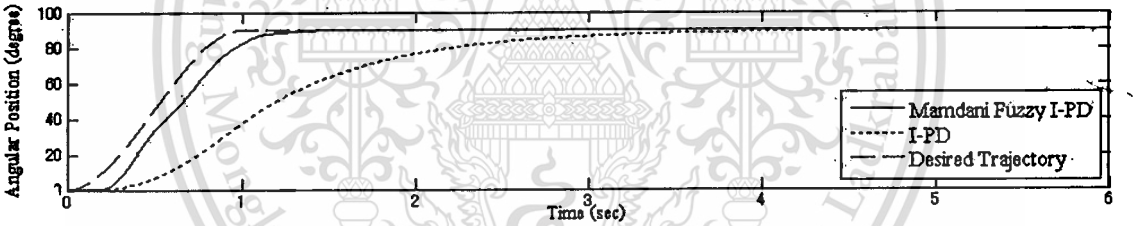

(d) Responses of the 2nd link.

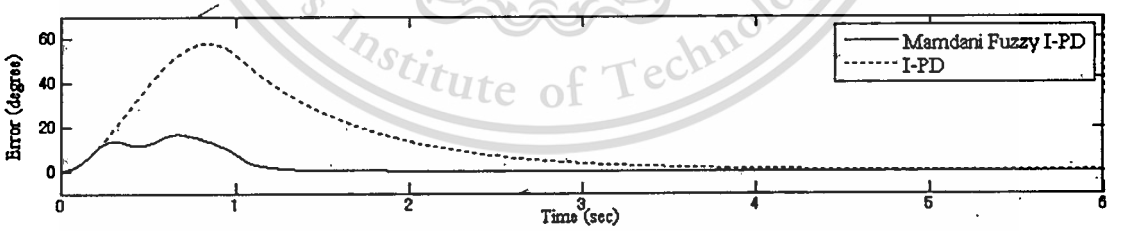

(e) Errors of the 2nd link.

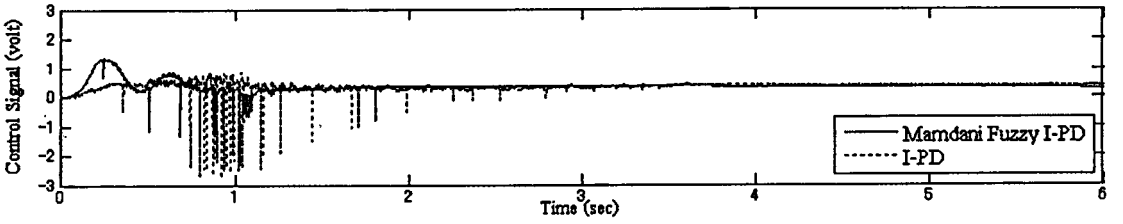

(f) Control signals of the 2nd link.

Figure 5.15 Experimental results for simultaneously control of both links (0.8kg load).

Form figure (5.15), it is seen that even if there is the 0.8 kg load mass at the end-effector and there are the coupling forces caused by the rotational movements of the both links of the robot manipulator, the both systems still can track the desired trajectories. But the tracking error s of Mamdani fuzzy I-PD control system is smaller and can track the desired trajectory faster than the conventional I-PD system while the oscillation of the control signals of the Mamdani fuzzy I-PD control system also occurred. It can be noticed that the lad mass of 0.8 kg will cause the larger control signals for both links when compared to the case of with no load.

Chapter 6

Conclusions and Future Works

6.1 Conclusions

The Mamdani fuzzy I-PD controller has been studied and proposed for controlling the angular position of two-link robot manipulator system. In order to obtain the fast response without steady-state error, the fuzzy principle is used to design the proposed controller which is the modification of the conventional I-PD controller designed by coefficient diagram method. Based on the small gain theorem, the parameters satisfying to the sufficient condition for stability have obtained for Mamdani fuzzy I-PD system. The simulation and experimental results indicated that the Mamdani fuzzy I-PD control controllers can control both links of the robot manipulator to follow the desired trajectories rapidly without steady-state errors. When the system is disturbed by adding a load mass, the system still be controlled with satisfactory performance without redesigning the controller parameters. Furthermore, even if the effect of the coupling between links occurred, the quick angular position tracking responses can be obtained. Hence, it can be concluded that the Mamdani fuzzy I-PD controller is successful in controlling the angular positions of the 1^{st} and the 2^{nd} links of robot manipulator.

6.2 Future Work

In order to control the two-link robot manipulator to follow the desired trajectory with small tracking error is an interested work. For the fuzzy controller, adjusting the parameters of the fuzzy controller in order to obtain the best performance, nowadays there is no standard. It depends on experience of the fuzzy controller designer. Thus, the study about the fuzzy tuning method is an interested thing for future study.

Nonlinear controller designed by high-speed switching law such as sliding mode controller which is a high-speed switching feedback controller that can drive the nonlinear plant's state trajectory onto a specified surface in the state space also be the interested controller for the future work of this tracking system.

REFERENCES

[1] R. K. Mittal, I. J. Nagrath. **Robotics and Control.** Tata McGraw Hill Publishing Company Limited. 2003.

[2] Robert J. Schilling. **Fundamentals of Robotics Analysis and Control.** Prentice-Hall International, Inc. 1990.

[3] สมพงษ์ ทานอก "การออกแบบตัวชดเชยไม่เป็นเชิงเส้นแบบปรับเปลี่ยนได้ร่วมกับตัวควบคุมพีดีสำหรับหุ่นยนต์สการา"วิทยานิพนธ์วิศวกรรมศาสตรมหาบัณฑิต สาขาวิชาวิศวกรรมระบบควบคุม คณะบัณฑิตวิทยาลัย สถาบันเทคโนโลยีพระจอมเกล้าเจ้าคุณทหารลาดกระบัง พ.ศ. 2549

[4] L. Dessaint, M. Saad and B. HCbert, "An Adaptive Controller for a Direct-Drive Scara Robot," IEEE Transactions on Industrial Electronics, vol 39, no.2, 1992.

[5] Baines, P.J. and Mills, J.K., "Feedback Linearized Joint Torque Control of A Geared, DC Motor Driven Industrial Robot," In Proceedings of IEEE International Conference on Robotics and Automation, 1995, pp3129 - 3136.

[6] R. Gourdeau, S. Blouin and R. Hurteau, "Computed Torque Control of Robots Without Joint Velocity Measurements," IEEE Canadian Conference on Electrical and Computer Engineering, 1999, pp. 1413 – 1418.

[7] H. Ying, **Fuzzy Control and Modeling: Analytical Foundations and Applications.** Institute of Electrical and Electronics Engineers, Inc., 2000.

[8] S.Manabe. "Coefficient Diagram Method." 14th IFAC Symposium on Automatic Control in Aerospace, 1998.

[9] Zadeh L.A. **Fuzzy Sets. Information & Control.** vol.8, 1965. pp.338-353.

[10] L. Wang, **Adaptive Fuzzy Systems and Control.** Prentice-Hall International, Inc. 1994.

[11] J. Angeles, A. Morozov and O. Navarro, "A Novel Manipulator Architecture for The Production of SCARA Motions," IEEE International Conference on Robotics and Automation, 2000, pp. 2370-2375.

[12] F.L, Lewis, C.T. Abdallah and D.M. Dawson, **Control of Robot Manipulators.** Macmillan Publishing Company, 1993.

[13] B. A. Chubb, **Modern Analytical Design of Instrument Servomechanisms.** Addison-Wesley, 1967.

Appendix A

Equipment Specifications

A.1 Outline Drawing of Two-Link Robot Manipulator

The two-link robot manipulator used in the experiments has outline drawing as shown in figure A.1.

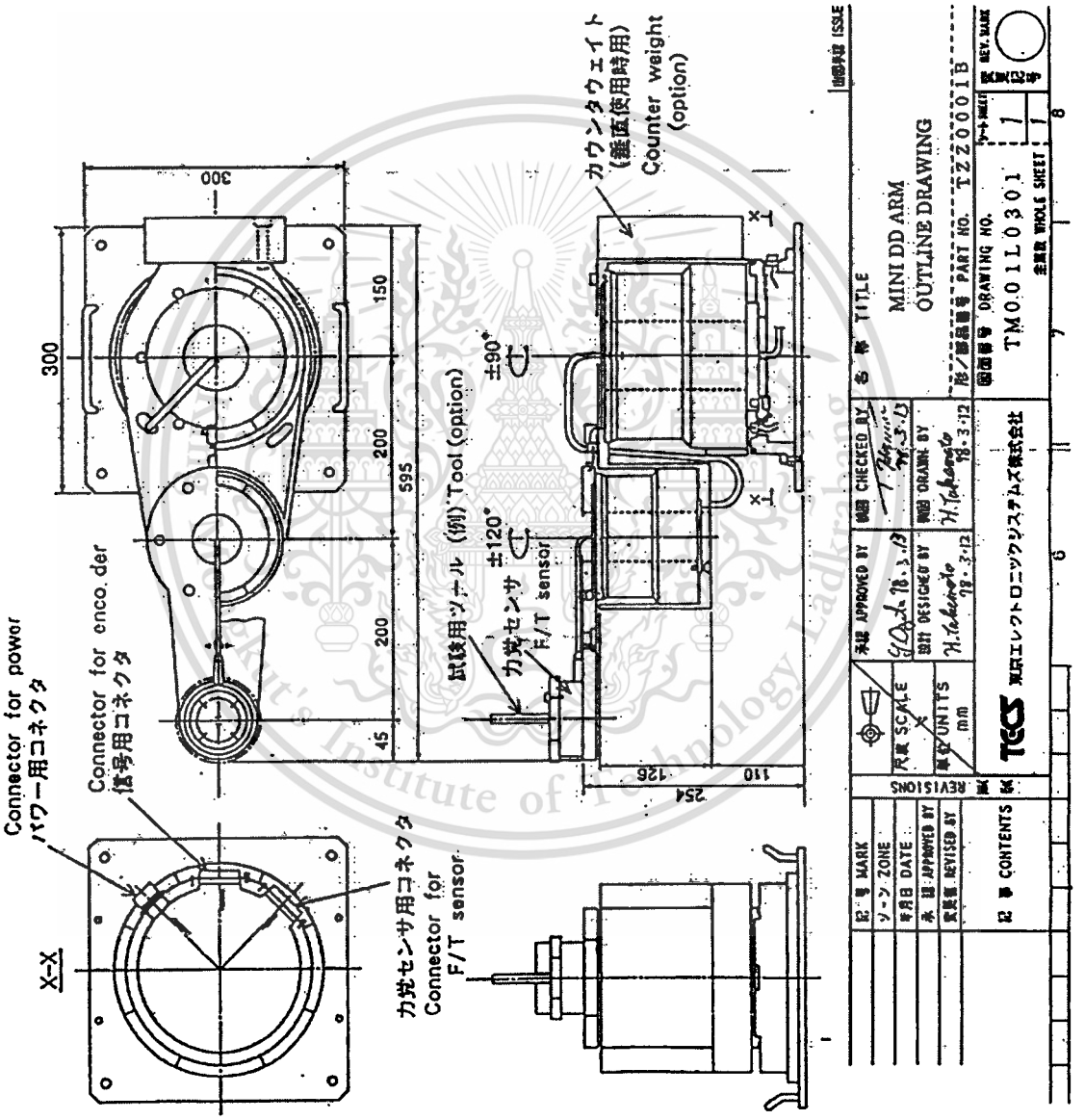

Figure A.1 Outline Drawing of Two-Link Robot Manipulator.

A.2 Actuators

The actuators driven the 1st and the 2nd links of the robot manipulator are AC servos of YOKOGAWA Precision Corporation. Their structures are identical as shown in figure A.2. The model for the 1st and the 2nd links are DR-1070E and DR-1015B. Their specification are shown in table A.1 and table A.2, respectively.

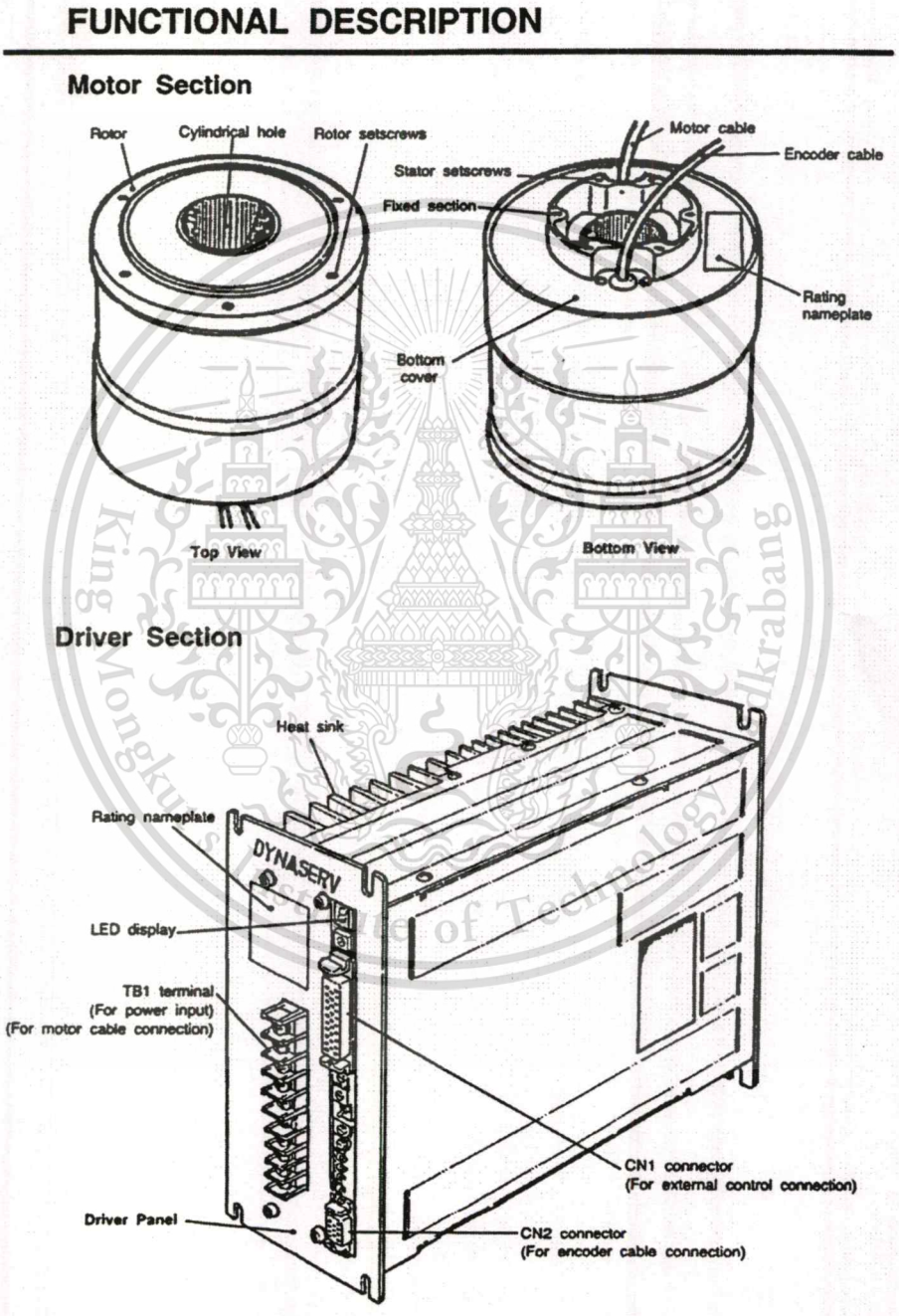

Figure A.2 Description of an Actuator.

Table A.1 Specifications of DYNASERV E Series.

Series				DR-E Series						
Model				DR1250E□0	DR1220E□0	DR1160E□0	DR1130E□0	DR1100E□0	DR1070E□0	DR1030E□0
Motor & driver coupling	Max. torque		(N·m)	250	220	160	130	100	70	30
	Max. speed (rps)	100 to 115V AC Model		0.7	0.7	1.0	1.2	1.5	2.0	2.0
		200 to 230V AC Model		1.2	1.2	1.2	1.2	2.4	2.4	2.4
	Rated output (W)	100 to 115V AC Model		265	224	170	132	212	224	95
		200 to 230V AC Model		425	375	335	265	315	300	125
	Rated torque		(N·m)	83	73	53	43	33	23	10
	Rated speed (rps)	100 to 115V AC Model		0.5	0.5	0.5	0.5	1.0	1.5	1.5
		200 to 230V AC Model		0.8	0.8	1.0	1.0	1.5	2.0	2.0
	Encoder resolution		(p/rev)	614,400						
	Positioning accuracy		(arc-sec)	±45						
	Repeatability		(arc-sec)	±5						
	Max. power consumption		(kVA)	3.2	3.0	2.8	2.5	2.3	2.0	1.8
Motor section	Rotor inertia		($kg \cdot m^2$)	185×10^{-3}	170×10^{-3}	140×10^{-3}	125×10^{-3}	100×10^{-3}	85×10^{-3}	72×10^{-3}
	Static max. load	Axial load (N)	Compression	4.0×10^{4}						
			Tension	2.0×10^{4}						
		Overhung load	(N·m)	400						
	Torsional stiffness	Axial stiffness (mm/N)	Compression	2.0×10^{-6}						
			Tension	3.0×10^{-6}						
		Radial stiffness	(rad/N·m)	4.0×10^{-7}						
	Weight		(kg)	48	44	36	32	26	22	18
	Dimensions		(mm) Roter dia. ×L.	ϕ205×355	ϕ205×327	ϕ205×271	ϕ205×243	ϕ205×210	ϕ205×183	ϕ205×156
	Common item			Motor insulation: class F / Insulation resistance: 10MΩ Min.(500V DC) / Withstanding voltage: 1500V AC, 1 min. / Color: Black / Excitation: 3 Phase						
Driver section	Model	100 to 115V AC		SR1250E□2-1□□	SR1220E□2-1□□	SR1160E□2-1□□	SR1130E□2-1□□	SR1100E□2-1□□	SR1070E□2-1□□	SR1030E□2-1□□
		200 to 230V AC		SR1250E□2-2□□	SR1220E□2-2□□	SR1160E□2-2□□	SR1130E□2-2□□	SR1100E□2-2□□	SR1070E□2-2□□	SR1030E□2-2□□
	Input signal	Speed input	Domestic model	Analog voltage: ±6V DC						
			Export model	Analog voltage: ±10V DC						
		Positioning input		Serial pulse 1.6MHz Max.						
		Rotation direction command		+6V(CW) to −6V(CCW)						
	Output signal	Speed output		H: CW L: CCW						
		Encorder output		Track A/B(400kHz Max.) Zero position signal(150p/rev)						
		Alarm output		Over current, Over voltage, Heat sink temperature rise, Voltage down, Encoder abnormal, CPU abnormal.						
		Monitor output		2.5Hz Step response output (test mode)						
	Power source			100 to 115V AC$^{\pm10\%}$ / 200 to 230V AC$^{\pm10\%}$ 50/60Hz						
	Power consumption driver (VA)	100 to 115V AC Model		1250	1120	900	750	1060	1120	710
		200 to 230V AC Model		1800	1600	1500	1250	1500	1400	900
	Weight		(kg)							

Table A.2 Specifications of DYNASERV A and B Series.

Series				DR-A Series						DR-B Series				
Model				DR1400A□0	DR1300A□0	DR1200A□0	DR1150A□0	DR1100A□0	DR1050A□0	DR1060B□0	DR1045B□0	DR1030B□0	DR1015B□0	DR1008B□0
Motor & driver coupling	Max. torque (N·m)			400	300	200	150	100	50	60	45	30	15	8
	Max. speed (rps)	100 to 115V AC Model		0.4	0.5	0.8	1.0	1.2	1.8	1.4	1.8	2.4		
		200 to 230V AC Model		0.8	1.0	1.2	1.2	1.2	1.8	2.4				
	Rated output (W)	100 to 115V AC Model		212	160	212	160	212	160	125	95	95	63	33.5
		200 to 230V AC Model		425	315	425	315	212	160	125	140	125	63	33.5
	Rated torque (N·m)			133	100	67	50	33	17	20	15	10	5	3
	Rated speed (rps)	100 to 115V AC Model		0.25	0.25	0.5	0.5	1.0	1.5	1.0	1.0	1.5	2.0	2.0
		200 to 230V AC Model		0.5	0.5	1.0	1.0	1.0	1.5	1.0	1.5	2.0	2.0	2.0
	Encoder resolution (p/rev)			819,200						507,904				
	Positioning accuracy (arc-sec)			±30						±45				
	Repeatability (arc-sec)			±5						±5				
	Max. power consumption(kVA)			3.2	3.2	3.0	3.0	2.5	2.5	2.3	2.1	1.8	1.4	1.0
Motor section	Rotor inertia (kg·m²)			400×10^{-3}	320×10^{-3}	285×10^{-3}	230×10^{-3}	200×10^{-3}	180×10^{-3}	33×10^{-3}	26×10^{-3}	24×10^{-3}	21×10^{-3}	15×10^{-3}
	Static max. load	Axial load (N)	Compression	4.0×10^{4}						3.0×10^{4}				
			Tension	2.0×10^{4}						1.0×10^{4}				
		Overhung load (N·m)		400						200				
	Torsional stiffness	Axial stiffness (mm/N)	Compression	2.0×10^{-6}						2.5×10^{-6}				
			Tension	3.0×10^{-6}						3.0×10^{-6}				
		Radial stiffness(rad/N·m)		4.0×10^{-7}						2.0×10^{-6}				
	Weight (kg)			65	55	45	36	31	26	15.5	13	11	9.0	6.0
	Dimensions(mm) Roter dia. xL*			ϕ264x358	ϕ264x304	ϕ264x250	ϕ264x212	ϕ264x185	ϕ264x158	ϕ150x207	ϕ150x179	ϕ150x151	ϕ150x123	ϕ145x85
	Common item			Motor insulation: class F / Insulation resistance: 10MΩ Min.(500V DC) / Withstanding voltage: 1500V AC, 1 min. / Color: Black / Excitation: 3 Phase										
Driver section	Model	100 to 115V AC		SR1400A□2-1□□	SR1300A□2-1□□	SR1200A□2-1□□	SR1150A□2-1□□	SR1100A□2-1□□	SR1050A□2-1□□	SR1060B□2-1□□	SR1045B□2-1□□	SR1030B□2-1□□	SR1015B□2-1□□	SR1008B□2-1□□
		200 to 230V AC		SR1400A□2-2□□	SR1300A□2-2□□	SR1200A□2-2□□	SR1150A□2-2□□	SR1100A□2-2□□	SR1050A□2-2□□	SR1060B□2-2□□	SR1045B□2-2□□	SR1030B□2-2□□	SR1015B□2-2□□	SR1008B□2-2□□
	Input signal	Speed input	Domestic model	Analog voltage: ±6V DC						Analog voltage: ±6V DC				
			Export model	Analog voltage: ±10V DC						Analog voltage: ±10V DC				
		Positioning input		Serial pulse 1.6MHz Max.						Serial pulse 1.6MHz Max.				
		Rotation direction command		+6V(CW) to -6V(CCW)						+6V(CW) to -6V(CCW)				
	Output signal	Speed output		H: CW L: CCW						H: CW L: CCW				
		Encorder output		Track A/B(400kHz Max.) Zero position signal(200p/rev)						Track A/B(400kHz Max.) Zero position signal(124p/rev)				
		Alarm output		Over current, Over voltage, Heat sink temperature rise, Voltage down, Encoder abnormal, CPU abnormal.						Over current, Over voltage, Heat sink temperature rise, Voltage down, Encoder abnormal, CPU abnormal.				
		Monitor output		2.5Hz Step response output (test mode)						2.5Hz Step response output (test mode)				
	Power source			100 to 115V AC±10% / 200 to 230V AC±10% 50/60Hz						100 to 115V AC±10% / 200 to 230V AC±10% 50/60Hz				
	Power consumption driver (VA)	100 to 115V AC Model		1120	900	1060	850	1120	1000	710	670	670	500	400
		200 to 230V AC Model		1800	1400	1900	1500	1120	1000	710	800	750	500	400
	Weight (kg)			6						6				

* See drawings

Appendix B

Coefficient Diagram Method

How to choose a proper controller to meet desired performance specifications is the general problem of control system design. Three main theories: Classical Control Theory, Modern Control Theory and Polynomial Approach, which is sometimes called the Algebraic Approach has been employed for a design procedure. The frequency response method and root-locus method, which are classical control methods, use the transfer function for the system representation. However, when the controlled system is represented by transfer function, it is easy to handle but it becomes inaccurate when pole-zero cancellation occurs due to uncontrollable or unobservable situations. The modern control method like pole-placement method and optimal control uses state-space representation. This representation is accurate and well-suited in machine computation. The Coefficient Diagram Method (CDM) is an algebraic control design approach. This method uses polynomials for system representation. The denominator and the numerator of the transfer function are considered independently from each other. Thus, the better results can be achieved against pole-zero cancellation. In this chapter, the CDM standard block diagram and the basic mathematical relations concerning the CDM will be described.

CDM design is based on the stability index γ_i and the equivalent time constant τ as defined later. The equivalent time constant τ specifies the response speed. The stability index γ_i specifies the stability and the wave form of the time response. The variation of stability index γ_i due to the plant parameter variation specifies the robustness.

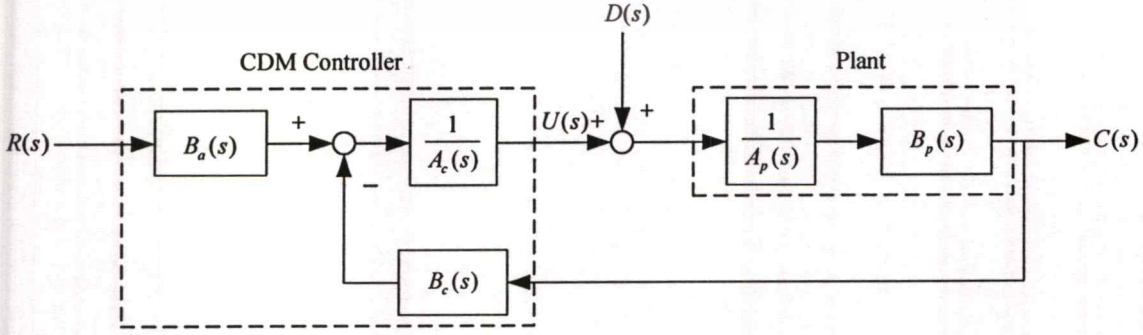

Figure B.1 CDM standard block diagram of SISO system.

The standard block diagram of the CDM design for a single-input-single-output system is shown in figure B.1. $A_p(s)$ and $B_p(s)$ are the polynomials of the plant, $A_c(s)$, $B_c(s)$ and $B_a(s)$ are the polynomials of the standard CDM controller. $D(s)$ is the disturbance entering to the controlled system. The transfer function of the plant in polynomial form can be expressed as

$$A_p(s) = p_k s^k + p_{k-1} s^{k-1} + \ldots + p_0 \tag{B.1}$$

$$B_p(s) = q_m s^m + q_{m-1} s^{m-1} + \ldots + q_0 \tag{B.2}$$

and the controller polynomials are given by

$$A_c(s) = l_\lambda s^\lambda + l_{\lambda-1} s^{\lambda-1} + \ldots + l_0 \tag{B.3}$$

$$B_c(s) = k_\lambda s^\lambda + k_{\lambda-1} s^{\lambda-1} + \ldots + k_0 \tag{B.4}$$

$$B_a(s) = p_\lambda s^\lambda + p_{\lambda-1} s^{\lambda-1} + \ldots + p_0 \tag{B.5}$$

where $\lambda < k$ and $m < k$. $B_a(s)$ is called pre-filter. The characteristic polynomial of the closed-loop system without pre-filter is defined as

$$P(s) = A_c(s)A_p(s) + B_c(s)B_p(s)$$

$$= a_n s^n + a_{n-1} s^{n-1} + \ldots + a_1 s + a_0 \tag{B.6}$$

$$= \sum_{i=0}^{n} a_i s^i$$

where $a_0, a_1, \ldots, a_n$ are the coefficients of the characteristic polynomial. The stability index γ_i, the equivalent time constant τ and stability limit γ_i^* are defined as follows.

$$\gamma_i = \frac{a_i^2}{a_{i+1} a_{i-1}} \tag{B.7}$$

$$\tau = \frac{a_1}{a_0} \tag{B.8}$$

$$\gamma_i^* = \frac{1}{\gamma_{i+1}} + \frac{1}{\gamma_{i-1}}; \gamma_0, \gamma_n = \infty \tag{B.9}$$

where $i = 1,\ldots,n-1$. From (B.7) and (B.8), the coefficient a_i can be written by

$$a_i = a_0 \tau^i \frac{1}{\gamma_{i-1} \cdots \gamma_2^{i-2} \gamma_1^{i-1}}$$

$$= a_0 \tau^i \prod_{j=1}^{i-1} \frac{1}{\left(\gamma_{i-j}\right)^j} \tag{B.10}$$

Substituting each coefficient a_i into equation (B.6), then the characteristic polynomial will be expressed in term of a_0, τ and γ_i as

$$P(s) = a_0 \left[\left\{ \sum_{i=2}^{n} \left(\prod_{j=1}^{i-1} \frac{1}{\gamma_{i-j}^j} \right) (\tau s)^i \right\} + \tau s + 1 \right]. \tag{B.11}$$

The coefficients of equation (B.6) can be computed from the equivalent time constant τ and stability index γ_i, which are chosen to satisfy the stability limit γ_i^*. Thus $\gamma_1 = 2$, $\gamma_2 = 4$, $\gamma_3 = 1.5917$ and $\tau = 0.45$ for the 1st link are chosen. Then the parameters K_i, K_p and K_d of controller for the 1st link can be assigned by equating equation (B.6) to the equation (B.11) and solving them for the solutions. The parameters of controller for the 2nd link can also be found by the using manner of the 1st link. When the stability index γ_i and the time constant τ are chosen to be $\gamma_1 = 2$, $\gamma_2 = 4$, $\gamma_3 = 3.5923$ and $\tau = 0.45$, controller parameter of the 2nd link can be obtained.

Appendix C

Cubic Polynomial Trajectory

For the robotic systems, the important task that can not be ignored is motion planning because of the robotic arms can not be operated without any order; they are required specific commands to move from the starting point to the desired position. The specific commands are like paths or the ways for the arms and are usually called "trajectory". The most well know and common used trajectory is cubic polynomial trajectory, thus in this thesis, the cubic polynomial trajectories are utilized as desired trajectories.

The motion of the robot manipulator begins at the time $t = t_0 = 0$ and ends at $t = t_g$. For a smooth motion between the initial and goal points, the function $q_d(t)$ and $\dot{q}_d(t)$ have to be smooth by the conditions:

$$\begin{aligned} q_d(0) &= q^s \\ q_d(t_g) &= q^g \\ \dot{q}_d(0) &= 0 \\ \dot{q}_d(t_g) &= 0. \end{aligned} \tag{C.1}$$

Assuming that the cubic polynomial is

$$q_d(t) = a_0 + a_1 t + a_2 t^2 + a_3 t^3 \tag{C.2}$$

which gives a parabolic velocity profile

$$\dot{q}_d(t) = a_1 + 2a_2 t + 3a_3 t^2 \tag{C.3}$$

and a linear acceleration profile

$$\ddot{q}_d(t) = 2a_2 + 6a_3 t^2. \tag{C.4}$$

Applying the constrains of equation (C.1) to equations (C.2), (C.3) and (C.4), four equations in four unknown are obtained by

$$\begin{aligned} a_0 &= q^s \\ a_0 + a_1 t_g + a_2 t_g^2 + a_3 t_g^3 &= q^g \\ a_1 &= 0 \\ a_1 + 2a_2 t_g + 3a_3 t_g^2 &= 0. \end{aligned} \tag{C.5}$$

From the equation (C.5), the coefficients of cubic polynomial in equation (C.2) are given by

$$\begin{aligned} a_0 &= q^s \\ a_1 &= 0 \\ a_2 &= \frac{3}{t_g^2}(q^g - q^s) \\ a_3 &= -\frac{2}{t_g^3}(q^g - q^s). \end{aligned} \tag{C.6}$$

Thus, the cubic polynomial for interpolating the path which connect the initial joint position to the final joint position are defined by

$$q_d(t) = q^s + \frac{3}{t_g^2}(q^g - q^s)t^2 - \frac{2}{t_g^3}(q^g - q^s)t^3. \tag{C.7}$$

When assigning the 1st link or 2nd link start to move from the angular position $q^s = 0$ degree to the goal $q^g = 90$ degree within 1 sec, then

$$q_d(t) = 270t^2 - 180t^3 \tag{C.8}$$

can be obtained. Its trajectory is shown in figure C.1.

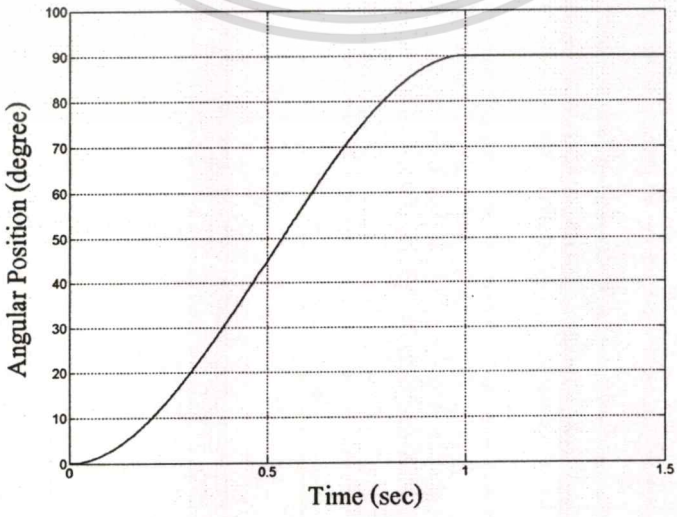

Figure C.1 Desired cubic polynomial trajectory.

Appendix D

Related Publication

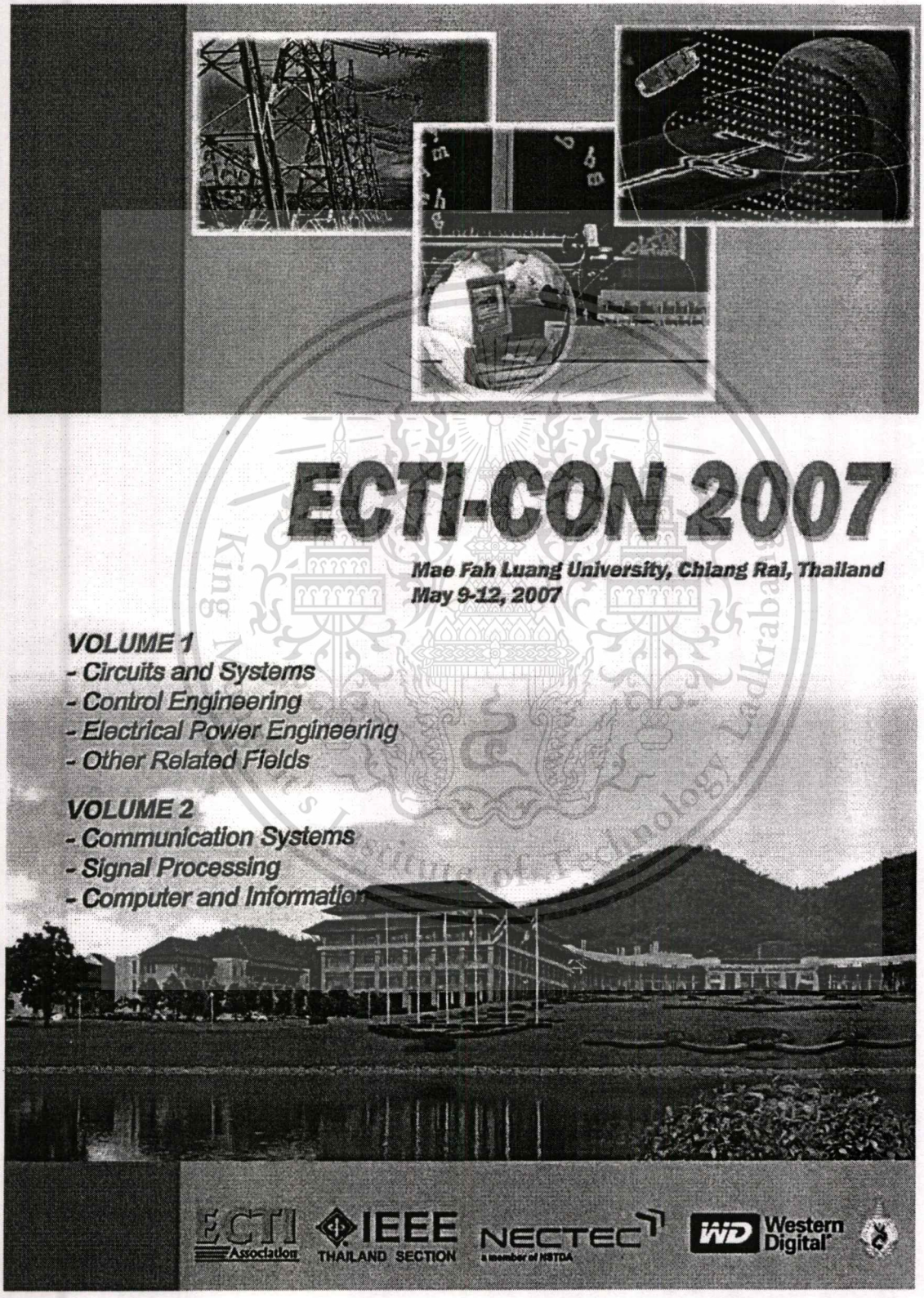

Fuzzy I-PD Controller for Two-Link Robot Manipulator

Wicharn Chatrattanawuth[1], Songmoung Nundrakwang[1], Taworn Benjanarasuth[1],
Jongkol Ngamwiwit[1] and Noriyuki Komine[2]
[1] Faculty of Engineering and ReCCIT, King Mongkut's Institute of Technology Ladkrabang, Bangkok, Thailand
(Tel: +662-739-2405, E-mail: knjongko@kmitl.ac.th)
[2] School of Information Science and Technology, Tokai University, Kanagawa, Japan
(Tel: +81-463-58-1211, E-mail: komine@keyaki.cc.u-tokai.ac.jp)

***Abstract*-This paper presents a fuzzy I-PD controller for two-link robot manipulator. The proposed controller consists of a Mamdani fuzzy I and a Mamdani fuzzy PD controller and its parameters are adjusted to make the manipulator follow to desired trajectory. The experimental results in controlling the two-link robot manipulator by using the proposed fuzzy I-PD controller with the same parameters (proportional gain, integral gain and derivative gain) as the conventional I-PD controller are also shown in this paper.**

I. Introduction

The most well-known and widely used controllers in the industries are the conventional PID-family controllers. The good points of the PID type controllers are the simple in adjusting their parameters to meet the desired control system performances by using the tuning method such as Zeigler-Nichols' (Z-N) tuning formula or coefficient diagram method (CDM) [1-2]. However, when the PID controller is used to control the nonlinear system such as a manipulator system, it is difficult to achieve the desired trajectory, since the manipulator systems contain uncertain components.

Recently, the fuzzy logic controller has been used in control system when the mathematical model of the process is vague or exhibits uncertainties or when PID-family controller can not generate the satisfactory performance [3]. However, due to popularity and simplicity of PID type controller, fuzzy PID-family controllers have been also employed in control system by combining the merits of both controllers.

It is known that I-PD controller has a property to avoid large changes in control signal due to the proportional and derivative actions when there is a sudden change in the reference input. Therefore, a fuzzy I-PD controller, which is the modification of conventional I-PD controller structure, is presented in this paper. Firstly, the conventional I-PD controller is divided into I controller part and PD controller part. After rearranging the structure of I and PD controllers, they will be constructed as a Mamdani fuzzy I controller and a Mamdani fuzzy PD controller. The inputs of Mamdani fuzzy I controller will consist of two inputs, error and change of error, and Mamdani fuzzy PD controller will consist of two inputs, output and change of output. The control signal of the controller is the subtraction value of the output of Mamdani fuzzy I controller and Mamdani fuzzy PD controller. The proposed controller is implemented to control two-link robot manipulator. The experimental results are shown that the parameters of Mamdani fuzzy I-PD controller can be adjusted to make the manipulator follow desired trajectory. The experimental results are also shown by comparing the proposed fuzzy I-PD controller to the conventional I-PD controller where the values of proportional gain, integral gain and derivative gain of fuzzy and conventional controllers are identical.

II. Two-Link Robot Manipulator

In Fig. 1, when the effect of gravity is negligible, the Lagrange dynamics of the two-link robot manipulator is [4]

$$M(q)\ddot{q}+V(q,\dot{q})+F(\dot{q})+\tau_d=\tau \qquad (1)$$

where $q,\dot{q}$ and $\ddot{q}\in R^2$ are joint angle, velocity and acceleration vectors, $M(q)\in R^{2\times2}$ is the inertia matrix, $V(q,\dot{q})\in R^2$ is the Coriolis/centripetal torque vector, $F(\dot{q})$ is the friction, τ_d and $\tau\in R^2$ are disturbance and input torque vectors. The term $M(q)$ and $V(q,\dot{q})$ in dynamic equations (1) are given by

$$M(q)=\begin{bmatrix} J_1+J_2+2rC_2 & J_2+rC_2 \\ J_2+rC_2 & J_2 \end{bmatrix} \qquad (2)$$

and

$$V(q,\dot{q})=\begin{bmatrix} -rS_2(2\dot{q}_1\dot{q}_2+\dot{q}_2^2) \\ rS_2\dot{q}_1^2 \end{bmatrix} \qquad (3)$$

where $J_1=I_1+m_1a_1^2+m_2\ell_1^2$, $J_2=I_2+m_2a_2^2$, $r=m_2\ell_1a_2$, $C_2=\cos q_2$, $S_2=\sin q_2$ and $q=[q_1\ q_2]^T$. $F(\dot{q})$ is assumed to be zero.

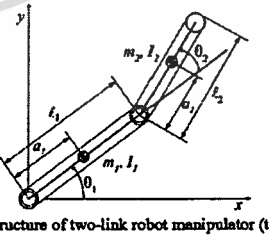

Figure 1. Structure of two-link robot manipulator (top view).

Fig. 2 shows the SCARA type robot manipulator which will be used in the experiments. The mass and the length of robot arms are m_1 = 4.37 kg, m_2 = 1.24 kg, $\ell_1=\ell_2$ = 200 mm,

$a_1 = 63$ mm and $a_2 = 80$ mm. Maximum torque of the 1st and the 2nd joint are 70 Nm and 15 Nm when the maximum torque commands are produced at ±8 V by 2 channels 24 bits D/A PC interface card. Optical encoders of the 1st joint and the 2nd joint are 614,400 and 507,904 pulse/rev.

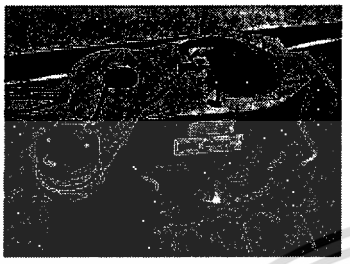

Figure 2. SCARA type robot manipulator.

III. Fuzzy I-PD Control System

The conventional I-PD controller and fuzzy I-PD control system structure which composes of a Mamdani fuzzy I controller and a Mamdani fuzzy PD controller, will be describe in this section.

A. Conventional I-PD Control System Structure

The conventional I-PD control system which consists of a plant, an integral controller and a PD feedback controller, is shown in Fig. 3. Here, K_i is the integral gain of the integral controller, and K_p and K_d are the proportional gain and derivative gain of the PD controller respectively.

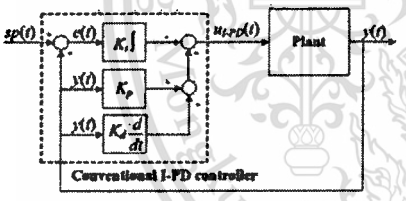

Figure 3. Conventional I-PD control system structure.

The control signal of the conventional I-PD controller of the control system shown in Fig. 3 can be expressed as

$$u_{I\text{-}PD}(t) = K_i \int_0^t e(t)dt - K_p y(t) - K_d \frac{dy(t)}{dt} \quad (4)$$

where $e(t)$ is the error signal and $y(t)$ is the output signal of the control system. After rearranging (4), it can be rewritten as

$$u_{I-PD}(t) = u_I(t) - u_{PD}(t) \quad (5)$$

where

$$u_I(t) = K_i \int_0^t e(t)dt \quad (6)$$

and

$$u_{PD}(t) = K_p y(t) + K_d \frac{dy(t)}{dt}. \quad (7)$$

The control signal of the system $u_{I\text{-}PD}(t)$ in (5) can be transformed into discrete time as

$$u_{I-PD}(nT) = u_I(nT) - u_{PD}(nT) \quad (8)$$

where T denotes the sampling time.

B. Fuzzy I-PD Control System Structure

The structure of the fuzzy I-PD control system shown in Fig. 4 consists of a process and a fuzzy I-PD controller which is the modification of the conventional I-PD controller. The control signal of the fuzzy I-PD controller $u_{I\text{-}PD}(nT)$ is the subtraction of Mamdani fuzzy I control signal and Mamdani fuzzy PD control signal.

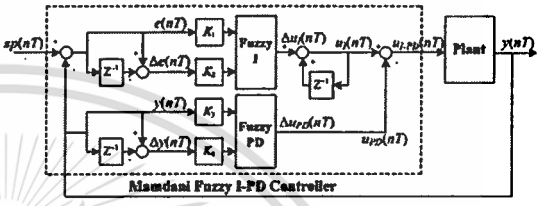

Figure 4. Fuzzy I-PD control system structure.

The output of Mamdani fuzzy I controller $u_I(nT)$ can be computed from (6) by approximating the integral term with the trapezoidal summation. Therefore

$$u_I(nT) = K_1 e(nT) - K_2 \Delta e(nT) + u_I(nT - T) \quad (9)$$

where the error $e(nT) = sp(nT) - y(nT)$, the change of error $\Delta e(nT) = e(nT) - e(nT\text{-}T)$, $K_1 = K_i T$ and $K_2 = K_i T/2$. When the term $K_1 e(nT) - K_2 \Delta e(nT)$ is replaced by $\Delta u_I(nT)$, the new output of Mamdani fuzzy I controller can be obtained as

$$u_I(nT) = \Delta u_I(nT) + u_I(nT - T) \quad (10)$$

where $\Delta u_I(nT)$ is the output change of fuzzy I controller whose inputs are $K_1 e(nT)$ and $K_2 \Delta e(nT)$.

In the same manner, the output of Mamdani fuzzy PD controller $u_{PD}(nT)$ can be directly computed from (7) by approximating the derivative term with two-point difference form. Then

$$u_{PD}(nT) = K_3 y(nT) + K_4 \Delta y(nT) \quad (11)$$

can be obtained, where $y(nT)$ is the output, $\Delta y(nT)$ is the change of output, $K_3 = K_p$ and $K_4 = K_d/T$. Define $\Delta u_{PD}(nT)$ to be $K_3 y(nT) + K_4 \Delta y(nT)$, the new output of Mamdani fuzzy PD controller becomes

$$u_{PD}(nT) = \Delta u_{PD}(nT). \quad (12)$$

IV. Fuzzy I-PD Controller Design

In this section, the Mamdani fuzzy I controller and the Mamdani fuzzy PD controller design will be described. The fuzzification, fuzzy rules and defuzzification are needed for designing the fuzzy controllers.

A. Fuzzification

In fuzzification, $K_1e(nT)$ and $K_2\Delta e(nT)$ are the Mamdani fuzzy I controller inputs and $K_3y(nT)$ and $K_4\Delta y(nT)$ are the Mamdani fuzzy PD controller inputs. Input scaling uses two input membership functions (n : negative and p : positive). Since the fuzzy I and fuzzy PD controllers have similar structure, the membership functions of all inputs are similarly selected with the adjustable constant L as shown in Fig. 5.

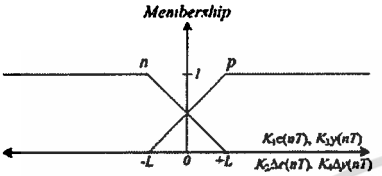

Figure 5. Input membership functions.

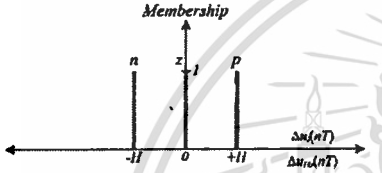

Figure 6. Output membership functions.

B. Fuzzy Rules

The output membership functions for Δu_I and Δu_{PD} are shown in Fig. 6. Three output membership functions are used (n : negative, z : zero and p : positive), where H is the adjustable constant. Based on the input membership functions in fuzzification stage and these output membership functions, the fuzzy control rules for the Mamdani fuzzy I controller are

R^1: IF $K_1e(nT)$ is n & $K_2\Delta e(nT)$ is n THEN $\Delta u_I(nT)$ is n
R^2: IF $K_1e(nT)$ is n & $K_2\Delta e(nT)$ is p THEN $\Delta u_I(nT)$ is z
R^3: IF $K_1e(nT)$ is p & $K_2\Delta e(nT)$ is n THEN $\Delta u_I(nT)$ is z
R^4: IF $K_1e(nT)$ is p & $K_2\Delta e(nT)$ is p THEN $\Delta u_I(nT)$ is p.

Similar rules are also applied for assigning the Mamadani fuzzy PD controller. Hence,

R^1: IF $K_3y(nT)$ is n & $K_4\Delta y(nT)$ is n THEN $\Delta u_{PD}(nT)$ is n
R^2: IF $K_3y(nT)$ is n & $K_4\Delta y(nT)$ is p THEN $\Delta u_{PD}(nT)$ is z
R^3: IF $K_3y(nT)$ is p & $K_4\Delta y(nT)$ is n THEN $\Delta u_{PD}(nT)$ is z
R^4: IF $K_3y(nT)$ is p & $K_4\Delta y(nT)$ is p THEN $\Delta u_{PD}(nT)$ is p.

C. Defuzzification

The centroid defuzzifier is used to calculate the output change $\Delta u_I(nT)$ of the Mamdani fuzzy I controller and $\Delta u_{PD}(nT)$ of the Mamdani fuzzy PD controller. The defuzzification results are respectively obtained from

$$\Delta u_I(nT)=\frac{\sum_{r=1}^{4}\mu_{I_r}\Delta u_{I_r}}{\sum_{r=1}^{4}\mu_{I_r}} \text{ and } \Delta u_{PD}(nT)=\frac{\sum_{r=1}^{4}\mu_{PD_r}\Delta u_{PD_r}}{\sum_{r=1}^{4}\mu_{PD_r}}, \quad (13)$$

where μ_{I_r} and μ_{PD_r} are the membership values at the r^{th} rule, Δu_{I_r} and Δu_{PD_r} are the singleton outputs at the r^{th} rule.

Fig. 7 and Fig. 8 show the input spaces of Mamdani fuzzy I and Mamdani fuzzy PD controller that can be decomposed into 12 different input spaces (ICs). The results of $\Delta u_I(nT)$ and $\Delta u_{PD}(nT)$ are obtained by applying defuzzification algorithm (13) to each membership area. The expressions of $\Delta u_I(nT)$ and $\Delta u_{PD}(nT)$ in IC1 to IC12 are shown in Table 1.

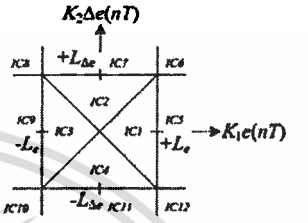

Figure 7. Input spaces of fuzzy I controller.

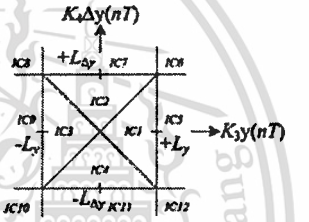

Figure 8. Input spaces of fuzzy PD controller.

TABLE I
IC1 to IC12 for $\Delta u_I(nT)$ and $\Delta u_{PD}(nT)$

IC#	$\Delta u_I(nT)$	$\Delta u_{PD}(nT)$
IC1	$\frac{2HL_{\Delta e}K_1e(nT)+2HL_eK_2\Delta e(nT)}{8L_eL_{\Delta e}-4L_{\Delta e}K_1e(nT)}$	$\frac{2HL_{\Delta y}K_3y(nT)+2HL_yK_4\Delta y(nT)}{8L_yL_{\Delta y}-4L_{\Delta y}K_3y(nT)}$
IC2	$\frac{2HL_{\Delta e}K_1e(nT)+2HL_eK_2\Delta e(nT)}{8L_eL_{\Delta e}-4L_eK_2\Delta e(nT)}$	$\frac{2HL_{\Delta y}K_3y(nT)+2HL_yK_4\Delta y(nT)}{8L_yL_{\Delta y}-4L_yK_4\Delta y(nT)}$
IC3	$\frac{2HL_{\Delta e}K_1e(nT)+2HL_eK_2\Delta e(nT)}{8L_eL_{\Delta e}+4L_{\Delta e}K_1e(nT)}$	$\frac{2HL_{\Delta y}K_3y(nT)+2HL_yK_4\Delta y(nT)}{8L_yL_{\Delta y}+4L_{\Delta y}K_3y(nT)}$
IC4	$\frac{2HL_{\Delta e}K_1e(nT)+2HL_eK_2\Delta e(nT)}{8L_eL_{\Delta e}+4L_eK_2\Delta e(nT)}$	$\frac{2HL_{\Delta y}K_3y(nT)+2HL_yK_4\Delta y(nT)}{8L_yL_{\Delta y}+4L_yK_4\Delta y(nT)}$
IC5	$\frac{HK_2\Delta e(nT)+HL_{\Delta e}}{2L_{\Delta e}}$	$\frac{HK_4\Delta y(nT)+HL_{\Delta y}}{2L_{\Delta y}}$
IC6	H	H
IC7	$\frac{HK_1e(nT)+HL_e}{2L_e}$	$\frac{HK_3y(nT)+HL_y}{2L_y}$
IC8	0	0
IC9	$\frac{HK_2\Delta e(nT)-HL_{\Delta e}}{2L_{\Delta e}}$	$\frac{HK_4\Delta y(nT)-HL_{\Delta y}}{2L_{\Delta y}}$
IC10	$-H$	$-H$
IC11	$\frac{HK_1e(nT)-HL_e}{2L_e}$	$\frac{HK_3y(nT)-HL_y}{2L_y}$
IC12	0	0

V. EXPERIMENTAL RESULTS

In this section, the proposed Mamdani fuzzy I-PD controller is implemented to control the two-link robot manipulator shown Fig. 2 in order to demonstrate the effectiveness of the proposed the controller. In the experiments, the sampling time T is chosen to be 0.001 second.

First, the parameters $K_I = 25.0$, $K_p = 25.0$ and $K_d = 10.0$ of the conventional I-PD controller are found from the CDM tuning method when the stability index $\gamma_2 = 4$ [5] and then they will be used for designing the proposed Mamdani fuzzy I-PD controller as stated in section III. Consequently, the gains for the Mamdani fuzzy I controller are $K_1 = 0.025$ and $K_2 = 0.0125$, and for the Mamdani fuzzy PD controller are $K_3 = 25.0$ and $K_4 = 10000$, respectively. The adjustable constants for 1st joint are chosen as $L_e = 600$, $L_{\Delta e} = 50000$, $L_y = 85000$, $L_{\Delta y} = 85000$, $H_{\Delta u_I} = 20400$ and $H_{\Delta u_{PD}} = 11400$. The adjustable constants for 2nd joint are chosen as $L_e = 7500$, $L_{\Delta e} = 500000$, $L_y = 850000$, $L_{\Delta y} = 650000$, $H_{\Delta u_I} = 14600$ and $H_{\Delta u_{PD}} = 12600$.

The experimental results of the Mamdani fuzzy I-PD and the conventional I-PD control systems are shown in Fig. 9 to Fig. 14. It is seen from Fig. 9 and Fig. 12 that the Mamdani fuzzy I-PD controller can control the robot manipulator rapidly follows the desired cubic polynomial trajectories [6] than the conventional I-PD controller. Both control systems can reach to the desired angular position at 90 degrees without steady-state error as shown in Fig. 10 and Fig. 13 where the smaller error of both links of the Mamdani fuzzy I-PD control system can be noticed. Furthermore, it can be seen that the magnitude of the control signals of the 1st link and the 2nd link of the fuzzy I-PD control system are smaller than the control signals of the conventional I-PD control system as shown in Fig. 11 and Fig. 14. Thus, the effectiveness of the Mamdani fuzzy I-PD controller for the two-link manipulator is confirmed by the experimental results.

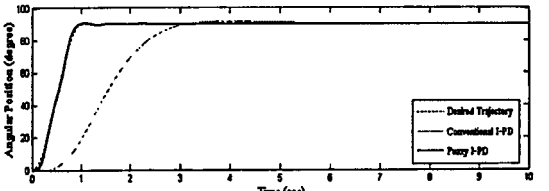

Figure 9. Responses of the 1st link.

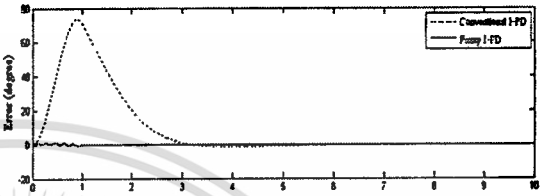

Figure 10. Errors of the 1st link.

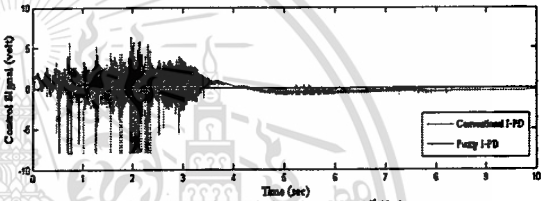

Figure 11. Control signals of the 1st link.

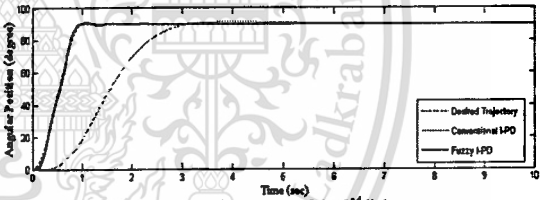

Figure 12. Responses of the 2nd link.

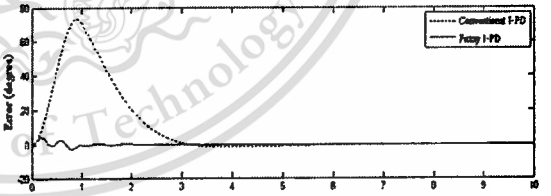

Figure 13. Errors of the 2nd link.

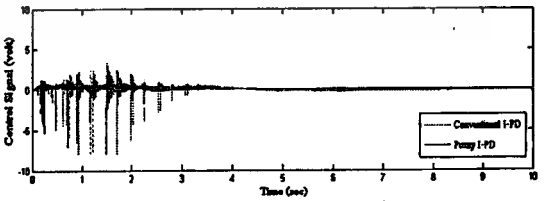

Figure 14. Control signals of the 2nd link.

VI. CONCLUSIONS

The Mamdani fuzzy I-PD controller has been proposed in this paper and has been implemented to control the angular position of the two-link robot manipulator. The proposed Mamdani fuzzy I-PD controller can control the robot manipulator to rapidly follow the desired trajectories without steady-state error. In conclusion, the proposed controller has the efficiency to handle the robot manipulator.

REFERENCES

[1] J. G Zeigler and N. B. Nichols, "Optimum Settings for Automatic Controllers," *ASME Trans.*, vol. 64, pp. 759-768, 1942.

[2] S. Manabe, "Coefficient Diagram Method," *14th IFAC Symposium on Automatic Control in Aerospace*, pp. 199-210, 1998.

[3] H. Ying, *Fuzzy Control and Modeling: Analytical Foundations and Applications*, Institute of Electrical and Electronics Engineers, Inc., 2000.

[4] F.L, Lewis, C.T. Abdallah and D.M. Dawson, *Control of Robot Manipulators*, Macmillan Publishing Company, 1993.

[5] A. Ucar and S.E. Hamamci, "A controller based on coefficient diagram method for the robotic manipulators," *The 7th IEEE International Conference on Electronics, Circuits and Systems*, Jounieh, Lebanon, vol. 2, pp. 777-780, December 17-18, 2000.

[6] R. K. Mittal and I. J. Nagrath, *Robot and Control*, Tata McGraw-Hill Publishing Company Limited, 2003.

Author Biography

The author, Wicharn Chatrattanawuth was born in Chon Buri, Thailand, on October 3, 1982. He received his B.Eng degree in Control Engineering in 2005 from King Mongkut's Institute of Technology Ladkrabang (KMITL). And then he enrolled in the Control Engineering Department, KMITL, as a graduate student and become a member of the Control and Mechatronics Laboratory, Research Center for Communications and Information Technology (ReCCIT) to work toward his M.Eng degree.

His main research interests include analysis and design of robot manipulator system as well as fuzzy logic controller.